P A P E R S

ROZPRAWY

RYSZARD ZEIDLER

Polish Academy of Sciences'
Institute of Hydro-Engineering — Gdańsk

HYDROMECHANICS OF THE WASTE- AND HEATED-WATER DISCHARGE TO THE MARINE ENVIRONMENT, AND RELATED PROBLEMS

Chapter 1

INTRODUCTION

The gross national products of the world's countries increase rapidly and so does the production of energy. Although sources of energy seem to be limited within the sphere of our current technological possibilities and the energy crisis has appeared as a new term in almost everyone's everyday life, yet the industrial development of many nations will certainly last for a considerable period. This trend is illustrated by Fig. 1.1

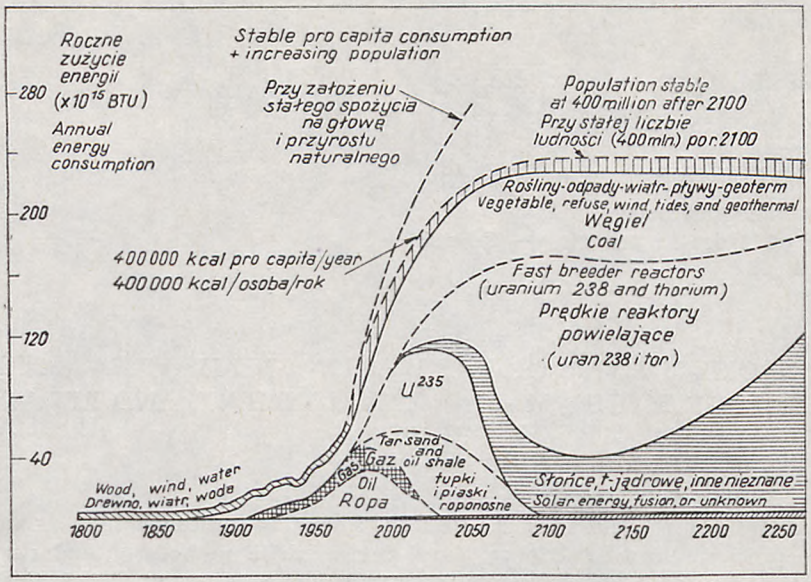

Fig. 1.1. U.S. power generation

Rys. 1.1. Produkcja energii w USA

with the curve of U.S. power generation predicted in the seventies. Under the conditions where fossil sources are becoming gradually depleted nuclear power is anticipated to increase the total generation. However controversial, such a trend might also characterize Poland, perhaps with a certain time lag.

Energy generation is closely related to environmental pollution: directly through liberation of heat, which must be ultimately transferred to either the atmosphere or hydrosphere, and indirectly through increasing amounts of industrial and municipal wastes discharged to water bodies.

There is a battle between those who would retain the current state of the environment or even advocate its return to the pristine state and those who insist that technological advancements are necessary and unavoidable in spite of the world's increasing pollution. Both groups are correct to some extent and one cannot advocate either environmental quality or technological advancements to the exclusion of the other. Increased effort must be exerted to identify all phases of the problem, develop various alternative solutions, and delineate the probable effects. This study is aimed at the extensive examination of the hydromechanical aspects of the problem with a broadened wision to encompass the full realization of other effects. In view of often uncontrollable energy

limitations (and resulting higher costs of waste management systems) it is assumed that some pollution is permitted; the engineer's task is to provide for the lowest and least hazardous contamination patterns possible under specific conditions.

Two procedures have been used for discharging heated water from power plants into an impoundment: surface discharges and bottom diffusers. The first procedure involves the spreading of the lighter, heated water on the surface of a water body as a jet, either boyant or non-buoyant (under certain circumstances), at short distances from the channel outlet, and subject to surface heat loss and ambient turbulence at a relative distance from the outlet. Bottom diffusers ensure the jet-like dispersion of heated water on its way to naviface and further surface spread under the effect of heat loss and ambient turbulence. Although the second procedure produces smaller surface temperatures above diffusers, which conforms better to pollution control requirements of some countries (e.g. some U.S. states permit 1.5°F rise in surface temperature within and area of 300-ft radius), the surface discharge imposes a weaker impact on the environment because of faster heat transfer to the atmosphere and a smaller total amount of heat restored in water. Typical layout and comparison is shown in Fig. 1.2.

Although industrial or munipical wastes are not usually disposed of in the sea through shoreline outlets, their discharge has much in common with the procedures for heated water. If forced out through bottom diffusers, waste water is affected by the same factors (momentum, buoyancy, ambient dynamics, etc.) which control the dispersion of heated water, with the exception of heat loss and associated phenomena, which are negligible for wastes. Fig. 1.2. shows the major types of discharges of both heated and waste-water along with some description of factors and definitions involved.

This work is intended to summarize the up-to-date knowledge of the phenomena on the basis of the Author's and others' findings so as to enable an engineer to design coastal discharges and to provide him with an insight into the physics of the problem (with associated aspects of other branches of science). Individual stages of waste dispersion and groups of governing factors are treated in 11 chapters. In almost every chapter the Author has been able to present his own ideas and empirical results against the background of the existing state of the art. Coastal advection and diffusion processes are dealt with first in Chapters 2 and 3, while ambient thermal phenomena (important especially for heated water) are discussed in short in Chapter 4. Initial dilution, common for heated water and waste water discharged from below the sea surface, mostly through pipe diffusers, is devoted more space

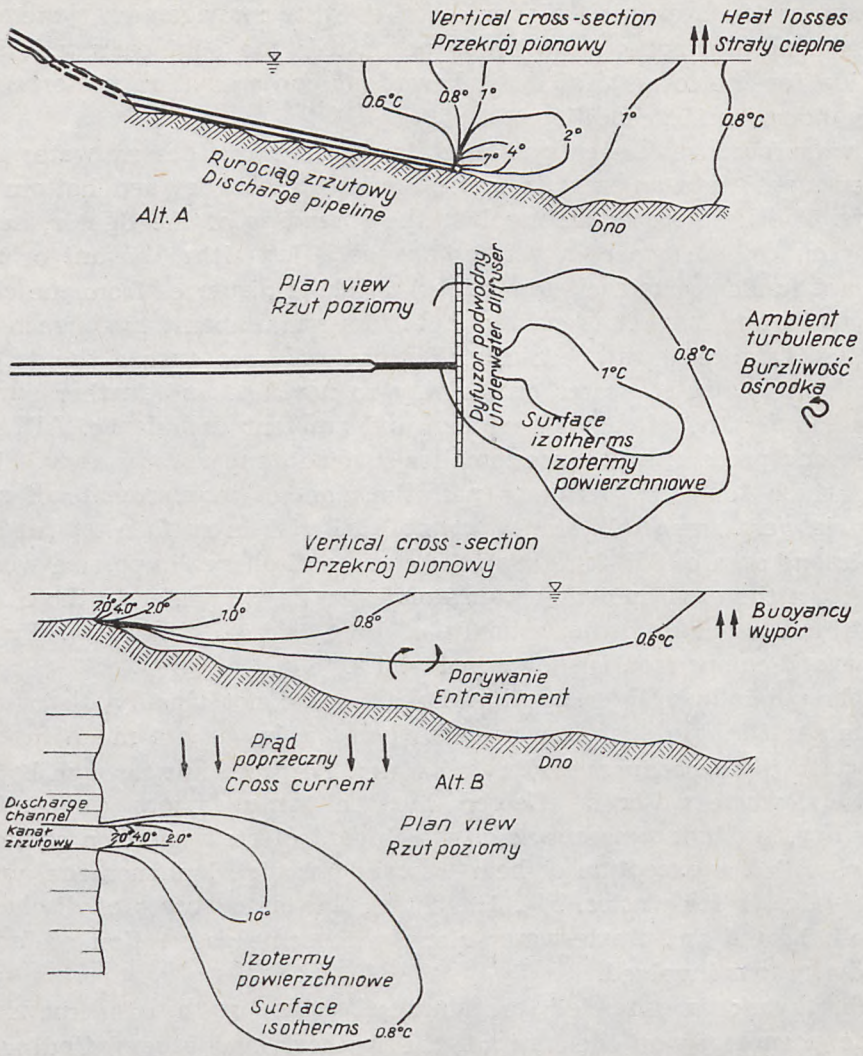

Fig. 1.2. Waste-and heated-water discharge alternatives
Rys. 1.2. Rozwiązania dla zrzutu ścieków i wody podgrzanej

because of its importance to both types of disposed water. Chapter 5, in which initial dilution is discussed, closes the first part of the study, in which physical prerequisites for a certain mode of heated- and waste-water behaviour are analysed. Chapter 6 is fully devoted to one of the alternative schemes for heated water — to surface discharges, the design of which requires the knowledge of all the components described previously (analogous basis for waste-water disposal has been summarized in Chapter 3). The further two chapters are of a methodological char-

acter as they outline the techniques used in assessment of the topics discussed elsewhere. Finally, the random character of the discharges in taken into account in Chapter 10. Thus far quasi-deterministic patterns were assumed to hold true in all stages of discharges. This would mean diffusion and dispersion only within bounds of jet-like structures moving in steady and stable advective fields. Introduction of randomness in those fields adds to dispersion and thus improves design features. Several techniques are examined and the most expedient is chosen. An attemmpt is also udertaken to include relevant factors (biological, engineering etc.) that might play some role in the design and which are presented in Chapter 9. Ultimately, the design procedure is incorporated in a computer program (outlined in Chapter 11), which embraces all the phenomena discussed in this study and constitutes the respective represenation of the procedures outlined in Chapter 10.

Chapter 2

INSHORE ADVECTION PROCESSES

The importance of advection in inshore zones is self-explanatory as it is the advection field that provides transport patterns for a discharged matter and that contributes primarily to the occurrence of this matter at a certain point while released elsewhere. Since most discharges of heated water and wastes take place in the inshore zone and undergo hydrodynamic changes due to inshore advection, it is reasonable to examine the pertinent processes thoroughly.

We shall start from the field and laboratory observations of currents within coastal regions made by the Author (1975) and others (e.g. Sonu 1972). As it is quite well known that from among wind-driven and wave-induced currents the latter are dominant in the inshore zone, our attention has been focussed on the inshore circulation patterns developed by waves.

The Author's quantitative field observations are carried out by means of tracers of neutral buoyancy photographed from above and by current meters at different locations. The laboratory investigations were conducted with standard techniques on a regularly alternating beach section. From the observations it follows that a general schematization can be provided for the seemingly pure random flow patterns in the inshore zone and numerical estimates can be given to some characteristics.

The limits of the surf zone, where the wave-induced currents prevail, vary considerably with characteristic wave heights and are less pronounced under weak waves and swell. Wave currents appear seawards of a breaking line to an extent which seems to depend upon the ratio $\frac{h}{H}$ ctg α. This ratio was found by subtracting the almost constant velocities of wind-driven currents far away from the breaking line from the overall velocities measured elsewhere. Under most common conditions the region of dominant wave currents is practically equivalent to the surf zone. Therefore the schematization of inshore currents presented in Fig. 2.1 and proposed earlier by Sonu proves itself valuable and instructive.

The details of the inshore circulation patterns observed by the Author off Benghazi (Libya) and Lubiatowo (Poland) may be seen in Figs. 2.2 and 2.3, respectively. Both beaches are sandy with parallel isobaths, but the Libyan shore is steeper than the Polish one (4 per cent vs 1 per cent) and does not exhibit underwater bars (with the exception of the inshore shoal, where distinct plunging occurs), while the number of the Baltic reefs sometimes amounts to four and the breaking between them often assumes the form of spilling or surfing.

The dissimilarity of both beaches observed allows the Author to draw the following conclusions from the analysis of all situations measured. The unidirectional flow occurs in the case of higher waves incident at an angle to shore line and if wave amplitude does not vary much along crests. Hence, type (a) of Fig. 2.1 occurs in most cases observed in the Baltic Sea (Fig. 2.3) and for stronger Mediterranean currents (27th February in Fig. 2.2), while normal wave indidence (as on 18th March in Fig. 2.2) is associated with bidirectional currents, when water flows towards the sea in the convergence zones, as in Fig. 2.1, scheme (b). The outflow is weaker at the surface and intensifies beneath, which is indicated by clear sediment clouds and has also been confirmed by Sonu (1972). There are two factors contributing to the bidirectional flow: (1) longshore variation of depth contours and (2) longshore variation of random wave amplitudes. Both factors were present on the Libyan cast, while the latter added only little to weak opposite currents at Lubiatowo. Bottom configuration is very important to the character of inshore currents. The laboratory tests carried out on both stable and movable bed (Tarnowska and Zeidler, 1976) have shown that the bottom reconstructed by storm changes the character of inshore circulation. Since this changes in turn the bed itself, the entire interaction process is fairly complex and requires further investigation.

Bottom configuration is also an important factor controlling the size

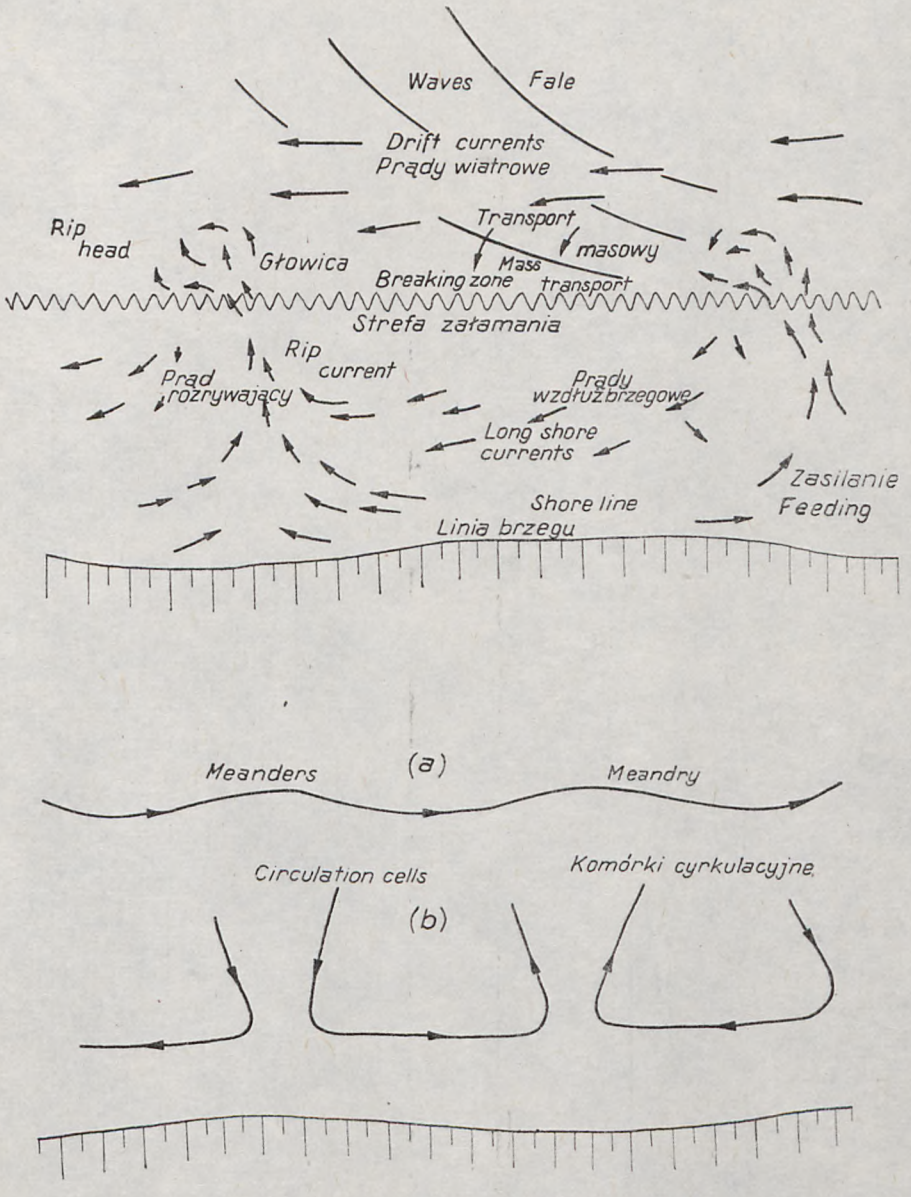

Fig. 2.1. Schematization of inshore currents
Rys. 2.1. Schematyzacja prądów przybrzeżnych

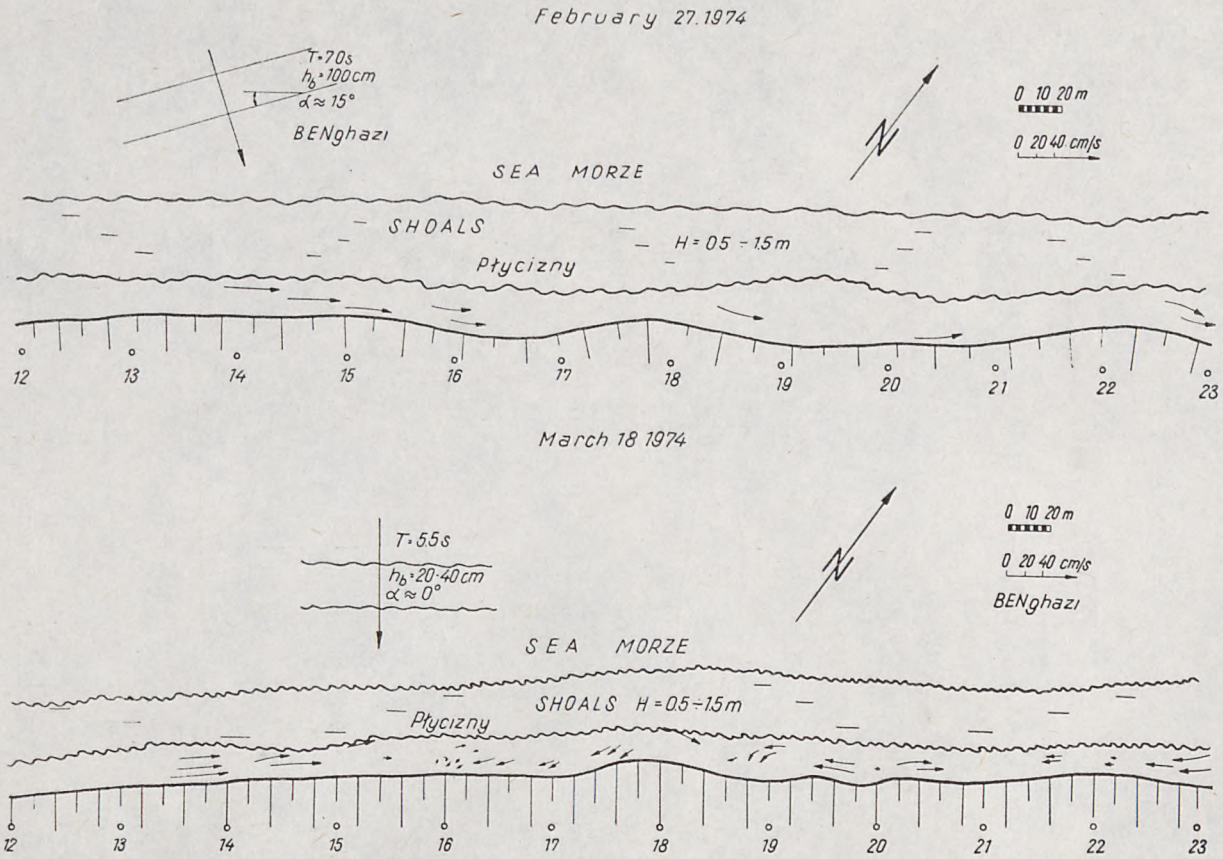

Fig. 2.2. Circulation system on the Benghazi (Libya) coastline on March 6, 1974

Rys. 2.2. Układ prądów w przybrzeżnej strefie Benghazi 6 marca 1974

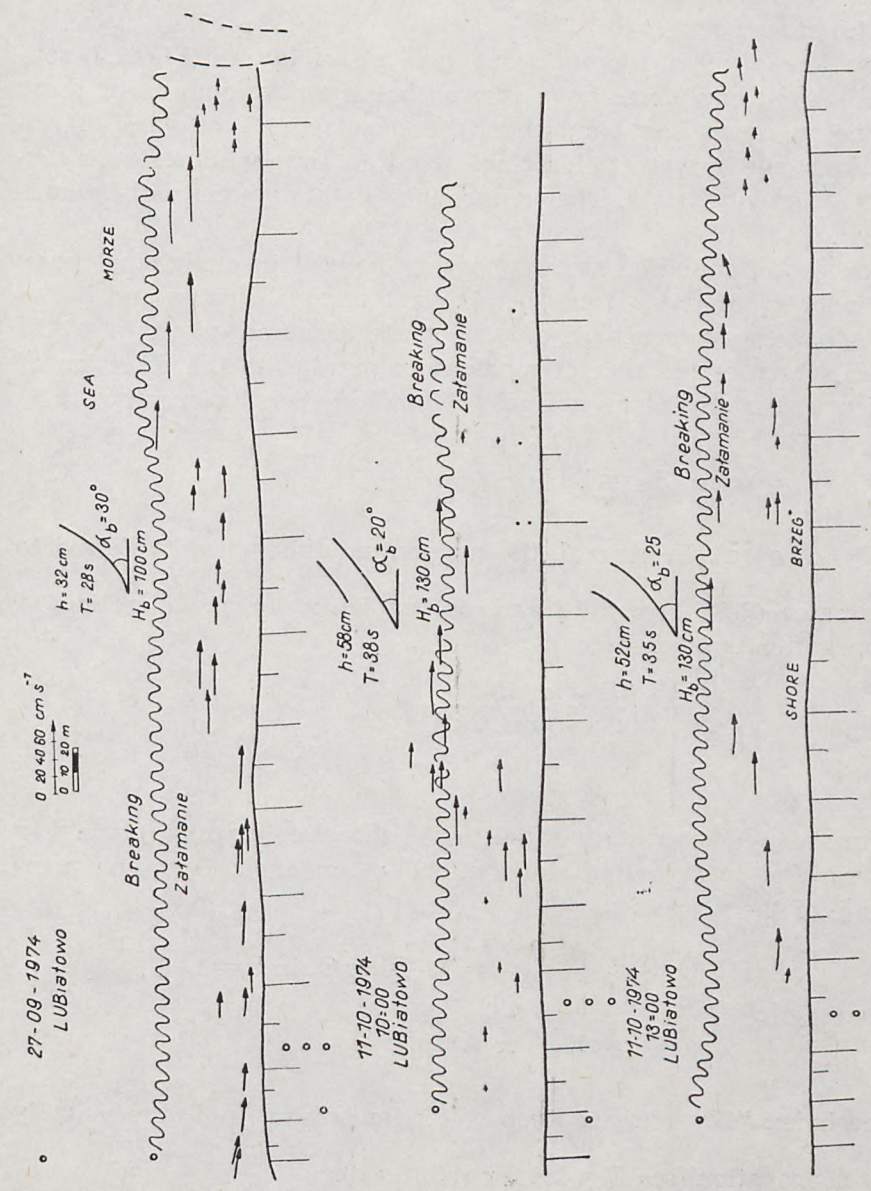

Fig. 2.3. Three flow regimes in the Baltic inshore zone

Rys. 2.3. Trzy rodzaje przepływów w przybrzeżnej strefie Bałtyku

of circulation cells. The distance between rip currents varied from 50 m on the Baltic and Mediterranean beaches to 500 m on the latter. The laboratory tests indicate that this distance is proportional to breaker height or the width of surf zone.

Observations of wave currents conducted at Lubiatowo (Fig. 2.3) several times during one storm have shown that the development of these currents needs much less time than the development of wind-driven currents. A change in wave field brings about an almost immediate alteration of the current system. The components of this system will be analysed below.

The concept of radiation stresses is very helpful in explaining many facets of inshore currents. It can be shown (Longuet-Higgins and Stewart, 1960) that the presence of a wave train of amplitude a in water of depth H increases the flux of momentum parallel to the direction of propagation across any plane normal to that direction by an amount

$$S_{11} = E\left(\frac{1}{2} + \frac{2kH}{\sinh 2kH}\right), \tag{2.1}$$

where $E = \frac{1}{2}\varrho g a^2$. In general, the momentum flux tensor, referred to the coordinates (ξ_1, ξ_2) parallel and perpendicular to the direction of wave propagation is given by

$$S_{ij} = \begin{bmatrix} E\left(\frac{1}{2} + \frac{2kH}{\sinh 2kH}\right) & 0 \\ 0 & E\frac{kH}{\sinh 2kH} \end{bmatrix}. \tag{2.2}$$

The flux of y-momentum parallel to the shoreline across a plane $x = \text{const}$, parallel to shoreline and inclined at an angle Θ to the principal axis ξ_i of the waves is

$$S_{xy} = \sum_{ij} S_{ij} \frac{\partial x}{\partial \xi_j} \frac{\partial y}{\partial \xi_j} = E\frac{C_g}{C}\cos\Theta\sin\Theta = E\frac{C_g}{C_o}\cos\Theta\sin\Theta_o$$

where the index "O" refers to deep water, and $C_g = \frac{d\delta}{dk}$ is the velocity of energy propagation (see Fig. 2.4 for reference).

A general equation of wave-induced currents in the surf zone can now be derived on the basis of the radiation-stress concept. This reads

$$-\frac{\partial S_{xy}}{\partial x} - \frac{\partial (H\tau_{xy})}{\partial x} + f_Y = 0. \tag{2.3}$$

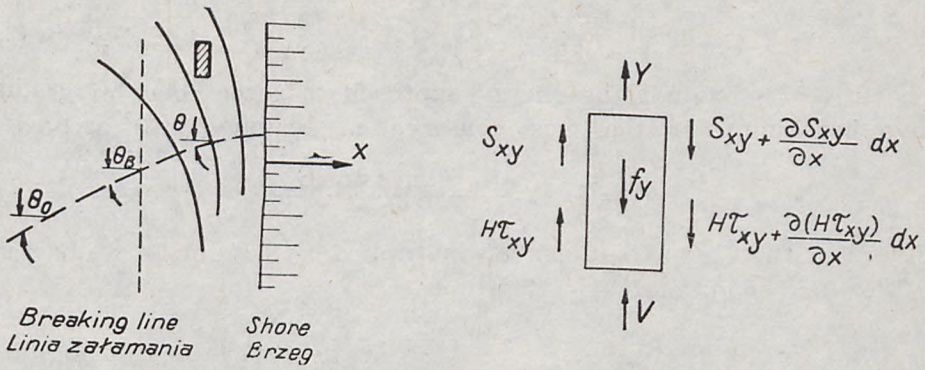

Fig. 2.4. Definition diagram for Eq. 2.3
Rys. 2.4. Objaśnienia do równania 2.3

The first term is the net momentum imparted by the radiation stress. The bottom friction is $f_y\,dx$ opposite to the velocity V. The usual form for the bottom stress is

$$f = -C_f \varrho |\vec{V}| \vec{V} \tag{2.4}$$

where V is the instantaneous fluid velocity (oscillatory plus current) and $C_f = 0.01$ is a representative value. The last term in Eq. 2.3 is the unit net momentum imparted by horizontal turbulence (Reynolds stress). In solving Eq. 2.3. Longuet-Higgins (1970) chose $U_m \sim \alpha(gH)^{1/2}$ as the velocity scale, and thus the coefficient of turbulent diffusion K_{xy} is equal to $N\varrho\sqrt{gH}|x|$. Incorporating all his assumptions in the momentum equation yields finally

$$\frac{\partial}{\partial x}\left[N\varrho|x|g^{1/2}H^{3/2}\frac{dV}{dx}\right] - \frac{2}{\pi}\varrho\alpha C_f\sqrt{gH}V = -\frac{5}{4}\alpha^2\varrho(gH)^{3/2}S\frac{\sin\Theta_b}{\sqrt{gH_b}}. \tag{2.5}$$

Eq. 2.5 can be solved numerically and the solution is shown in Fig. 2.5 as a function of the parameter P measuring the relative importance of eddy diffusion to bottom friction.

Until quite recently the longshore currents described by using the above concept of radiation stresses were analysed merely in terms of either conservation laws for mass energy and momentum after wave breaking or empirical relationships. In the most common Putnam, Munk and Taylor's energy approach it was assumed that a portion s of breaker energy is balanced by bottom friction, from which is follows

$$V = \left[0.871\ g\frac{s}{f}\frac{m\,h_b^2}{T}\sin 2\Theta_b\right]^{1/3}. \tag{2.6}$$

An analogous expression for momentum conservation is

$$V = 1.305 \frac{m H_b \cos \Theta_b}{f T} \left[\sqrt{1 + \frac{c f t \operatorname{tg} \Theta_b}{0.65 m H_b}} - 1 \right]. \tag{2.7}$$

Shadrin (1972) extends the energy approach to three zones of gradual wave breaking. For the mass conservation Bruun (1963) arrived at

$$V = \sqrt{C'_f \frac{H_b^{3/2} \cdot m \cdot \sin 2\Theta_b}{T}} \tag{2.8.}$$

with C'_f as the Chezy coefficient C_f multiplied by 0.25 for laboratory and 0.13 for field conditions.

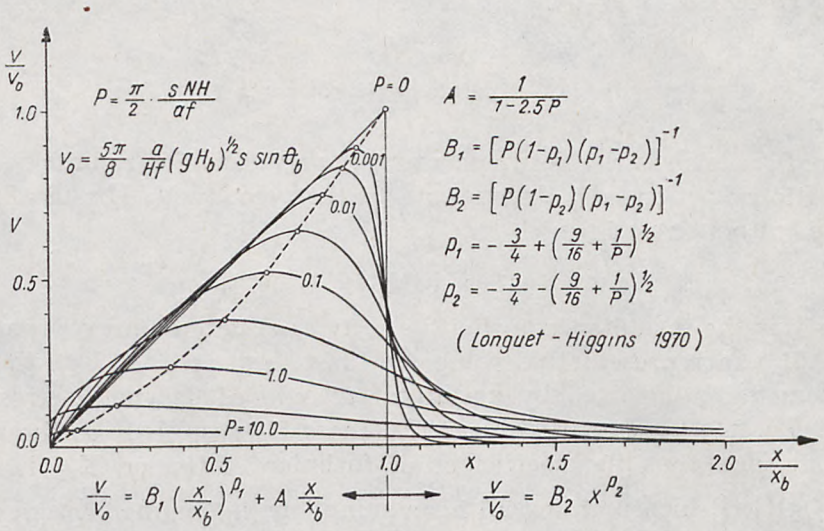

Fig. 2.5. Longshore currents after Longuet-Higgins (1970)
Rys. 2.5. Prądy wzdłużbrzegowe według Longuet-Higginsa (1970)

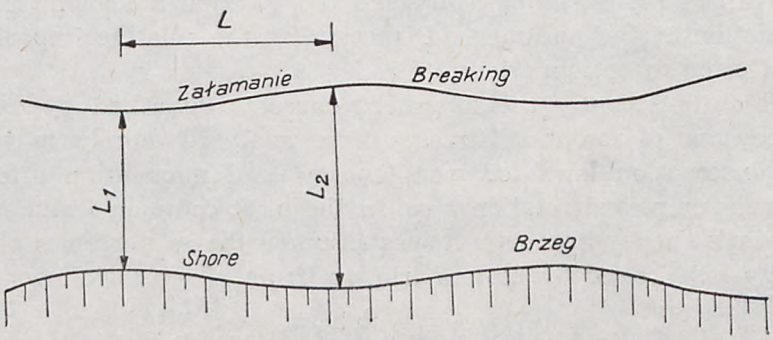

Fig. 2.6. Gradiential components of longshore currents. Notation
Rys. 2.6. Składowe gradientalne prądów wzdłużbrzegowych. Oznaczenia

Table 2.1

Day — Site	Field measurements: T s	h(h_b) cm	H cm	H_b cm	α_b o	Theoretical (cm s^{-1}): V_{gr} cm/s	V_{en} cm/s	V_{gr} (2.10)	V_{en} (2.8)	V_{en} (2.9)	P	V	V_{en} (L-H)
Sep 16'72 Lub	3.0	35	100	130	8.5	25		19	7	7	0.075	16	9
Sep 20'72 Lub	4.0	35	60	150	12.5	55		16	6	13	0.043	23	14
Sep 22'72 Lub	3.2	56	150	200	18	90		24	11	15	0.075	39	22
Feb 26'74 Ben	6.5	70	150	150	8	20		25					
Feb 27'74 Ben	7.0	100	150	200	10—15	20	50	31	20	93	0.20	183	74
Mar 1'74 Ben	4.7	60	150	150	0	35		27			0.25		
Mar 2'74 Ben	5.0	30	100	100	0	25		15			0.33		
Mar 7'74 Ben	7.0	150	200	250	0	40		43			0.17		
Mar 11'74 Ben	5.0	50	100	150	5—10	30	30	23	12	41	0.30	78	37
Mar 12'74 Ben	7.2	50	100	150	5—10	30	45	19	10	59	0.30	78	37
Mar 15'74 Ben	8.2	120	200	250	0	25		36			0.21		
Mar 17'74 Ben	8.0	75	150	200	8	25	50	24	13	69	0.27	92	37
Mar 18'74 Ben	5.5	30	100	100	0	20		14			0.33		
Sep 27'74 Lub	2.8	32	100	100	30	15	35	18	10	19	0.08	50	30
Oct 3'74 Lub	5.4	60	100	130	15	20	30	21	9	21	0.054	43	27
Oct 9'74 10 a.m.	3.0	29	100	100	20	12	35	16	7	15	0.075	31	18
Oct 9'74 1 p.m.	4.7	57	100	130	20	15	30	22	10	24	0.057	54	32
Oct 10'74 10 a.m.	4.3	71	100	150	8	25	15	26	9	9	0.050	25	15
Oct 10'74 1 p.m.	4.3	60	100	130	10	10	15	23	8	12	0.054	28	17
Oct 10'74 4 p.m.	3.7	50	100	130	25	20	40	22	11	22	0.065	55	32
Oct. 11'74 10 a.m.	3.8	58	100	130	20	20	40	25	12	19	0.056	54	32
Oct 11'74 1 p.m.	3.5	52	100	130	25	14	40	23	12	21	0.063	59	33
Oct. 13'74 Lub	3.0	52	100	130	30	15	35	25	10	20	0.063	70	39
Oct 16'74 Lub	2.7	39	100	130	20	0	12	21	10	14	0.083	35	19
Galvin —Eagleson, 1965									+	+			+
Shadrin, 1972						raw data		+	–				
Brebner — Kamphuis, 1963													+
Author: Mass transport;								(2.14) +	(2.13) +				

Notations: Ben — Benghazi, Lub — Lubiatowo, h— Lubiatowo, h_b — Benghazi
If not stated otherwise, measurements at 1:00 p.m.
$N = 0.008$, $C_f = 0.01$, $C_f' = 130$
Recommended use of Egs (30) and (32).
L-H = Longuet-Higgins, 1970

From other mass considerations Galvin and Eagleson (1965) found

$$V = K\, g\, m\, T \sin 2\Theta_b, \tag{2.9}$$

where $K = \dfrac{1 + \dfrac{H_b}{h_b} - \dfrac{a_i}{h_b}}{2(H_{b/h_b})^2}$.

Aside from energy currents there are other wave-induced components, primarily due to the three—dimensionality of waves and water level along the shore line, as already mentioned. Although the gradiental components of the first kind (variation of wave height along crests) are usually negligible for their local character, the others are still considerable and may be computed from the formula (Shadrin 1972)

$$V_g = \sqrt{1.11 \frac{h}{T} \sqrt{gh} \left(1 - \frac{L_1}{L_2}\right)} \tag{2.10}$$

with the notation as in Fig. 2.6.

The formulae presented above have been compared against the experimental data obtained from field measurements in Benghazi and Lubiatowo. From the comparison in Table 2.1 it is evident that the Longuet-Higgins formula fits best the empirical evidence for the energy currents, while Shadrin's (2.10) gives the closest approximation of the gradiental currents. The formulae derived by Bruun (2.8) and Galvin and Eagleson (2.9) are not satisfactory in the Author's opinion, although their authors claim they are correct within the range of their experiments.

Table 2.1 also indicates the validity of two other formulae for the mass-transport by waves. Until recently the most complete description of mass transport was given by the following formula of Longuet-Higgins (1953):

$$U = \frac{\pi^2 h^2}{4TL \sinh^2 kH} \left\{ 3 + 2\cosh\left[2kH\left(\frac{z}{H} - 1\right)\right] + \right.$$
$$+ kH \sinh 2kH \left[3\left(\frac{z}{H}\right)^2 - 4\left(\frac{z}{h}\right) + 1\right] +$$
$$\left. + 3\left[\frac{\sinh 2kH}{2kH} + \frac{3}{2}\right]\left[\left(\frac{z}{H}\right)^2 - 1\right]\right\}. \tag{2.11}$$

This formula does not take into account changes in the surface boundary loyer. This was accomplished by Huang (1970), who obtained

$$U = \frac{\pi^2 h^2}{4\, TL \sinh^2 kH} \left\{ 2\cosh\left[2kH\left(1 - \frac{z}{H}\right) - \frac{3}{2}\left[1 - \left(\frac{z}{H}\right)^2\right]\right.\right.\cdot$$
$$\left.\left. \cdot \frac{\sinh 2kH}{kH} + \frac{9}{2}\left(\frac{z}{H}\right)^2 - \frac{3}{2}\right\} \tag{2.12}$$

for pure water and

$$U = \frac{\pi^2 h^2}{4\,TL \sinh^2 kH}\left\{2\cosh\left[2kH\left(1-\frac{z}{H}\right)\right]+\left[9\left(\frac{z}{H}\right)^2-6\frac{z}{H}\right]+\right.$$
$$+3\left[\left(\frac{z}{H}\right)^2-4\left(\frac{z}{H}\right)+1\right]\cosh^2 kH+$$
$$\left.+\frac{6}{kH}\left[\left(\frac{z}{H}\right)^2-\left(\frac{z}{H}\right)\right]\sinh 2kH\right\} \tag{2.13}$$

for a contaminating surface film; Huang's solutions being much better for kH above 1.5.

Sleath (1972) has shown that some disagreement exists between the Longuet-Higgins theory and empirical data because of the order of approximation rather than turbulence as suggested at times. Sleath's second-order approximation for mass transport is

$$U = U_1 + \left(\frac{u_\infty k}{\delta}\right)^3 U_\infty \left[F_1(z) + AF_2(z) + A^2 F_3(z)\right] \tag{2.14}$$

with the functions F shown in Fig. 2.7.

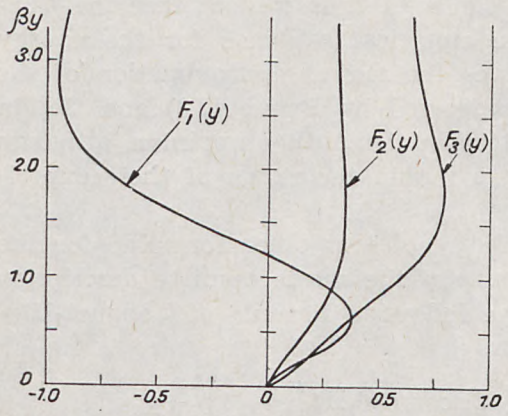

Fig. 2.7. F_1, F_2, and F_3 after Sleatch (1972)

Rys. 2.7. F_1, F_2 F_3 wg Sleatha (1972)

The Navier-Stokes equations make it possible to derive the fields of wind-driven currents in coastal zones, although complex boundary conditions introduce considerable difficulties. For uniform and weak bottom slopes the velocities are:

$$u = \frac{1}{K_z}\tau_x (H - z) + \sqrt{\frac{\tau_x}{\eta\varrho}}, \tag{2.15.1}$$

$$v = \frac{1}{4K_z}\tau_y\left(H - 4z + 3\cdot\frac{z^2}{H}\right) - \frac{1}{2}\sqrt{\frac{\tau_y}{\eta\varrho}}\left(1 - 3\frac{z^2}{H^2}\right), \tag{2.15.2}$$

$$w = -z\,\mathrm{tg}\beta\left[\frac{1}{4}\frac{\tau_y}{K_z}\left(1-\frac{z^2}{H}\right)+\sqrt{\frac{\tau_y}{\eta\varrho}}\cdot\frac{z^2}{H^2}\right], \tag{2.15.3}$$

where the tangential wind stresses have the components

$$\tau_x = \varkappa \varrho_a \vec{W} \vec{W}_x \simeq 3.0 \cdot 10^{-6} W^2 \sin \Theta,$$

$$\tau_x = \varkappa \varrho_a \vec{W} \vec{W}_y \simeq 3.0 \cdot 10^{-6} W^2 \cos \Theta.$$

Formulae (2.15) may serve as first approximations with an accuracy of 5% for $\operatorname{tg} \beta \leqslant 0.04$ and 10% for $0.04 \leqslant \operatorname{tg} \beta \leqslant 0.09$ (Shadrin, 1972).

More helpful in practical computations is the Bretschneider formula

$$\frac{u}{W} = \sqrt{\frac{k}{k^*} \sin \Theta} \tanh \left\{ \frac{Wt}{H} \sqrt{k\, k^* \sin \Theta} \right\} \tag{2.16.1}$$

with $k = 3 \cdot 10^{-6}$ and $k^* = 15\, n^2\, H^{-1/3}$ (Engl. sys.),
which for shallow water and longer times t yields

$$\frac{u}{W} = \sqrt{\frac{k}{k^*} \cdot \sin \Theta}. \tag{2.16.2}$$

The angle between wind and current depends on the wind-incidence angle Θ and reaches 40 to 45° for $\Theta = 25°$. Together with values of u/W for the Baltic conditions, it may be found in the work of Soskin (1962).

Moreover, an analysis performed by the Author has confirmed that the quotient u/W varies within rather narrow limits from fractions of a percent to about 3 percent, which in fact depend primarily on depth and Θ. For several cycles of the Author's data the values of u/W are shown in Fig. 2.8, whih can be used as a tool in fast computations.

Formulae (2.16) are averaged over surface layers. For the vertical profile of wind-driven currents Shemdin (1972) observed

$$\frac{u(z) - u(z_o)}{u_*} = \frac{1}{\varkappa} \ln \frac{z}{z_o} \tag{2.17}$$

in his laboratory experiments. An analogous distribution was observed by Bye (1967) in field measurements. Also, compare Hopkins (1974). The vertical variation is more complex in stratified media (Csanady 1972).

The z-axis in formula 2.17 oriented vertically upward from the actual bottom. This fact might bring about certain difficulties in our further mathematical considerations, where the z-axis starts an the bottom of the deep-water region and the origin of the system of co-ordinates is situated at shore line (cf. Fig. 3.9). Thus, it is appropriate to assume the power distribution of velocities in the vertical cross-section.

$$u(z) = u_{surf} \left(\frac{H_o}{z} \right)^n \tag{2.17.1}$$

with the exponent n chosen so as to approximate the logarithmic profile. This can be done with $n = 1/7$ at a depth of H_o and $n = 1$ at depth of

$H_{0/2}$ and smaller (the accuracy is better than 20 per cent for $z = 0.2H$ on the local depths $H = 1/4\ H_o$). Should merely one exponent n be chosen for all depth H from H_o to 0 in the problem of coastal turbulent diffusion, then $n = \frac{1}{3}$ to $\frac{1}{7}$ can be taken if the beach is steep and reaches $H_o =$ = const close to the shore line or $n = \frac{1}{2}$ if the solution is sought for gradually increasing depths from 0 to H_o and the region of constant depth is small.

An additional difficulty in correct compution of inshore currents is caused by their nonstationarity and heterogeneity. Temporal instability of wind and associated wave and current parameters may be neglected if

$$\frac{\partial W}{\partial t} \ll \frac{fW}{2}, \tag{2.18}$$

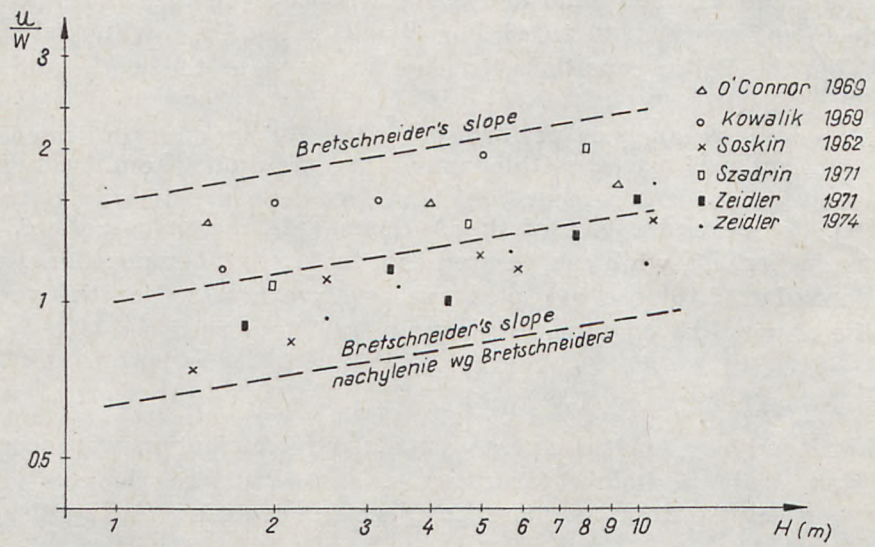

Fig. 2.8. Current-wind velocity ratio vs depth. Each value obtained from averaging more than 200 data taken every 3 seconds

Rys. 2.8. Zależność stosunku prędkości prądu i wiatru od głębokości. Każdą wartość uśredniono dla ponad 200 danych z 3-sekundowego próbkowania

which requires that a 6-m/s wind changes at a rate less than 10 m/s per hour (Pease 1972). Correlation analysis by Hupfer (1974) has shown that wind currents develop during 2 hours, while Zeidler (1971) found 6 hours. Short-term variation of coastal circulation constitutes an essential factor of "secondary" turbulence adding to the "primary" turbulence understood as fluctuations within regular and steady flow structures. This

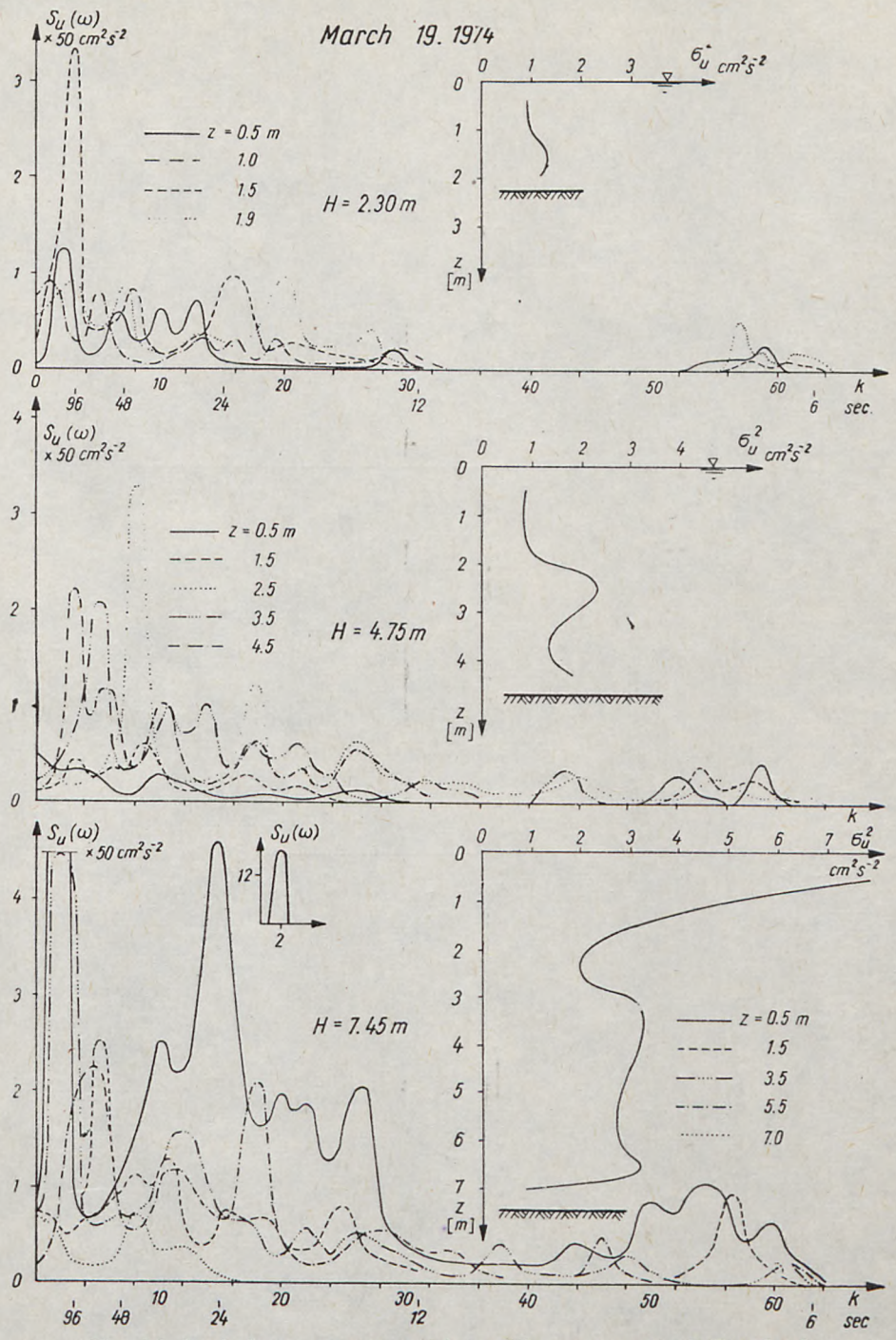

Fig. 2.9. Turbulence spectra and intensities measured off Benghazi

Rys. 2.9. Widma i intensywność turbulencji pomierzone w Benghazi

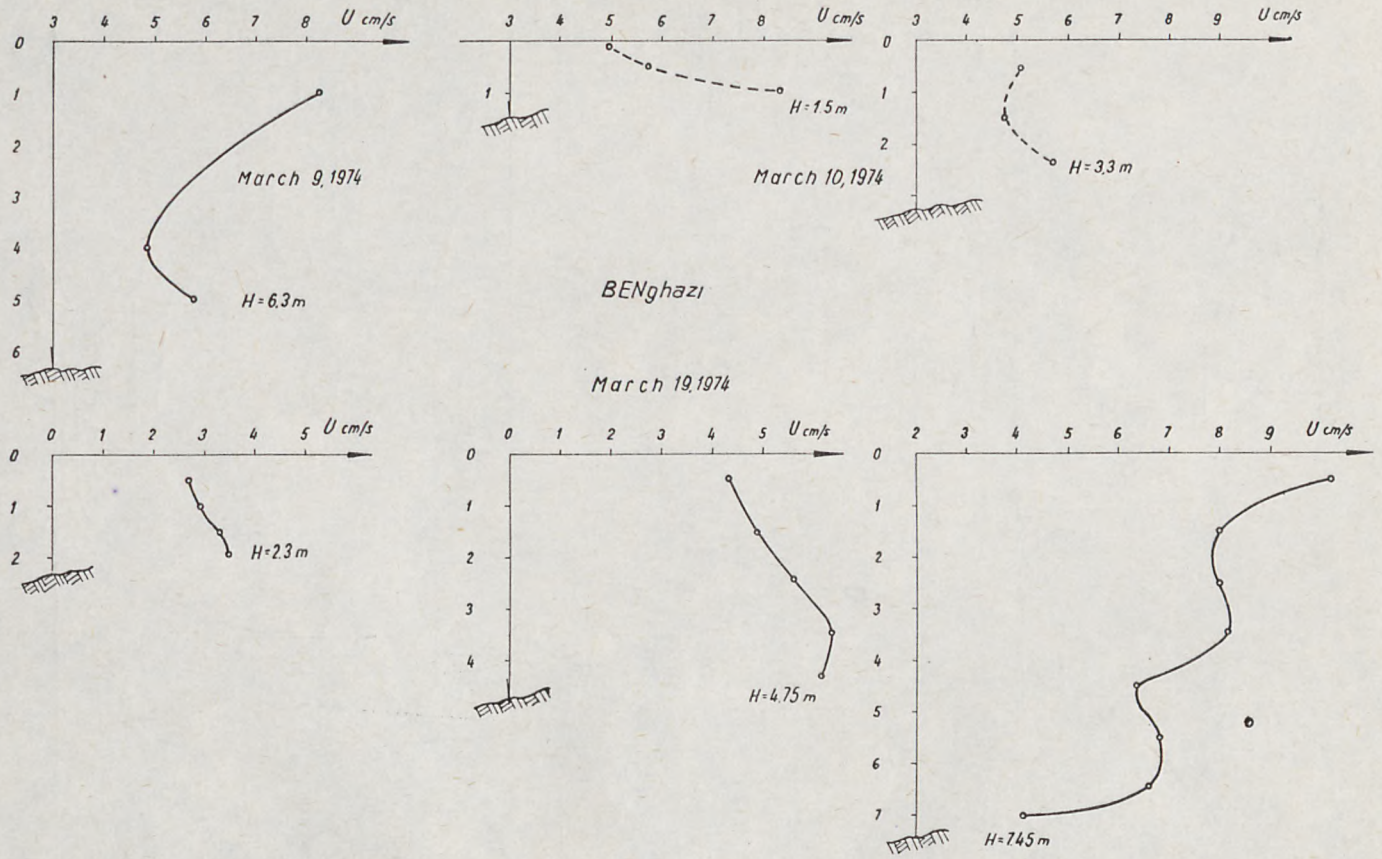

Fig. 2.10. Vertical profiles of water velocity
Rys. 2.10. Pionowe rozkłady prędkości wody

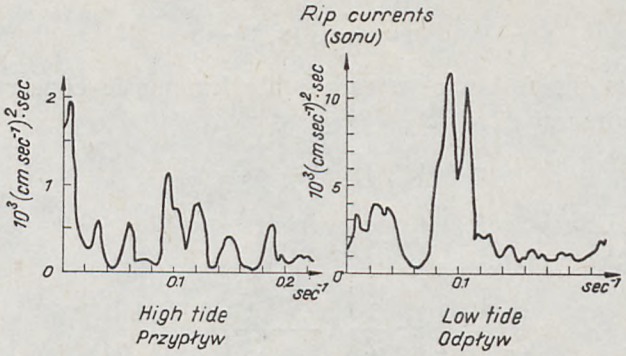

Fig. 2.11. Meso- and micro-scale turbulence spectra

Rys. 2.11. Widma turbulencji mezoskalnej i mikroskalowej

point is more fully analysed in Chapter 10, and hence two-dimensional spectra for currents are only outlined here whereas their impact on dispersion will be discussed later.

The spectra of inshore currents presented in Fig. 2.9 were measured by the Author for different wind and wave conditions, beach topography, depths and averaging scales. Although the data is modest, some general conclusions may be drawn on the spectral structure of the currents. The bandwidths remain rather unchanged with depth and the distance from the shoreline, but the peak of maximum energy moves towards higher frequencies at lower depths. The longer the averaging time, the smaller is the peak frequency. The spectra of wind-driven currents seem wider than those of wave-induced ones. Respective ranges of important spectra at different depths off Benghazi are shown in Fig. 2.9. Most energy is contained in the harmonics with periods of 6... 7, 25 and 50 (the time constant was 3 s). Maximum energies appear at the water surface and the lowest σ^2 are observed near mid-depths. This fact might imply the generation of turbulence at the beach bottom. Relative turbulence intensity may be found by comparing Fig. 2.9 with Fig. 2.10 (mean velocities); it varies from 20 to 30 per cent. — An analogous spectral diagram for rip currents after Sonu (1972) is presented in Fig. 2.11.

Since nonlinear wave-wave interaction can redistribute energy in the spectrum but, as far as the overall energy level is concerned, this weak interaction cannot compare with the effective exchange of energy between current and wave motions (Phillips, 1966) we shall confine our short discussion to the latter case.

For wave motion coupled with a current, the total frequency can be decomposed into the intrinsic frequency σ and the convective frequency, i.e.

$$n = \vec{k}\ U(\vec{x}, t) + \sigma. \tag{2.19}$$

This gives us the following steady-state kinematic conservation law for waves and currents

$$n = \vec{k}\,\vec{U}(\vec{x}, t) + \sigma = \sigma_o, \tag{2.20}$$

where the subscript refers to no current.

Phillips has shown:

$$\frac{c}{C_o} = \frac{1}{2} + \frac{1}{2}\left(1 + \frac{4U}{C_o}\right)^{1/2} = \left(\frac{k_o}{k}\right)^{1/2}. \tag{2,21}$$

Combining Eqs. (2.20) and (2.21) gives

$$gk = \frac{n^2}{\left[\frac{1}{2} + \frac{1}{2}\left(1 + \frac{4Un}{g}\right)^{1/2}\right]^2}, \tag{2.22}$$

which is a more general form of the dispersion relationship including the influence of currents. If we let the energy density of the waves under current be $\bar{\Phi}(n)\,dn$ then we have

$$\frac{1}{2}\,c_o^2\,\Phi(n)\,dn = \left(\frac{c}{2} + U\right) c\,\bar{\Phi}(n)\,dn. \tag{2.23}$$

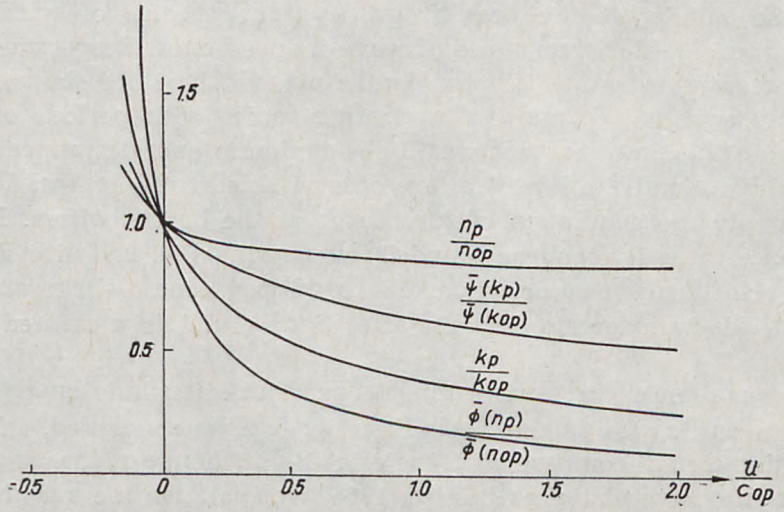

Fig. 2.12. Changes in peak location and magnitude for spectra under different current conditions (after Huang et al, 1972)

Rys. 2.12. Zmiany w położeniu i wielkości maksimum widm falowych dla różnych warunków prądowych (wg Huanga i in., 1972)

The ratio of respective spectra is

$$\frac{\bar{\Phi}(n)}{\Phi(n)} = \frac{4}{\left[1 + \left(1 + \frac{4\,Un}{g}\right)^{1/2}\right]\left[\left(1 + \frac{4\,Un}{g}\right)^{1/2} + \left(1 + \frac{4\,Un}{g}\right)\right]}. \tag{2.24}$$

From energy considerations we have

$$\bar{\Phi}(n)\,dn = \bar{\psi}(k)\,dk. \tag{2.25}$$

Fig. 2.12 plots the changes in the peak location and magnitude of the frequency and wave number spectra as a function of U/c_{op}, where C_{op} is the speed of the waves corresponding to peaks of the frequency or wave number spectrum under no current. From this diagram it appears that under wave-current interactions and for a given current velocity wave numbers decrease drastically with wave energy. This phenomenon may have serious implications to diffusion processes, as discussed in Chapter 3.

Two important mixing mechanisms are coupled with inshore currents. The first is associated with the breaking wave and its bore, which produce rapid mixing in an in-offshore direction, while the other is advective and is attributed to inshore circulation cells. For constant longshore discharge of water between cells Q_t, this process gives a concentration N_n in the nth cell down-current from a continuously injected source of dye of

$$N_n = N_o \left(\frac{Q_t}{Q_m}\right)^n \tag{2.26}$$

where N_o is the concentration leaving the injection cell and Q_m is the maximum longshore discharge within a cell. As an approximation (Inman et al., 1971), the concentration decreases exponentially with distance y from the injection point when n is replaced by y/Y, where Y is the spacing between rip currents.

In the close proximity of shore line (up to a few hundred meters off shore) velocities of longshore currents are proportional to $y^{1/7}$. This exponent results from the Author's diffusion tests and does not differ much from that obtained for wind-driven currents analyzed both theoretically and empirically. The distributions of wave-induced gradiential currents depend considerably on bottom and beach configuration, so that in practical computations one often has to assume their average constant value throughout the coastal zone. The exponents for wave-induced energy currents vary within wide intervals, their velocity ratio v/V_o being a power binomial. In practical computations, the curves v/V_o

in the surf zone can be splitted up into two branches with dominating factors of 1 and p_1 after Longuet-Higgins, respectively.

At greater distances from shore an exponent of 1/7 changes and shear profiles can be suggested with some reason.

Should simple power relationships be taken in the prediction of waste disposal, the proportionality factors of the power functions $v/V_o \sim (y/Y_o)^n$ can be found by using the formulae given for V_o for a certain characteristic distance off shore (say, $Y_o = 500$ m). Taking into account the vertical variations discussed formerly one has

$$u = u_{surf}\left(\frac{z}{H}\right)^n = \frac{u_{500}}{500^{1/7}}\, y^{1/7}\left(\frac{z}{H}\right)^{1\div 1/7} \tag{2.27}$$

This formula is employed in the theoretical analysis of turbulent diffusion (Chapter 3).

At the end of this chapter it is worthwhile mentioning that the above discussion holds generally for a fairly monotonous coastline with longshore currents which can deviate from the approximate beach-parallel direction only at a certain distance far off shore. At the outer boundary of the coastal zone there occurs a wide spectrum of external circulation components, which have to be computed by methods different from these presented here for inshore currents. Among them, wind-driven currents due to the motion of air masses over the whole Baltic are very characteristic for our conditions. The procedures presented by Polish authors, also in Oceanologia, are applicable in wind-driven current computations, including special configurations of coastline with embayments, islands, underwater troughs, etc.

Chapter 3

TURBULENT DIFFUSION PROCESSES IN COASTAL ZONES QUASI-DETERMINISTIC METHODS OF ANALYSIS

3.1. Quantitative discussion of turbulent diffusion phenomena

The energy of air motion is transferred to the water underneath as

$$\frac{\partial E}{\partial t} = \frac{1}{\varrho}\left(\tau_x \frac{\partial u}{\partial z} + \tau_y \frac{\partial v}{\partial z}\right) - \frac{g}{\varrho}\overline{w'\varrho'} - \frac{1}{\varrho}\frac{\partial Q}{\partial z} - \varepsilon, \tag{3.1}$$

where the first RHS term represents the energy contribution from the atmosphere due to the velocity gradient, the second is associated with

buoyancy, and the third depicts energy transfer through vertical pulsations.

In turn, the energy of mean water flow is also conveyed to turbulence. This is described by an analogous equation of turbulence energy

$$\frac{\partial E_t}{\partial t} + \frac{\partial}{\partial x_\alpha}\left(E_t \bar{u}_\alpha + \frac{1}{2}\varrho \overline{u'_\beta u'_\beta u'_\alpha} + \overline{p' u'_\alpha} - \overline{u_\beta \sigma'_{\alpha\beta}}\right) =$$

$$= \varrho \overline{u'_\alpha X'_\alpha} - \varrho \bar{\varepsilon}_t - \varrho \overline{u'_\alpha \cdot u'_\beta} \frac{\partial \bar{u}_\beta}{\partial x_\alpha} \qquad (3.2)$$

for a density—homogeneous medium, where $\varrho \bar{\varepsilon}_t$ represents the mean specific dissipation of the energy of turbulent pulsations due to viscosity. It is the last term at the right-hand side that reflects the transfer of energy between the mean flow and turbulence.

Once a flow regime has been established (in the statistical sense), large eddies form smaller ones, and so on up to complete dissipation through viscosity and heat. However, unlike idealized cases of flow in rivers, channels, pipes, etc., the motion of seas and lakes is characterized by more than one band of energy input (Fig. 3.1).

On the next pages we discuss the problems related to all aspects of a diversified oceanic turbulence field.

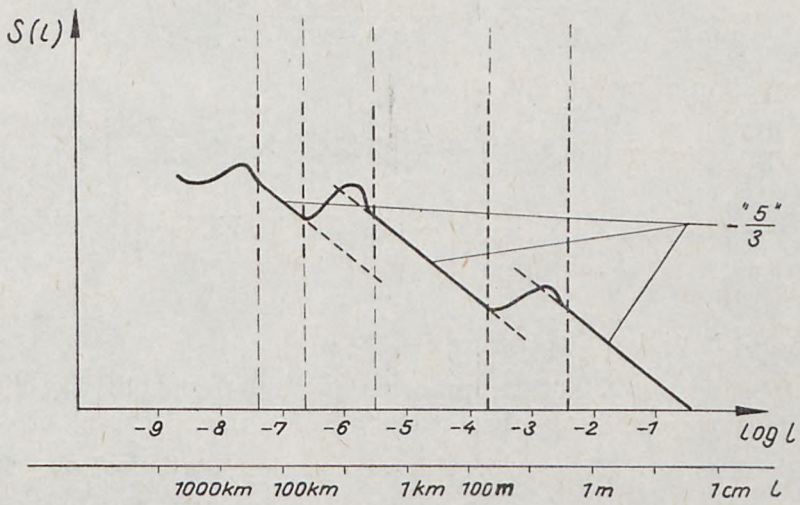

Fig. 3.1. Ozmidov's oceanic energy spectrum

Rys. 3.1. Widmo energii w oceanie wg Ozmidowa

As is well-known, the best description of a field of pollutants (or, in principle, of any physical quantity subject to turbulent flow) can be gained through the Lagrangian approach. For the sake of definition, let us consider a group of (fluid or solid matter) particles (Fig. 3.2). At

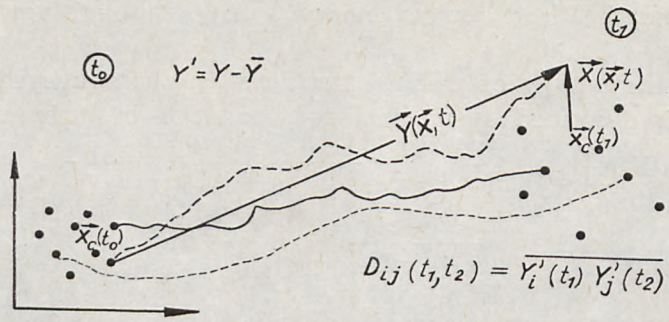

Fig. 3.2. Definition diagram for Lagrangian characteristics
Rys. 3.2. Schemat oznaczeń dla współrzędnych Lagrange'a

time t_0 the particles are at positions denoted by $\vec{x}$, while, in general, at any time t their places are designated by $\vec{X}(\vec{x}, t)$. The goal we strive for is as complete a description of the random vector $\vec{X}(\vec{x}, t)$ as possible in view of complex stochastic flow patterns. A closed system of equations for the dynamics of an incompressible viscid fluid in Lagrangian terms consists of the equation of continuity

$$[X_1, X_2, X_3] = \frac{\partial(X_1, X_2, X_3)}{\partial(x_1, x_2, x_3)} = 1 \tag{3.3}$$

and the equation of motion

$$\frac{\partial^2 X_i}{\partial t^2} = -\frac{1}{\varrho}[X_j, X_k, p] + \nu\left\{\left[X_2, X_3, \left[X_2, X_3, \frac{\partial X_i}{\partial t}\right]\right] + \right.$$
$$\left. + \left[X_3, X_1, \left[X_3, X_1, \frac{\partial X_i}{\partial t}\right]\right] + \left[X_1, X_2, \left[X_1, X_2, \frac{\partial X_i}{\partial t}\right]\right]\right\}, \tag{3.4}$$

where:

$i = 1, 2, 3$, p — pressure.

Since the vector $\vec{X}(\vec{x}, t)$ is random, it is reasonable to observe it through its probabilistic characteristics. The most general of these, probability density $p(\vec{X}|\vec{x}, t)$ provides a complete statistical description of $\vec{X}(\vec{x}, t)$. However, in most practical cases it is difficult to utilize the density $p(\vec{X}|\vec{x}, t)$ for the representation of turbulent diffusion (or, better, diffusive advection). This is due to high dimensionality of $p(\vec{X}|\vec{x}, t)$: it is $3n + m$ — dimensional for n particles considered at m times. Moreover, the complete knowledge of a turbulent field is warranted by the function $p(\vec{X}, \vec{V}|\vec{x}, t)$, which includes the Langrangian velocity V. There-

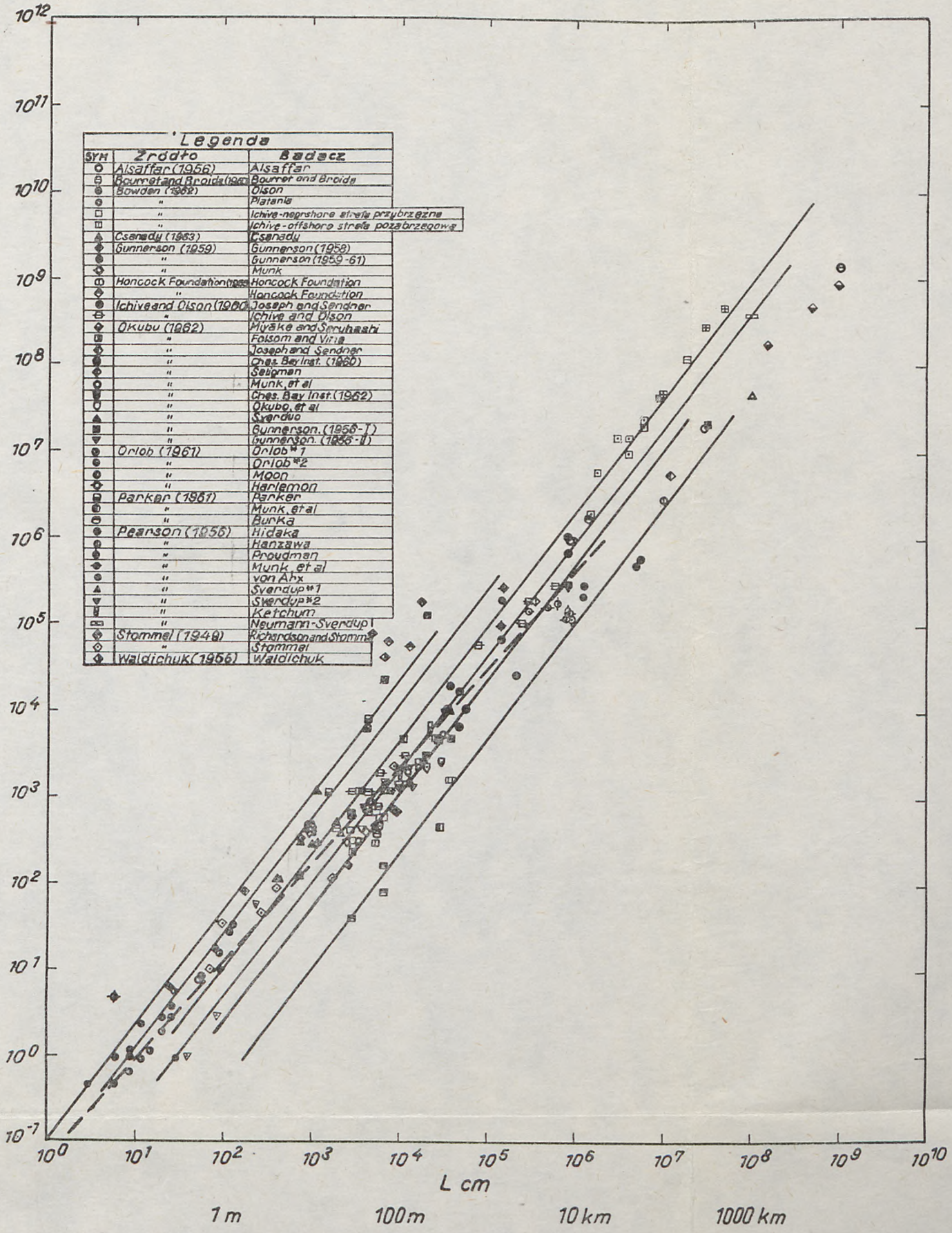

Fig. 3.3. Eddy viscosity, cm^2s^{-1}, vs turbulence scale

Ryc. 3.3. Zależność współczynnika dyfuzji, cm^2s^{-1}, od skali burzliwości

fore we often have to recourse to the first two statistical moments of the vector $\vec{X}(\vec{x}, t)$ $\left(\text{or } \vec{Y}(\vec{x}, t)\right)$, which we refer to on the following pages.

Let us turn to the point of our essential interest in this work. We denote by $\vartheta(\vec{X}, t)$ the concentration of a matter conveyed by a flow with the initial field of Eulerian velocity $\vec{u}_o(\vec{X}) = \vec{u}(\vec{x}, t_o)$. For homogeneous boundary conditions, the dependence of $\vartheta(\vec{X}, t)$ on $\vartheta_o(\vec{X}) = \vartheta(\vec{x}, t_o)$ is given by the equation

$$\vartheta(\vec{X},) = A\,[u_o(X),t]\,\vartheta_o(\vec{X}). \tag{3.5}$$

In most cases one is interested in mean values of $\vartheta(\vec{X}, t)$. Owing to linearity of the equation of matter conservation

$$\frac{\partial \vartheta}{\partial t} + \frac{\partial}{\partial X_i} u_i \vartheta = \chi \Delta u_i \tag{3.6}$$

and its boundary condition

$$\chi \frac{\partial \vartheta}{\partial n} + \beta \vartheta = f(t), \tag{3.7}$$

where:

χ is the coefficient of molecular diffusion,

n — straight line normal to the boundary, and

β — a constant that depends on the properties of the boundary;

for negligible molecular diffusion it can easily be proved that

$$\overline{\vartheta(\vec{X}, t)} = \overline{A}(t)\,\vartheta_o(\vec{X}) = \int p(\vec{X}|\vec{x}, t)\,\vartheta_o(\vec{x})\,d\vec{x}. \tag{3.8}$$

It is this equation that bears some prospects of determining a field of polluted water through the probability density $p(\vec{X}|\vec{x}, t)$ discussed above.

By neglecting the molecular diffusion in Eq. 3.6 and through classic introduction of mean and pulsational components ($\vartheta = \overline{\vartheta} + \vartheta'$, $u_i = \overline{u} + u_i'$ and subsequent averaging one obtains

$$\frac{\partial \overline{\vartheta}}{\partial t} + \frac{\partial \overline{u_i \vartheta}}{\partial X_\alpha} = -\frac{\partial S_i}{\partial X_i}. \tag{3.9}$$

At this point, the common semiempirical approach consists in assuming the proportionality

$$S_i = \overline{u_i' \vartheta'} = -K_{i_j} \frac{\partial \overline{\vartheta}}{\partial X_j} \tag{3.10}$$

in which the tensor of the coefficients of turbulent diffusion (eddy diffusivities) is, in general, time- and space-dependent.

Since some misconception exists as to the meaning of the coefficients of diffusion in quite a few studies carried out mainly with reference to pollution control problems, it is appropriate to provide some space for a discussion of $K_{ij}(\vec{X}, t)$.

Eq. 3.9 is satisfied by the probability density $p(\vec{X}|\vec{x}, t) = \vartheta(\vec{X}, t)$ for Gaussian distribution of $\vec{X}$ if the diffusion coefficients are

$$K_{ij} = \frac{1}{2}\frac{d\, D_{ij}(t - t_o)}{dt} = \frac{1}{2}\int_o^{t-t_o} \left[B_{ij}^{(L)}(\tau) + B_{ji}^{(L)}(\tau)\right] d\tau \qquad (3.11)$$

with $B_{ij}^{(L)}(\tau) = \overline{v_i'(t)\, v_j'(t+\tau)}$; Batchelor (1949).

This is, however, a case of little practical importance, since the Gaussian distribution of $\vartheta(\vec{X}, t)$ is known á priori.

On the other hand, Kolmogorov (1933) proved that provided some general conditiins are satisfied for $p(\vec{X}|\vec{x}, t)$, which guarantees that the Markov function $\vec{X}(t)$ is continuous, the derivatives

$$\overline{\vec{V}(\vec{x}, t_o)} = \left[\frac{\partial}{\partial t}\overline{\vec{Y}(\vec{x}, t)}\right]_{t=to} \qquad (3.12)$$

$$2\, K_{ij}(\vec{x}, t_o) = \left[\frac{\partial}{\partial t}\overline{Y'(\vec{x}, t)\, Y_j'(\vec{x}, t)}\right]_{t=to} \qquad (3.13)$$

exist and satisfy Eq. 3.9 with

$$V_i - \frac{\partial K_{ij}}{\partial X_j} = \overline{u_i} \qquad (3.14)$$

This does not imply, however, the validity of $K_{ij} = \frac{1}{2}\frac{D_{ij}(\tau)}{\partial \tau}$ for all kinds of turbulent fields; such a definition of K_{ij} is true only for turbulent fluctuations, as shown by Eq. 3.13. In fact, for the field

$$V_1(t) = \Gamma X_3(t) + V'(t); \quad V_2(t) = V_2'(t); \; V_3(t) = V'_3(t) \qquad (3.15)$$

one readily obtains (for longer times τ)

$$D_{11}(\tau) = \frac{2}{3}\Gamma^2 \overline{u_3'^2}\, T_3 \cdot \tau^3, \qquad D_{13}(\tau) = \Gamma \overline{u_3'^2}\, T_3 \cdot \tau^2, \qquad (3.16)$$

which shows the diffusion acceleration effect due to the vertical gradient Γ. Attributing overall $D_{ij}(\tau)$ to turbulent fluctuations and implying $K_{ij} =$

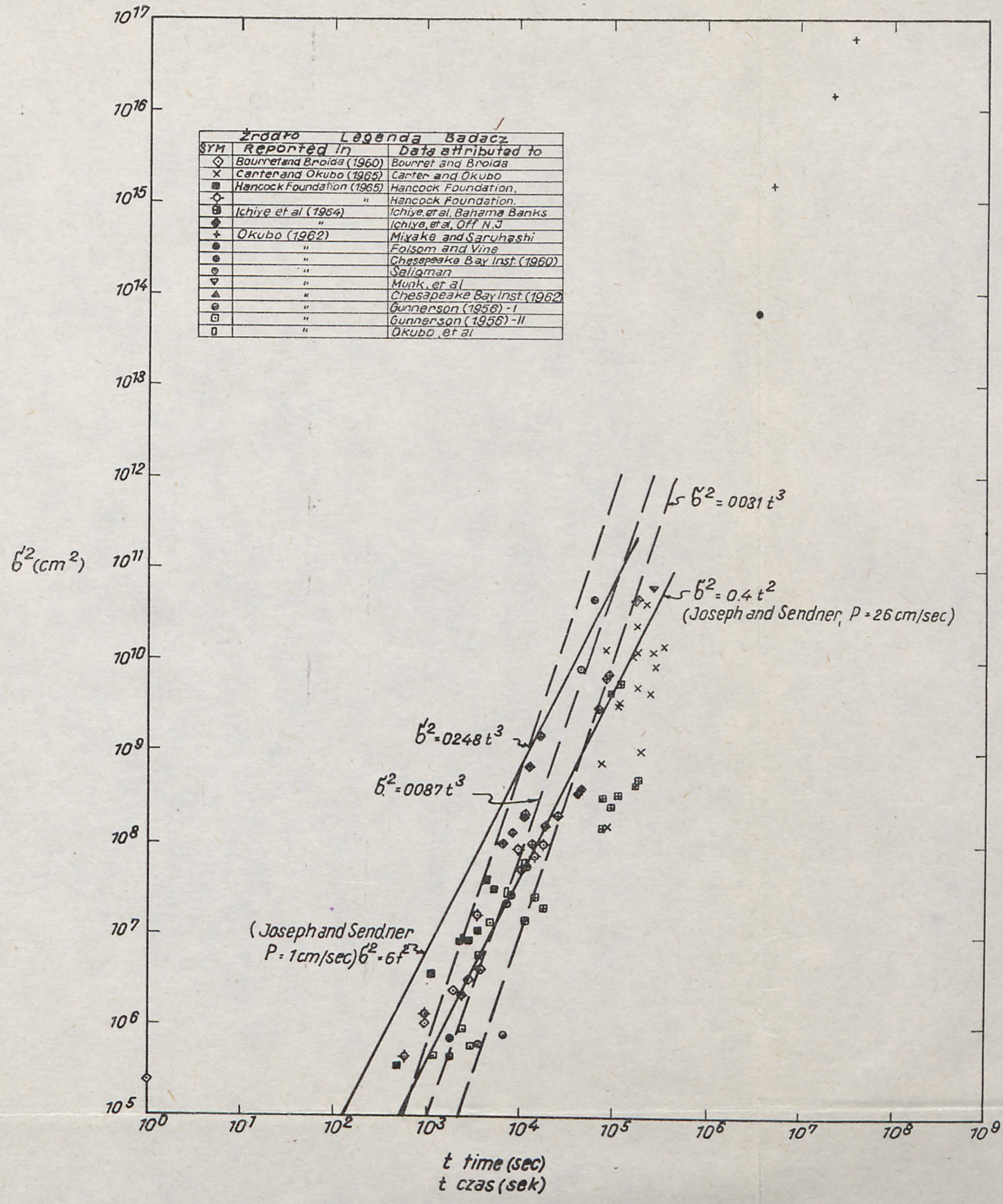

Fig. 3.4. Variance variation with time $\sigma^2(t)$

Ryc. 3.4. Czasowa zmienność wariancji $\sigma^2(t)$

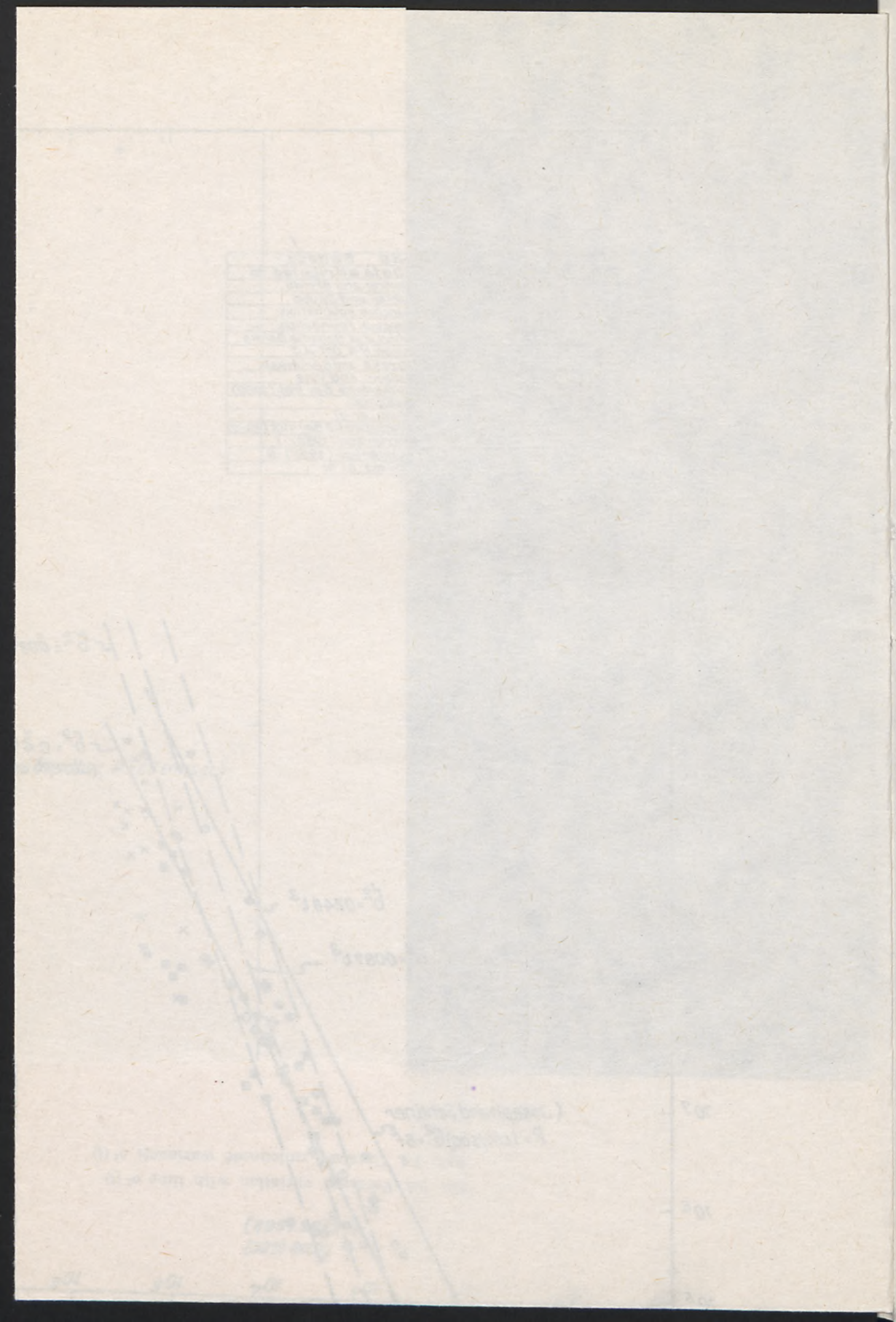

$\frac{1}{2}\frac{\partial}{\partial t} D_{ij}(\tau)$ would be quite erroneous. For deeper insight into the tensor K_{ij} refer to Kamenkovich (1967).

Another point at which theoretical results are too hastily applied to the interpretation of empirical findings, concentrates around the so-called 4/3 — law. For the isotropic turbulence it can be readily shown from the dimensional analysis (bolstered by physical considerations as to validity of some factors and negligence of others) that the dispersion tensor $D_{ii}(\tau)$ is proportional to the third power of time τ, which yields

$$K_{ii}(\tau) = \frac{1}{2}\frac{\partial D_{ii}(\tau)}{\partial(\tau)} \sim \tau^2 \sim D_{ii}^{2/3} \sim l^{4/3} \tag{3.17}$$

or $K(l) = c \cdot \varepsilon^{1/3} \cdot l^{4/3}$.

where l is regarded as a characteristic eddy length parameter (e.g. $\sqrt{D_{ii}}$). As was mentioned earlier, hardly ever is turbulence isotropic or even homogeneous in the marine environment (or particularly in coastal zones). Nonetheless, one can often encounter, especially in less recent

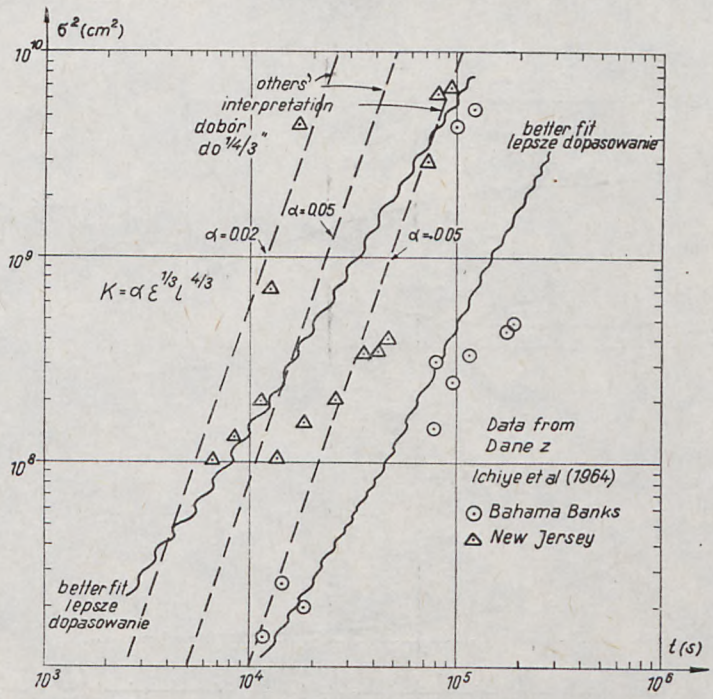

Fig. 3.5. Matching of data for the 4/3 law after Ichiye et al. (1964)

Rys. 3.5. Dopasowanie danych pomiarowych do prawa 4/3 wg danych Ichiye i in. (1964)

works, attempts to represent the coefficient K_{ij} in terms of the 4/3 law. This statement can be illustrated by the summary made by Yudelson (1967).

The data collected in Fig. 3.3 is approximated by six straight lines, each of the 4/3 slope. However, it is felt that 4/3 bands are fairly narrow. This can also be concluded on careful examination of respective sets of data from various authors. The results in Fig. 3.4 should be better represented by the second power of time instead of the third power, as is sometimes aimed at (or $K \sim \tau \sim \sqrt{D} \sim l$ instead of $K \sim l^{4/3}$). Finally, the data from Ichiye et al. (1964) also show a tendency to smaller exponents, in spite of the bias of some authors to conform to the "4/3" law (Fig. 3.5).

As has been pointed out earlier (see Fig. 3.1), the external energy penetrates a turbulent medium within specific frequency bands and one cannot preclude the validity of the 4/3 law (or 5/3 for energy) between these bands. This is essentially what Ozmidov claims on the basis of field findings.

The hypothesis on the partial applicability of the "4/3" law seems quite acceptable for a deep sea. It is however much more controversial

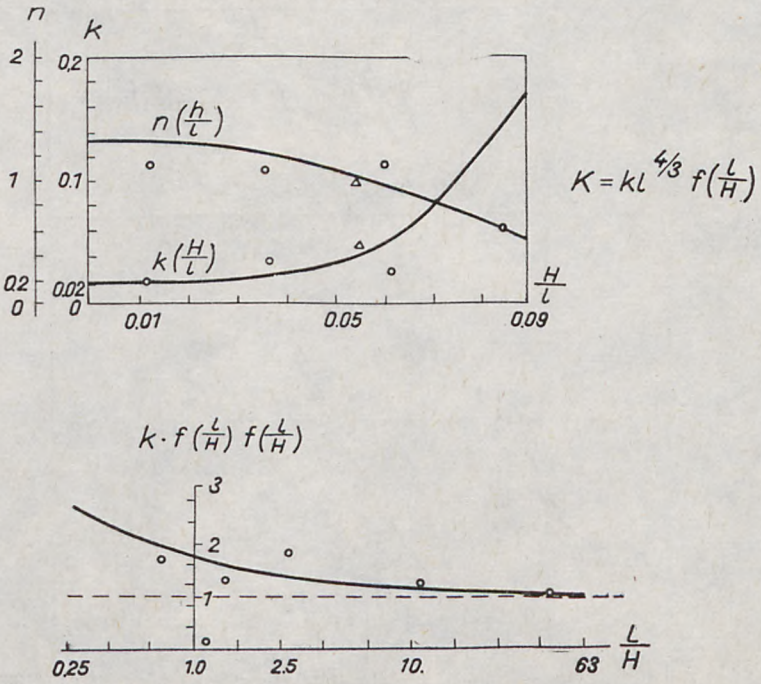

Fig. 3.6. Ozmidov's correction to the 4/3 law

Rys. 3.6. Poprawka Ozmidova do prawa 4/3

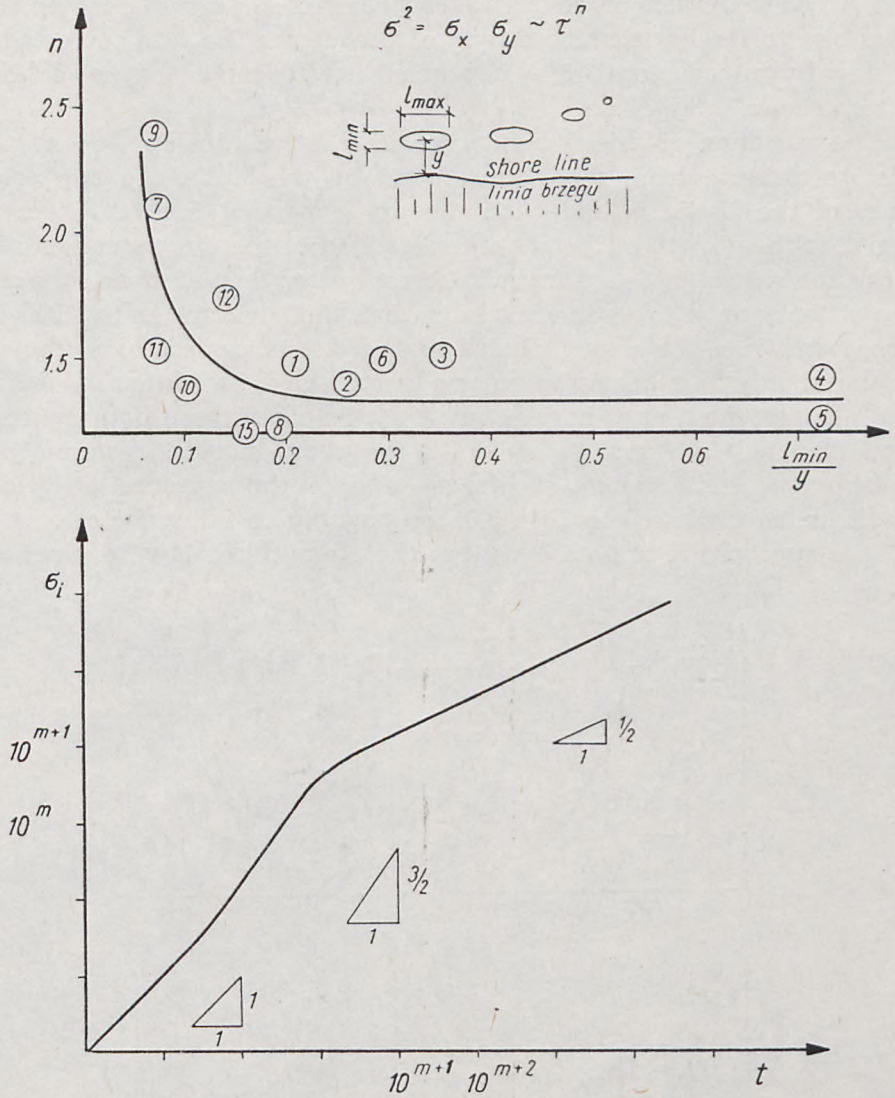

Fig. 3.7. The effect of shore on the temporal growth of dispersion (upper section) and the temporal variation of dispersion for homogeneous turbulence (lower section)

Rys. 3.7. Wpływ brzegu na wzrost rozproszenia w czasie (górna część) i czasowa zmienność wariancji w polu turbulencji jednorodnej (dolna część)

with regard to shallow water areas, where a great number of complications enter the problem. Nevertheless, (Ozmidov 1961—1970) found that a redistribution of eddies takes place in shallow waters and this gives rise to the horizontal isotropy of turbulence. He also corrected the 4/3 law by introducing l/H — dependent coefficient k and power factor n, both shown in Fig. 3.6.

The variation of the exponent n in the relatinship $D \sim \tau^n$ with relative distance from shore line, found by the Author in two coastal zones of the Baltic, is shown in the upper part of Fig. 3.7. It can be seen that the growth of turbulent eddies (and of the dye patches studied) with time is subejct to a dramatic decrease after they approach the shore at a distance only a few times greater than their lengths and widths l_{min}. The quantity of the data included in Fig. 3.7 is moderate, as they are employed only to indicate the general trend. Since the Author's remaining data are presented elsewhere, is must not be stated here if the phenomenon depicted in Fig. 3.7 is due to the shore-induced rearrangement of turbulent eddies alone or also — due to the presence of velocity gradients, as discussed in Par. 3.3., or possibly to other factors.

It is appropriate to note here that the „four-thirds law" is character-

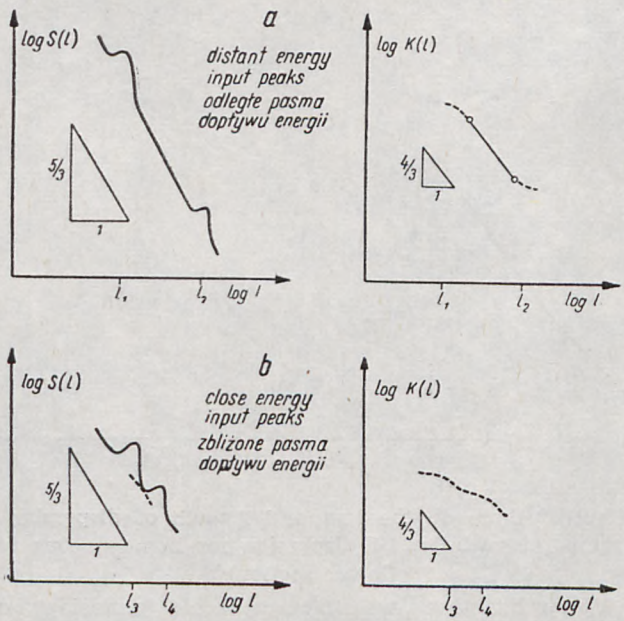

Fig. 3.8. Turbulence characteristics in the inertical subrange between two spectral peakes of energy imput

Rys. 3.8. Charakterystki turbulencji w podrozdziale bezwładnościowym między dwoma pasmami dopływu energii

istic for homogeneous turbulence, but only within the so-called inertial subrange (depicted by the central branch in the lower diagram in Fig. 3.7), that is, for intermediate diffusion times. Both for longer times of diffusion and for shorter temporal intervals, the dependence of K on turbulence scales (or diffusion time) is weaker. However, even in the inertial subrange the occurence of the „four-thirds law" can be disturbed if two energy inputs (of. Fig. 3.1) lie close to each other, so that the ipertial subrange between them is strongly affected by the input bands (Fig. 3.8). In the coastal zone, it is likely that two close frequency bands recive energy from two external sources of turbulence energy: waves and the „morphological" interaction between flowing water and the sea bed. The „morphological" Langmuir-type circulation cells might be coupled with local depths. With inreasing distance from shore the depth increases and the wave number (frequency) of the morphological circulation decreases, thus expanding the interval between both bands of energy input, sometimes making it wide enough for the „four-thirds law" to reappear.

3.2. Theoretical solutions to the equation of turbulent diffusive advection

The most common and reasonable approach to the mathematical formulation of the coastal pollution problem consists in analysing jet-like structures of spreading pollutants in terms of conservation laws. From such an approach one has the following well-known convective diffusion equation for any matter not affecting a flow field:

$$\frac{\partial \bar{\vartheta}}{\partial t} + u_i \frac{\partial \bar{\vartheta}}{\partial x_i} - w \frac{\partial \bar{\vartheta}}{\partial z} + \alpha \bar{\vartheta} = \frac{\partial}{\partial x_i} K_{ij} \frac{\partial \bar{\vartheta}}{\partial x_j}, \tag{3.18}$$

which follows from Eq. 3.9 upon assumption of the independence of u_i and ϑ together with constant velocity u_i along X_i. Equation 3.18 also includes substance decay in accordance with a first order reaction (its half-life being $T_o = \frac{\ln 2}{\alpha}$) and gravitational fall with a setling velocity of w.

A fairly general boundary condition desribing all practical cases at any wall (normal to n)

$$K_\eta \frac{\partial \bar{\vartheta}}{\partial n} + w_n \vartheta = \beta \vartheta \tag{3.19}$$

where β is a certain constant having the dimension of velocity; $\beta = 0$ corresponds to the complete "reflection" of a matter from the wall (and

$\frac{\partial \bar{\vartheta}}{\partial z} = \frac{\partial \bar{\vartheta}}{\partial n} = 0$ for $\mathcal{W} = 0$), while $\beta = \infty$ pertains to absorption. Details for this are included in the works of Calder (1961) and Monin (1959). In general, $\mathcal{W}$ may be substituted by f (x_i) due to secondary bottom deposits. Identical balance of turbulent fluxes must take place at the free surface, while the conditions of disappearance must be satisfied far from a source of substances, $X_i \to \infty$.

As to initial conditions, they may be of continuous or discontinuous type. In the first case a source starts flowing at $t = 0$, and then the concentration is equal to zero. The delta function is often employed for the discontinuous type of source, when a certain amount of matter is suddenly discharged.

Let us illustrate the instantaneous discharge in the framework of a general method derived by Aitsam (1967) for the solution of Eq. 3.18. Here the initial condition is

$$\bar{\vartheta}(x, y, z, 0) = G_o \, \delta(x) \, \delta(y) \, \delta(z - z_1), \tag{3.20}$$

where G_o is the source strength.

Let us denote by $\bar{\vartheta}_{ou}(x, y, z, z_1)$ a solution to Eq. 3.18 for $K = 0$ and homogeneous boudary conditions at the bottom. A solution for inhomogeneous boundary conditions can be written as

$$\bar{\vartheta}_u = \bar{\vartheta}_{uo} + \frac{1}{G_o} \int_{-\infty}^{+\infty} \int f(x - x', y - y') \, \bar{\vartheta}_{uo}(x', y', z, H) \, dx' \, dy' \tag{3,21}$$

For the homogeneous boundary conditions, the initial conditions as

$$f(x, y, z, 0) \Rightarrow f(x) \, f(y) \, f(z) \tag{3.22}$$

and diffusion coefficients

$$K_x = K_x(x), \quad K_y = K_y(y), \quad K_z = K_z(z) \tag{3.23}$$

the solution of Eq. 3.18 may be presented as

$$\bar{\vartheta}_u(x, y, z, t) = \frac{1}{G_o} \, \bar{\vartheta}_u(x) \, \bar{\vartheta}_y(y) \, \bar{\vartheta}_z(z), \tag{3.24}$$

where $\bar{\vartheta}_u(x)$, $\bar{\vartheta}_u(y)$, $\bar{\vartheta}_u(z)$ are the respective solutions to the following equations

$$\frac{\partial \bar{\vartheta}}{\partial t} + \bar{u} \frac{\partial \bar{\vartheta}}{\partial x} = \frac{\partial}{\partial x}\left(K_x \frac{\partial \bar{\vartheta}}{\partial x}\right) \tag{3.25.1}$$

$$\frac{\partial \bar{\vartheta}}{\partial t} = \frac{\partial}{\partial y}\left(K_y \frac{\partial \bar{\vartheta}}{\partial y}\right) \tag{3.25.2}$$

$$\frac{\partial \bar{\vartheta}}{\partial t} = \frac{\partial}{\partial z}\left(K_z \frac{\partial \bar{\vartheta}}{\partial z}\right), \tag{3.25.3}$$

with the initial conditions

$$\bar{\vartheta}(x, 0) = G_o \delta(x) \tag{3.26.1}$$

$$\bar{\vartheta}(y, 0) = G_o \delta(y) \tag{3.26.2}$$

$$\bar{\vartheta}(z, 0) = G_o \delta(z - z_1) \tag{3.26.3}$$

boundary conditions (3.18) and (3.21).

The one-dimensional problems (3.26) can be solved by integral transforms. Applying the Laplace transformation to Eq. 3.25.1 yields

$$\frac{\partial}{\partial x}\left[K_x \frac{\partial \bar{\vartheta}_L}{\partial x}\right] - u \frac{\partial \bar{\vartheta}_L}{\partial x} - p\,\bar{\vartheta}_L = \delta(x)\, G_o \tag{3.27}$$

with $\bar{\vartheta}_L(x, p)$ as the Laplace transform of $\bar{\vartheta}$.
A solution to Eq. 3.27 with the boundary condition

$$x \to \infty \qquad \bar{\vartheta}_L \to 0$$

may be further sought without the right-hand side member, and subsequently the inhomogeneous solution of Eq. 3.27 can be obtained by the variation of constants in the homogeneous solution.

Classical methods of the theory of partial differential equations may be used together with the above method in finding partial solutions for coastal pollution problems. We shall examine some of them separately for instantaneous (I) and continuous (C) sources, both point (P), line (L), and plane (Pl).

Instantaneous sources

(IP) For u, K_x, K_y, $K_z \equiv$ const in an infinite medium:

$$\vartheta = \frac{G_o}{\varrho\,(4\pi t)^{3/2}\sqrt{K_x K_y K_z}} \exp\left\{-\frac{[(x - x_1) - ut]^2}{4 K_x t} - \frac{(y - y_1)^2}{4 K_y t} - \right.$$
$$\left. - \frac{(z - z_1)^2}{4 K_z t} - \alpha t\right\} \tag{3.28}$$

(IL) For u, K_x, K_j, K_z = const in an infinite medium:

$$\vartheta = \frac{G_o}{4\pi\varrho\sqrt{K_x K_y t}} \exp\left(-\left\{\frac{[(x - x_1) - ut]^2}{4 K_x t} + \frac{(y - y_1)^2}{4 K_y t} + Kt\right\}\right) \tag{3.29}$$

where G_o' is a unit strength of the source.

(IPl) For u, K_x, K_y, K_z = const in an infinite medium:

$$\vartheta = \frac{G_o}{\varrho\sqrt{4\pi K_x t}} \exp\left(-\left\{\frac{[(x - x_1) - ut]^2}{4 K_x t} \alpha t\right\}\right) \tag{3.30}$$

As it is rather impossible to derive (I) solutions for more complex velocity and diffusion coefficient fields, efforts have been made to determine at least some characteristics of pollution fields. One method consists in substituting Eq. 3.12 by an infinite set of equations for statistical moments

$$\Theta_{nm}(z, t) = \int_{-\infty}^{+\infty} \int \bar{\vartheta}(x, y, z, t)\, x^n y^m \, dxdy \tag{3.31}$$

which can be consecutively solved for the individual moments Θ_{00}, Θ_{01}, Θ_{10} etc. (the first moments up to $n = 2$, $m = 2$ being of primary practical importance) and reduces the problem to the diffusion along the z-axis alone, subsequently supplemented by estimates for horizontal diffusion. For $n=0$ $m=0$ one has

$$\frac{\partial \Theta_{00}}{\partial t} = \frac{\partial}{\partial z}\left[K_z(z) \frac{\partial \Theta_{00}}{\partial z}\right] \tag{3.32}$$

with the boundary and initial conditions modified respectively.

Such a formulation is very helpful because the distribution over the planes $z = \text{const}$ does not depend anyhow on a velocity profile and the variation of diffusion coefficients. For

$$u(z) = u_1 z^m, \; K_x(z) = K_1 z^k, \; K_y(z) = K_2 z^l, \; K_z(z) = K_3 z^n$$

$$\text{and } 0 < n < 2$$

one obtains (Saffman 1962)

$$\begin{aligned} \langle X \rangle &= \frac{\Theta_{10}}{\Theta_{00}} = b\, u_1\, \tau\, (K_3 \tau)^{\frac{m}{2-n}} \quad \langle Y \rangle = \frac{\Theta_{01}}{\Theta_{00}}, \\ \sigma^2_{\vartheta x} &= \frac{\Theta_{20}}{\Theta_{00}} = b_1\, u_1^2\, \tau^2\, (K_3 \tau)^{\frac{2m}{2-n}} + b_2\, K_1\, \tau\, (K_3 \tau)^{\frac{k}{2-n}}, \\ \sigma^1_{\vartheta y} &= b_3\, K_2\, \tau\, (K_3 \tau)^{\frac{l}{2-n}}, \end{aligned} \tag{3.33}$$

where u_1, k_1, k_2, k_3, b, b_1, b_2, and b_3 are constants.

This solution proves again that the presense of z-shear always plays a dominant role in the dispersion along the x- and y- axes.

If considering radial diffusion only one may arrive at the following equation (Okubo 1962)

$$\frac{\partial \bar{\vartheta}}{\partial t} = \frac{1}{r} \frac{\partial}{\partial r}\left\{a\, f(t)\, r^{m+1} \frac{\partial \bar{\vartheta}}{\partial t}\right\}, \tag{3.34}$$

where r is the radial distance from the origin, a and m are arbitrary

constants, and f (t) is a function of time. Equation 3.34 incorporates a number of other diffusion equations derived for particular m and f (t), including that of Joseph and Sendner (f (t) = 1, m = 1). Under the following ditions (with averaging upper bars deleted henceforth)

$$\vartheta(r, 0) = \frac{M\delta(r)}{\pi r} \tag{3.35}$$

$$\lim_{r\to\infty} \vartheta(r, t) = 0 \qquad \text{for all } t \geqslant 0$$

$$\vartheta(r, t) = 0 \qquad \text{for } r < 0, \text{ all } t \geqslant 0$$

the solution for $0 \leqslant m < 2$ and $\Psi(t) = \int_0^t f(t_1)\, dt_1$ is given by

$$\vartheta(r, t) = \frac{(2-m)\, M}{2\pi (2-m)^{\frac{4}{2-m}} \Gamma\left(\frac{2}{2-m}\right) a^{\frac{2}{2-m}} \{\psi(t)\}^{\frac{2}{2-m}}} \exp\left[-\frac{r^{2-m}}{(2-m)^2 a \Psi(t)}\right] \tag{3.36}$$

Continuous sources

Fairly general concentration fields of substances flowing permanently out of their source at the point P (0, y_o, z_o) and moved by ambient water with a speed of u_x (y, z) and u_y (y, z) in a region of variable depth H (y) can be obtained by solving the equation

$$u_x \frac{\partial \vartheta}{\partial x} + u_y \frac{\partial \vartheta}{\partial y} = \frac{\partial}{\partial y} K_y \frac{\partial \vartheta}{\partial y} + \frac{\partial \vartheta}{\partial z} K_z \frac{\partial \vartheta}{\partial z} \tag{3.37}$$

with longitudinal advection prevailing over longitudinal diffusion. Solutions for line sources can be found from integration of solutions to (3.37). The Author managed to solve Eq. 3.37 in the system of co-ordinates shown in Fig. 3.9. On the basis of theoretical considerations, confirmed by empirical data, discussed briefly in this paper, the following distributions can be assumed as good approximations for velocities and eddy diffusivities:

$$u_x = u_{x_o}\, y^{\alpha_x}\, z^{n_x} \qquad u_y = u_{y_o}\, y^{\alpha_y}\, z^{n_y} \tag{3.37a}$$

$$K_y = k_y\, y^{\beta_y} \exp[-0.001\,(H_o - z)] \qquad K_z = k_z\, y^{\beta_z} \exp[-0.001\,(H_o - z)]$$

Together with Eq. 3.7, the boundary conditions should also take into account the disapperance of concentration at infinity and the matching of near field and far field (Fig. 3.9) created by a continuous source

$$\vartheta(x, y, z)\big|_{x,y\to\infty} = O$$

$$\vartheta(O, y_o, z_o) = \frac{Q}{S_o\, u(y_o, z_o)}\, \delta(y - y_o)\, \delta(z - z_o) \tag{3.37b}$$

A solution to Eq. 3.37 can be sought by the Fourier method as

$$\vartheta(x, y, z) = \vartheta_x(x) \cdot \vartheta_y(y) \cdot \vartheta_z(z) \tag{3.38}$$

After Eqs. 3.37 a ÷ c are included in Eq. 3.37 the latter becomes a system of three second-order differential equations.
There arises the problem of eigen-functions that can be found after the order of magnitude of individual terms in the component equations is estimated and some minor terms are rejected. A simple substitution of variables leads to solutions of Eq. 3.37 in the form of Bessel functions, e.g. for $\vartheta_y(y)$:

$$\vartheta_y(y) = A\, y^{\frac{\alpha+\varkappa}{\sigma}}\, \alpha^{-\frac{\alpha+\varkappa}{\sigma}}\, I_n(\beta\, y^{\frac{\gamma}{\sigma}}\, \alpha^{-\frac{\gamma}{\sigma}}) + B\, y^{\frac{\alpha+\varkappa}{\sigma}}\, \alpha^{-\frac{\alpha+\varkappa}{\sigma}}\, Y_n(\beta\, y^{\frac{\gamma}{\sigma}}\, \alpha^{-\frac{\gamma}{\sigma}}) \tag{3.39}$$

where a, α, β, γ, $\varkappa$, and σ are constants and exponents, which depend on the exponents in Eqs. 3.37 and 3.37.a., while A and B must be determined from the boundary conditions. The order n of the Bessel function I_n and Y_n also depends on these exponents.

After employing a rather arduous procedure one may find $\vartheta_x(x)$, $\vartheta_y(y)$, and $\vartheta_z(z)$, and come to the final solution, but this is troublesome and requires computer-aided techniques, since the resulting constants of integration must be found from implicit boundary conditions. The problem becomes much simpler, and the procedure outlined can be applied more successfully if one neglects u_y in Eqs. 3.37. and 3.37.a. and assumes

$$K_y = k_y \cdot y^{\beta_y} z^{n_x} \qquad K_z = k_z\, y^{\alpha_x}\, z^{n_z}\,. \tag{3.37c}$$

In this case one obtains

$$\vartheta(x, y, z) = A\, \frac{y^{\frac{1-\beta_y}{2}}}{x} \exp\left[-\frac{(y^{2+\alpha_x-\beta_y} + y_o^{2+\alpha_x-\beta_y})\, u_{x_o}}{(2+\alpha_x-\beta_y)^2\, k_y\, x}\right] \cdot$$

$$\cdot \left\{1 + B\, z^{\frac{1-n_z}{2}} \sum_{k=1}^{\infty} \frac{J_{-2}(\delta_k)}{J_{-n}} \left[\delta_k \left(\frac{z_o}{H}\right)^{\frac{2+n_x-n_z}{2}}\right] \exp(-q\, \delta_k^2\, x)\right\}. \tag{3.40}$$

$$\cdot I_{\frac{\beta_y-1}{2+\alpha_x-\beta_y}} \left(D\, \frac{y^{\frac{2+\alpha_x-\beta_y}{2}}}{x}\right),$$

where:

$$A = \frac{Q(n_x+1)}{(2+\alpha_x-\beta_y)\, k_y\, H^{n_x+1}} \cdot y_o^{\frac{1-\beta_y}{2}}\,; \quad B = \frac{1-n_z}{n(n_x+1)\, H^{1-n_z}} \cdot Z_o^{\frac{1-n_z}{2}}$$

$$D = \frac{2\, u_{x_o}}{k_y (2+\alpha_x-\beta_y)^2} \cdot y_o^{\frac{2+\alpha_x-\beta_y}{2}}\,; \quad n = \frac{1-n_z}{2+n_x-n_z}\,;$$

$$q = \frac{k_z (1 - n_z)^2}{4 n^2 u_{x_0} H^{2+n_k-n_z}} \quad ; \quad J_{-n+1}(\delta_k) = 0.$$

cf Goroshko, 1974, with his graphs in the lower part of Fig. 3.9).

The concentration profiles shown in Fig. 3.9 delineate a very special featur of concentration fields, also observed by the Author in certain coastal zones. It consists in the asymmetry of concentration profiles along the y-axis on both sides of the discharge point $P(0, y_o, z_o)$. The nearshore concentrations are higher than the offshore ones at the same distance from the source, as if the substance discharged were entrapped near shore. In the considered case of homogeneous density this effect can be attributed to velocities and eddy diffusivities increasing with dinstance from shore. A similar coastal entrapment phenomenon due to density effects was analyzed by Csanady (1969).

In the case of an infinite linear source streching along the y-axis the respective diffusional term in Eq. 3.37 (either first R.H.S. or second R.H.S) disappears and the solution with K_y (or K_z) of Eq. 3.37 and $n_x = 0$ (or $\alpha_x = 0$) becomes (assume now source along the z-axis):

$$\vartheta(x, y) = \frac{(\alpha_x - \beta_y + 2)\, q}{u_{x_0}\, \Gamma\left(\frac{\alpha_x + 1}{\alpha_x - \beta_y + 2}\right)} \left[\frac{u_{x_0}}{(\alpha_x - \beta_y + 2)^2 k_y x}\right]^{\frac{\alpha_x+1}{\alpha_x-\beta y+2}} \cdot \exp\left[-\frac{u_{x_0} y^{\alpha_x - \beta_y + 2}}{(\alpha_x - \beta_y + 2)^2 k_y x}\right] \tag{3.41}$$

for $\alpha_x - \beta_y + 2 > 0$,
where q = strength of the linear source.
A more genral solution for a source at $y = y_o$ is:

$$\vartheta(x, y) = \frac{Q \cdot (H \cdot y_o)^{\frac{1-\beta_y}{2}}}{(\alpha_x - \beta_y + 2) \cdot k_y \cdot x} \exp\left[\frac{-u_{x_0}(y^{\alpha x - \beta y + 2} + y_o{}^{\alpha x - \beta y + 2})}{(\alpha_x - \beta_y + 2)^2 \cdot k_y \cdot x}\right] \cdot \cdot I_p\left(\frac{2 u_{x_0} (Hy)^{\alpha x - \beta y + 2}}{(\alpha_x - \beta_y + 2)^2 \cdot k_y \cdot x}\right), \tag{3.42}$$

where I_p is the Bessel function of imaginary argument with the index

$$p = \frac{1 - \beta_y}{\alpha_x - \beta_y + 2}.$$

Solution for a line source of finite length can be obtained by integration of Eqs. 3.40., 3.41., and 3.42.

To end this paragraph it should be mentioned that, on the one hand, the solutions presented are of practical importance in the design of marine disposal of pollutants, and, on the other hand, they can be used as

tools to check the assumptions made for diffusion coefficients. Therefore Par. 3.2. precedes the description of horizontal and vertical diffusion in the following paragraphs.

3.3. Horizontal diffusion

Indirect determination of diffusion characteristics (primarily eddy diffusivities) from matching empirical data with the theoretical solutions presented in Par. 3.2. can be inaccurate, since different combinations of u and K can yield similar concentration fields. The measurement of Reynolds stresses and velocity gradients appearing in the classical definition

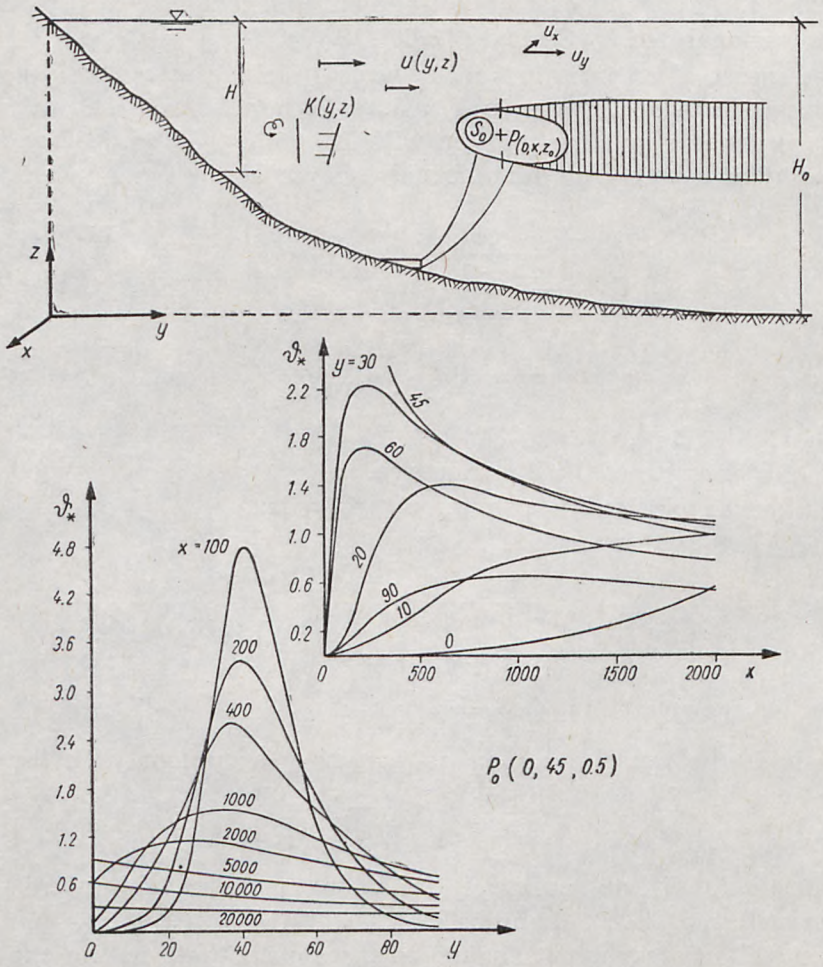

Fig. 3.9. Solutions 3.40 of the turbulent diffusion equation
Rys. 3.9. Rozwiązania 3.40 dla równania burzliwej dyfuzji

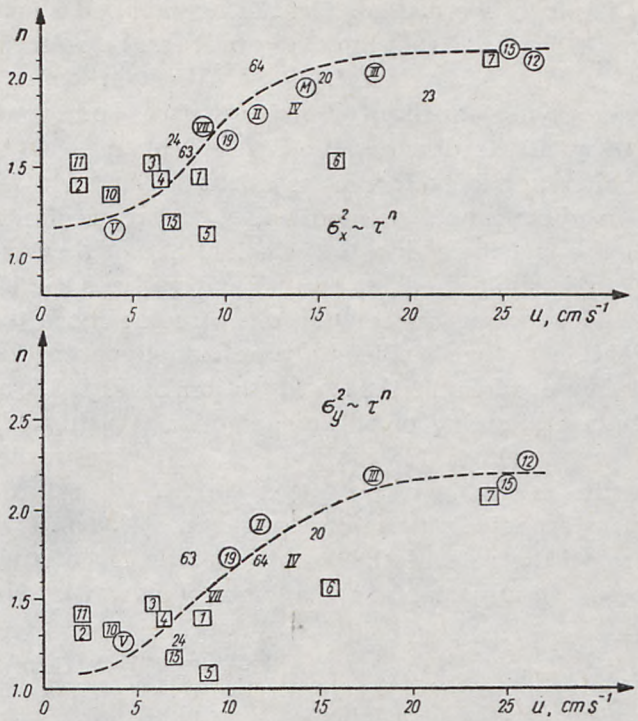

Fig. 3.10. The effect of velocity on the temporal growth of dispersion
Rys. 3.10. Wpływ prędkości na wzrost rozproszenia w czasie

$$\overline{u_i' u_j'} = K_{ij} \left(\frac{\partial \bar{u}_j}{\partial x_j} + \frac{\partial \bar{u}_i}{\partial x_i} \right), \tag{3.43}$$

or analogous correlations for heat, etc., makes it possible to find K_{ij} directly, without resorting to transitional assumptions. Within such direct-examination approach we will now discuss the data available on horizontal diffusion.

From a review of several field studies (cited in the List of References) made by the Author it follows that D_{ii} (where $i = 1,2$) varies with time (or length) as a power function with an exponent from 1 to 3 (cf Fig. 3.7), although figures higher than 2 are coupled with rough sea and occur far off shore. A couple fo factors are responsible for this variation: wind, currents, waves, thermal and density effects, bottom topography, etc.. The weight of each of them is difficult to establish because of their combined action. The regressional analysis has shown that current velocity is one of the essential factors.

Fig. 3.10 shows the variation of n_ϑ with current velocity. The tracers propagated with water in patches. Various techniques of investigation

described in Chapter 7 were used. The Author applied rhodamine B and droques shown in Fig. 7.7. From the diagram it can be seen that n increases with velocity and is characterized by a certain point of inflexion. While the lower asymptotic limit of n for density-homogeneous medium lies somewhere at 1, the upper value reached by n is slightly above 2. The transitional region of velocities is about 15 cm/s. However unclear from the purely dimensional point of view, variation of n_i is indicative of changes in the structure due to velocity. At higher velocities the rearrangement of turbulent eddies occurs, and perhaps some shear efects, difficult to avoid under natural conditions, become more pronounced. It should be mentioned that sufficient time and apparently homogeneus velocity fields were taken in the construction of Fig. 3.9 and 3.10, but until complete uderstanding of this phenomena is achieved, the figures should serve as quidelines for marine outfall design rather than as a basis for scientific debate.

In looking for a possible cause of changes in diffusion laws it is interesting to examine the role of the Eulerian intensity of turbulence. Let us briefly repeat two important results for the dispersion tensor:

$$D_{ii}(\tau) \approx \overline{2u_i'^2} \int_0^\infty (\tau - s)\, R_{ii}^{(L)}(s)\, ds \approx 2\,\overline{u'^2}\,(T_i\tau - S_i) \qquad (3.44)$$

(homogeneous turbulence)

or

$$D_{11}(\tau) \approx 2/3\,\Gamma^2 \cdot \overline{u_3'^2} \cdot T_3\,\tau^3 \qquad (3.44a)$$

for large τ in shear flow $V_1(t) = \Gamma \cdot X_3(t) + V'(t)$

These results suggest that irrespective of the type of flow the exponent of D_{ii} t vs n_i for a given flow remains unchanged in spite of turbulence intensity. This statement can be confirmed by field observations of plume widths. One such example is shown in Fig. 3.11, constructed from the data given by Kenney (1967). In can be seen that the plume

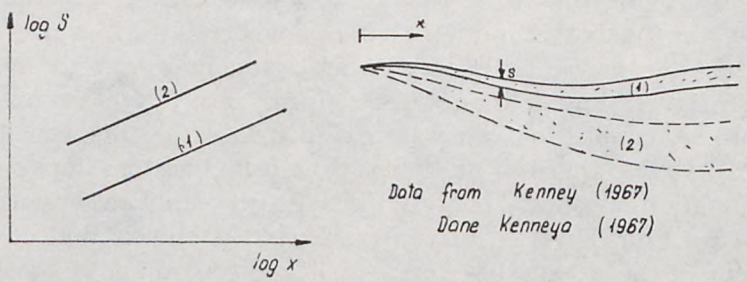

Fig. 3.11. Indepedence of the growth of jet width of the intensity of turbulence
Rys. 3.11. Niezależność wzrostu szerokości strugi od intensywności turbulencji

width increases with distance to an almost identical exponent. The two plumes developed from the same continuous source within a few hours.

Interesting observations of the dispersion very close to the shore line were carried out by the Author in a Bay of Puck area around the Gdynia mucicipal waste-water discharge channel. Since the Baltic Sea is very shallow within that region and the waste water was much lighter than the ambient medium, it is acceptable to assume the model of the linear vertical source. Coliform bacteria and rhodamine B were used as indicators of the concentration. The test layout and techniques applied are described in Chapter 7. Figures 3.12 and 3.13 show the data obtained for the longshore and transverse decay of concentration. Let us refer to the model described by Eq. 3.41. By comparing the exponent.

$$\frac{\alpha_x + 1}{\alpha_x - \beta_y + 2} = \frac{8}{9}$$

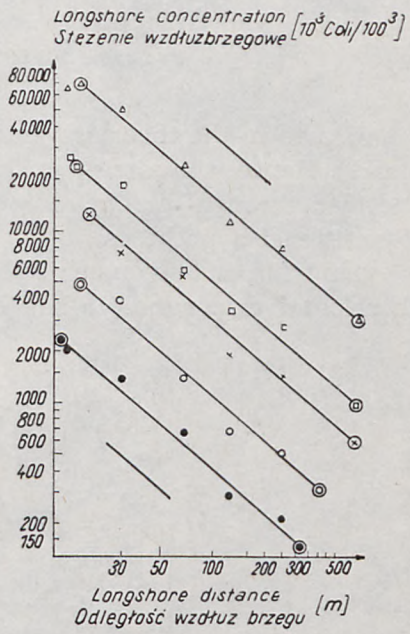

Fig. 3.12. Longshore concentration from a continuous point source on beach

Rys. 3.12. Wzdłużbrzegowe stężenie trasera zrzuconego z ciągłego punktowego źródła nabrzegowego

and the exponent

$$\alpha_x - \beta_y + 2 = \frac{9}{7}$$

one can easily find $\alpha_x = \frac{1}{7}$ and $\beta_y = \frac{6}{7}$, which gives a velocity field close to the logarithmic profile with $K_y(y) \sim {}^{6/7}$; such a current field is quite often encountered under field conditions of surf zones and is

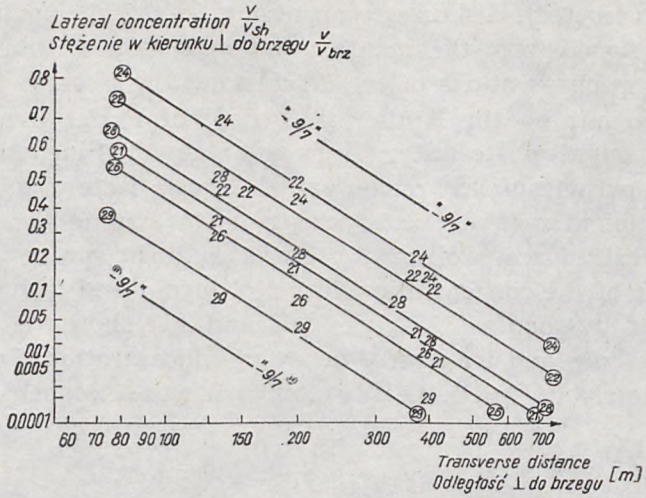

Fig. 3.13. Lateral variation of concentration from a continuous point source on beach
Rys. 3.13. Stężenie w kierunku ⊥ do brzegu

confirmed in the theories based on the concept of radiation stress (Chapter 2). Hence, the almost linear form od K_y (y) can be theated as being derived through direct reasoning and empirical evidence unobscured by transitional hypotheses.

Thus far, not too much light has been shed on the effect of waves on horizontal dispersion. It has been determined qualitatively that waves

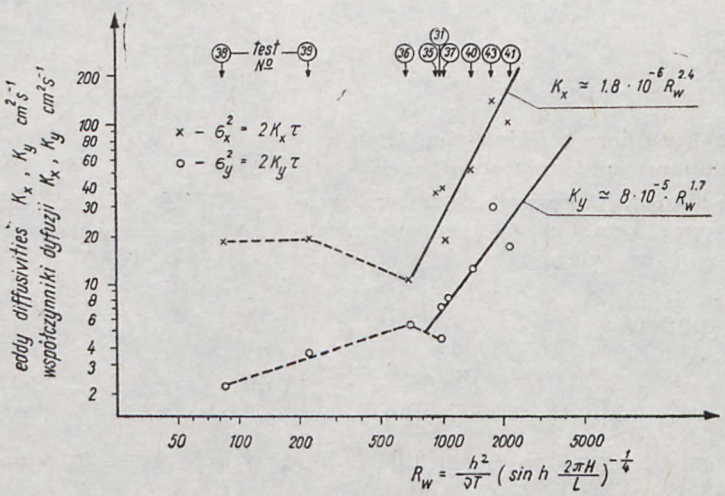

Fig. 3.14. Dependence of diffusion coefficients on wave parameters
Rys. 3.14. Zależność współczynników dyfuzji od parametrów fal

affect the power factors n_i quite considerably; waves and swell seem to be the primary agents in raising n_i to the level of 3. The field data for considerably large waves presented in Fig. 3.10, however scarce, indicate the tendency quite clearly. Nevertheless, more studies are required to elucidate the problem. In order to explain at least some of the aspects the Author undertook hydraulic laboratory tests on the dispersion under waves.

The test tank with test facilities is shown in Fig. 7.4. The applied tracers consisted of ping-pong balls partly filled with water. They were photographed from above and the dispersion was calculated from the photographs. Quite surprisingly, the components D_{ii} ($i = 1,2$) were found to be directly proportional to time (or length). One is thus justified in accepting the simple formula

$$K_{ii} = \frac{1}{2} \frac{\partial D_{ii}(t)}{\partial t} .$$

The coefficients of hirizontal diffusion calculated from this relationship are drawn in Fig. 3.14. As a consequence of several trials it has been found that the parameter

$$\alpha = \frac{h^2}{\nu T} \left(\sinh \frac{2\pi H}{L} \right)^{-1/4}$$

is characteristic as a variable for K_{ii}. As is illustrated in Fig. 3.14, there are two regions of the inerease of K_{ii}, which can be roughly described as laminar and turbulent ones. The power factor of the functions $K_{ii} = f_i$ is much higher in the turbulent region and approaches "—2.4" for K_x and "—1.65" for K_y.

In view of the distinction between the wave-induced dispersion in the field and that observed under laboratory conditions it is reasonable to assume that the higher field dispersion rate (almost 3 versus 1 as the exponent in $D_{ii} \sim {}^{n}\tau$) is due to different modes of interactions within the fields of waves and currents.

Let us assume that the "regular" field of concentration $\vartheta(z)$ due to currents varies randomly by $\vartheta'_1(z)$ due to oscillatory wave motion and by $\vartheta'_2(z)$ due to random displacements of water particles from their indisturbed position (x_o, z_o). In the linear wave theory approximation, the sum of both components can be estimated as a simple binomial

$$\vartheta'(z) = \vartheta'_1(z) + \vartheta'_2(z) = \frac{d\bar{\vartheta}}{dz}(z_o) \cdot h \cdot e^{-kz_o} \left[\cos(k x_o + \omega t) + \frac{8}{\pi^2} \right] + \tag{3.45}$$

$$+ \frac{d^2\bar{\vartheta}}{dz^2}(z_o) \cdot \frac{h^2}{2} \cdot e^{-2kz_o} \cos^2(k x_o + \omega t)$$

Both ϑ (z) and ϑ' (z) can be expanded in power series of a small parameter ε (e.g. wave steepness):

$$\begin{aligned} \bar{\vartheta}(z) &= \bar{\vartheta}^{(o)}(z) + \varepsilon\,\bar{\vartheta}^{(1)}(z) + \varepsilon^2\,\bar{\vartheta}^{(2)}(z) + \ldots \\ \vartheta'(z) &= \vartheta^{(o)}(z) + \varepsilon\,\vartheta'^{(1)}(z) + \varepsilon^2\,\vartheta'^{(2)} + \ldots \end{aligned} \tag{3.46}$$

Upon substitution of Eqs. 3.45 and 3.46 for $\vartheta(z) = \bar{\vartheta}(z) + \vartheta'(z)$ in Eq. 3.18 and on determination of the order of magnitude of all terms one obtains:

$$\left(\frac{\partial}{\partial t} - K_x \frac{\partial^2}{\partial x^2} - K_z \frac{\partial^2}{\partial z^2}\right) \varepsilon\vartheta'^{(1)} = u_z \frac{\partial \bar{\vartheta}^{(o)}}{\partial z}, \tag{3.46.1}$$

$$-K_z \frac{\partial \bar{\vartheta}^{(o)}}{\partial z} = \overline{u_z \vartheta'}\,|_{z=o}, \tag{3.46.2}$$

$$-K_z \frac{\partial\, \varepsilon^2 \vartheta^{(2)}(z)}{\partial z} \overline{u_z \vartheta'}. \tag{3.46.3.}$$

where u_z is the vertical orbital velocity component and the bar denotes statistical averaging. The term $\varepsilon^2 \bar{\vartheta}^{(2)}(z)$ describes the effect of waves on the current-induced concentration field. Solutions for $\vartheta'^{(1)}(z)$, and $\varepsilon^2 \bar{\vartheta}^2(z) = \bar{\vartheta}(z) - \bar{\vartheta}^{(o)}(z)$ in Eqs. 3.36.1.—3.46.3 are sought in the form of the Fourier-Stjeltjes integral:

$$f(t, x, y, z) = \int \exp(-i\omega t)\, d Z_f(\omega, x, y, z). \tag{3.47}$$

If one omits $K_z \dfrac{\partial^2 \bar{\vartheta}}{\partial z^2}$ in comparison with $u_z \dfrac{\partial \bar{\vartheta}^{(o)}}{\partial z}$, from the combination of Eqs. 3.46.1 and 3.47. it follows:

$$d Z_\vartheta = \frac{-P_e}{i + P_e} \frac{d\,\vartheta^{(o)}}{dz} e^{-kz}\, d Z_\zeta, \tag{3.48}$$

where $P_e = \dfrac{c}{K_x k}$ = Peclet number,

c = wave celerity,

$d Z_\zeta$ = random increment in free surface oscillations.

Thus, the spectral density $f_{\vartheta'}$ of the fluctuations ϑ' (z) is given by

$$f_{\vartheta'}(\omega, \alpha, z)\, d\omega\, d\alpha = \overline{d Z_{\vartheta'} \cdot d Z^*_{\vartheta'}} \frac{P_e^2}{P_e^2 + 1} \left(\frac{d\,\bar{\vartheta}^{(o)}}{dz}\right)^2 e^{-2kz} f_\vartheta(\omega, \alpha), \tag{3.48.1}$$

where $f_\vartheta(\omega, \alpha)$ = two-dimensional spectral density of free surface oscillations

and asterisk denotes conjugation.
Similarly, one has

$$f_{\vartheta, u_z} \cdot d\omega\, d\alpha = \overline{d Z_\vartheta \cdot d Z^*_{u_z}} = - \frac{P_e + i P_e^2}{P_e^2 + 1} \omega \frac{\partial \bar{\vartheta}^{(o)}}{\partial z} e^{-2kz} f_\zeta (\omega, \alpha). \quad (3.49)$$

Consequently, the mean value of the turbulent flux $\overline{\vartheta' u_z}$ reads

$$\overline{\vartheta' u_z} = \int\int f_{\vartheta' u} \, d\omega \, d\alpha =$$

$$= -4 \frac{\partial \bar{\vartheta}^{(o)}}{\partial z} \int_0^{\frac{\pi}{2}} \int_0^{\infty} \frac{g^2 K_x \omega^4}{g^4 + K_2^x \omega^6} \exp\left(-2 \frac{z}{g} \omega^2\right) f_\zeta (\omega, \alpha) \, dx \, d\omega \quad (3.49.1)$$

By analogy to Boussinesque classical definition, which employs this flux, one can regard the double integral in Eq. 3.49.1. as spectral eddy diffusivity due to waves and currents.

Comparison of the spectral eddy diffusivity with the values measured by the Author in known fields of waves and currents has shown that the difference is much smaller than in the case of diffusion coefficients coupled only with waves and wave-wave interactions. However, it is still unclear whether the ultralinear increase in dispersion with the time observed in the sea is shaped only by characteristics of advection (primarily, shear flows), the structure of turbulent eddies in the inertial subrange (with its four-thirds law) and some other factors, or possibly that a combination of waves and currents accelerates dispersion. Again, field studies have pointed to a very important part played by the angle between waves and currents. Waves begin to act as a strong dispersion-accelerating factor after they turn by a certain critical angle with respect to the direction of resulting advection, even if they are not very high.

The problem of horizontal diffusion in density-heterogeneous media has more to do with the vertical structure of turbulence and is therefore treated in the next paragraph.

3.4. Vertical diffusion

Vertical diffusion depends very much on the character of the medium under consideration. This is primarily true for the density or thermal heterogeneity of the medium.

Turbulent diffusion in a density-homogeneous medium is explored only superficially. It is fairly customary to assume homogeneous turbulence patterns, i.e. $D_z(t) \sim t$, etc. This immediately implies constancy

of K_z and the only question that remains under such a formulation is the value of K_z. It was found to vary from a fraction of unity under very calm conditions to several tens in rough seas. Koh and Fan (1970) found

$$K_z = 0.02 \frac{h^2}{T}$$

for the coefficient of vertical diffusion under waves of height h and period T. Aside from the empirical results presented hereafter, this is practically all we know about the relation of vertical diffusion characteristics to diffusion-inducing factors in idealized density-homogeneous media.

Our knowledge of density-stratified media is greater. As is well known, the turbulence in these media in governed by an additional factor i.e. buoyancy. The buoyancy forces hinder the penetration of surface energy into deeper layers. Therefore with regard to our needs, the following questions arise: (1) occurrence and structure of stratification (2) the effect of stratification on horizontal diffusion (3) the effect of stratification on vertical diffusion.

The equation of turbulence energy, E_t in a stratified medium reads

$$\frac{\partial E_t}{\partial t} = - \frac{\partial}{\partial z} \overline{\left(\frac{1}{2} u'_\alpha \cdot u'_\alpha + \frac{p'}{\varrho} \right) w'} - \overline{u' w'} \frac{\partial \bar{u}}{\partial z} + \frac{g}{T} \overline{T' w'} - \bar{\varepsilon}_t \quad (3.50)$$

and included the additional (in comparison with homogeneous medium) term

$\frac{g}{T} \overline{T' w'}$, which accounts for buoyancy. By comparing the magnitude of this term against the energy transmitted from mean flow to turbulence $\overline{u' w'} \frac{\partial \bar{u}}{\partial z}$ one obtains

$$Rf = - \frac{g}{\bar{T}} \frac{\overline{T' w'}}{\overline{u' w'} \frac{\partial \bar{u}}{\partial z}} \quad (3.51)$$

or after substituting $\overline{u' w'} = K \frac{\partial \bar{u}}{\partial z}$ and $\overline{w' T'} = K_T \frac{\partial \bar{T}}{\partial z}$

$$Rf = - \frac{K_T}{K} \cdot \frac{g}{\bar{T}} \frac{\frac{\partial \bar{T}}{\partial z}}{\left(\frac{\partial \bar{u}}{\partial z} \right)^2} = \alpha R_i, \quad (3.52)$$

where R_i is the Richardson number and Rf its dynamic version. These numbers describe the status of turbulence in dimensionless form. For

$$K_T = c^2 l^2 \left[\alpha_b \frac{\partial^2 E_t}{\partial z^2} + \frac{\partial \bar{u}}{\partial z} - \frac{g}{\bar{T}} \alpha \frac{\partial \bar{T}}{\partial z} \right]^{1/2}$$

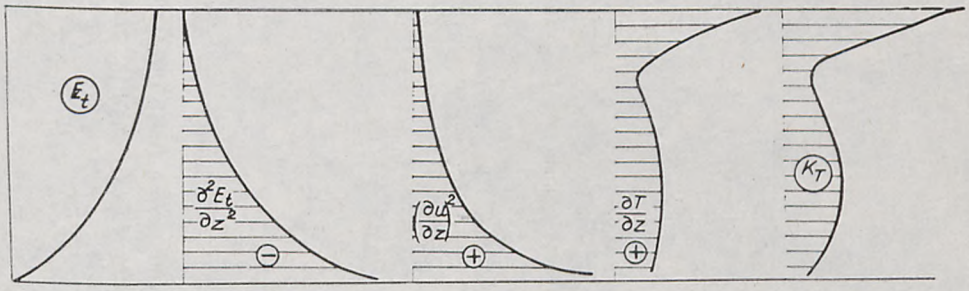

Fig. 3.15. Hypothetical form of the diffusion coefficient in stratified media
Rys. 3.15. Hipotetyczna postać współczynnika dyfuzji w ośrodkach uwarstwionych

example, by taking into account the two terms $-\overline{u' w'} \frac{\partial \bar{u}}{\partial z}$ and $\frac{g}{\bar{T}} \overline{T' w'}$ in the case of stratified media and only the former term in homogeneous media, the coefficient of vertical diffusion becoms

$$K^{str} = K (1 - \alpha \, Ri). \tag{3.53}$$

Similar results can be obtained by considering (in semiempirical formulation) K as a product of characteristic length and velocity, which also depend on stratification. From various assumptions as to the mixing lenght L based on the empirical findings of Kazanskiy and Monin and theoretical considerations of Obukhov (compare Kitaigorodskii 1961) it turns out that the power factor in Eq. 3.53 varies from 1 to 1.2:

$$K^{str} = K (1 - Ri)^{1 \div 1.2} \tag{3.54}$$

This result is equivalent to

$$K^{str} = K (1 + a \, Ri)^{-b} \tag{3.55}$$

derived by Rossby and Montgomery by assuming that the only important parameter, mixing length l depends on stratification.

The depth of thermocline at which an abrupt jump in temperature and density profiles occurs, is affected by many factors, such as surface heat transfer, extraterrestrial radiation, etc., which are dealt with elsewhere (Chapter 4). Therefore we confine ourselves to the description of the interlayer between waste water (or, generally, heated water) and the ambient density-heterogeneous medium. The depth of penetration is determined by the critical Richardson number, which reflects the equilibrium of the buoyancy and inertia forces. This equality yields

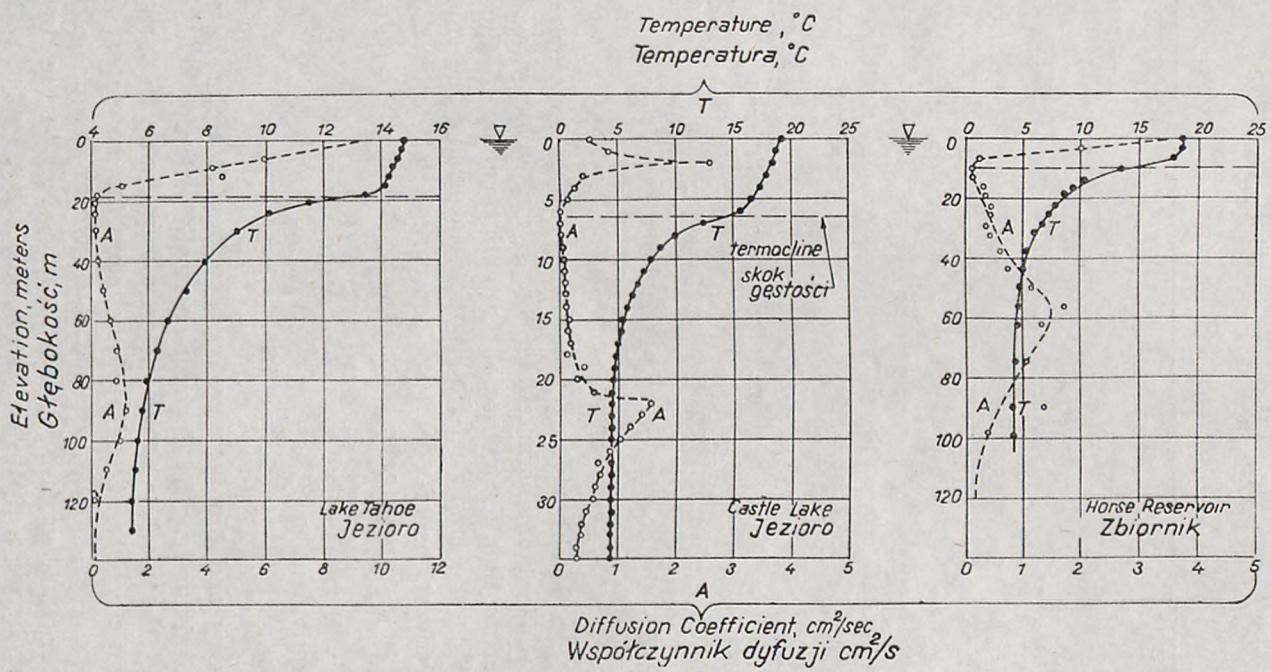

Fig. 3.16. Effective diffusion and temperature profiles for selected impoundments (from Orlob et al., 1969)

Rys. 3.16. Profile temperatury i współczynnika dyfuzji dla wybranych zbiorników (wg Orloba i in., 1969)

$$\left(\frac{\partial u}{\partial z}\right)_{cr} = \sqrt{\frac{g}{\varrho}\frac{\partial \varrho}{\partial z}\frac{1}{R_{icr}}}, \tag{3.56}$$

where $R_{icr} = 1$, and ϱ is space-dependent waste water density, which, in turn, is a simple function of concentration

$$\varrho = \vartheta \varrho_o + (1 - \vartheta)\, \varrho_w, \tag{3.57}$$

where ϱ_o is the outlet density of waste water and ϱ_w — water density. For a given assembly of governing factors (velocity and diffusion characteristics, which implicitly depend again on stratification) ϑ can be determined analytically as

$$\vartheta = f(x, y, z, u, K_i \ldots). \tag{3.58}$$

The combination of Eqs. 3.56, 3.57, and 3.58 gives the equation of the boundary $R_i = 1$, which depicts the turbulence penetration interface

$$F(x, y, z, u, g_o, K_i \ldots) = 0. \tag{3.59}$$

If there is no water propagating in the ambient medium, it is interesting to determine the patterns of depth changes in the coefficient of vertical diffusion. Turning back to Eq. 3.50 without the pressure component, by making a couple of semi-empirical assumptions for flow along the x_i-axis

$$-\varrho\, \overline{u'_i u'_j} = \varrho K \frac{\partial u_i}{\partial x_j}, \tag{3.60.1}$$

$$\overline{E'_t u'_i} = \alpha_E K \frac{\partial E_t}{\partial x_i}, \tag{3.60.2}$$

$$K = l\sqrt{E_t}, \tag{3.60.3}$$

$$\overline{\varepsilon_t} = \frac{E_t^{3/2}}{c^4 l} = \frac{K^3}{c^4 l^4} \tag{3.60.4}$$

one obtains the following equation

$$\frac{\partial E_t}{\partial t} = \frac{\partial}{\partial z}\alpha_b K \frac{\partial E_t}{\partial z} + K\left(\frac{\partial u}{\partial z}\right)^2 - \frac{g}{T}\alpha K \frac{\partial \overline{T}}{\partial z} - \frac{K^3}{c^4 l^4} \tag{3.61}$$

with the same order of components as in Eq. 3.50. For the stationary case one has

$$K = c^2 l^2 \left[\alpha_b \frac{\partial^2 E_t}{\partial z^2} + \left(\frac{\partial \overline{u}}{\partial z}\right)^2 - \frac{g}{\overline{T}}\alpha \frac{\partial \overline{T}}{\partial z}\right]^{1/2} \tag{3.62}$$

from which at least an order of magnitude and qualitative variation can be determined for K. Fig. 3.15 presents the three right-hand components

of Eq. 3.62 and the resulting coefficient K for the following set of parameters:

$$c = 1.5 \quad l = 10.0 \quad \alpha_b = 1.5 \quad \alpha = 0.1$$

It can be seen that this type of analysis results in a pronounced decrease in the coefficient of diffusion throughout the surface layer and rather insignificant differentiation with much smaller values in the lower stratum. General agreement of the curve with empirical findings can be concluded on the basis of the data shown in Fig. 3.16 after Orlob, Roesner, and Norton (1969). The analysis presented herein enables one to elucidate the origin of a characteristic inflexion of the curves for the diffusion coefficient. Such an inflexion is also found for other experiments (see Fig. 3.17). It is thus reasonable to describe the vertical variation of the diffusion coefficient as follows:

$$K = K_o e^{-\eta z_u} \text{ for the upper layer (I)} \tag{3.63.1}$$

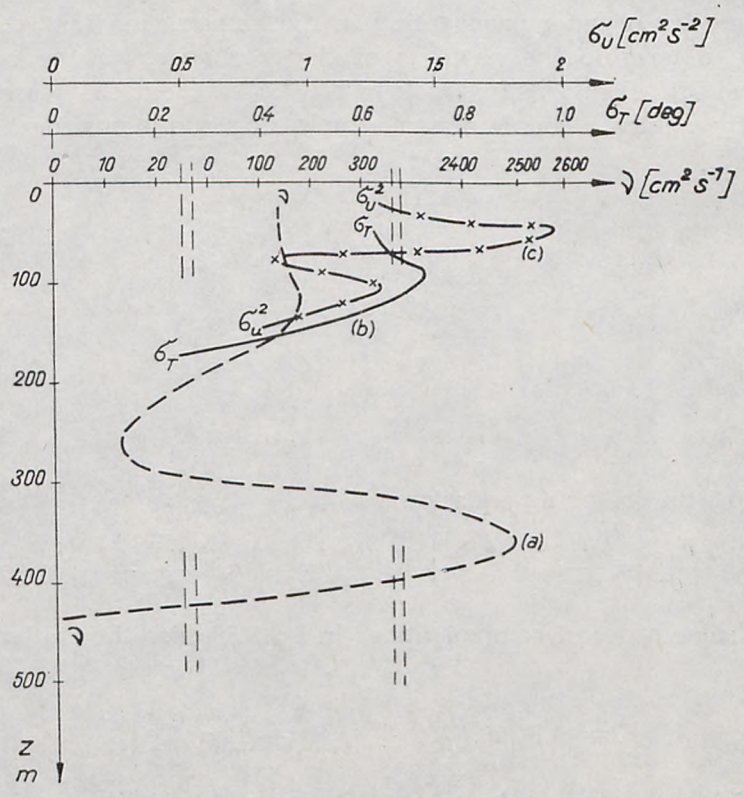

Fig. 3.17. Variation of temperature and eddy diffusivity, Ozmidov (1973)
Rys. 3.17. Zmienność temperatury i współczynnika dyfuzji, Ozmidov (1973)

$$K = b\,E^{-a}\left(E = -\frac{1}{\varrho}\frac{\partial \varrho}{\partial z}\right) \text{ at thermocline} \qquad (3.63.2)$$

$$K = K_1\, e^{-\eta_1 (z - z_i)^2} \text{ for lower layer (II).}$$

The following figures can serve as preliminary guidelines for the parameters a, b, η, η_1, z_1, K_o, and K_1.

Let us now consider the question of how the thermal or density heterogeneity affects the horizontal and vertical diffusion. From theoretical reasoning and empirical evidence it turns out that in unstratified media the horizontal and vertical diffusion are of the same order of magnitude unless the bottom of a reservoir or thermocline constrains the vertical eddies. This is illustrated in Fig. 3.18, where the horizontal lines depict the limits to growth due to vertical or horizontal constraints (the lower or upper line, respectively). Incidentally, in the drawing it is assumed that the 4/3 law holds throughout a considerable range of turbulence scales.

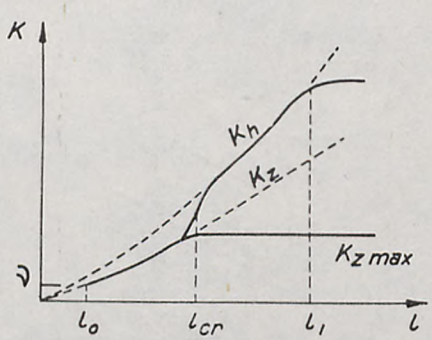

Fig. 3.18. Limits to growth of diffusion coefficients, Ozmidov, 1968

Rys. 3.18. Ograniczenia wzrostu współczynników dyfuzji, Ozmidov, 1968

In view of turbulence damping due to buoyancy it is generally accepted that the vertical diffusion coefficient decreases with increasing density gradient, or more specifically, with increasing Ri, as in Eqs. 3.53—3.55. It has not yet been resolved definitely how the horizontal diffusion behaves after the vertical eddies reach their limits. One may again resort to the equation or turbulence energy (3.1) and (3.50). For the case of negligible buoyancy the energy equation does not include the term $\frac{g}{\overline{T}}\,\alpha K\,\frac{\partial \overline{T}}{\partial z}$, which becomes, however, quite considerable under heterogeneous conditions. In order to conserve energy (which occurs in fact) the first and second right hand components of Eq. 3.61 must increase, energy dissipation being relatively insensitive to the density structure. It seems that the increase comes mostly from the first

term, i.e. strong gradient of $\overline{u'_\alpha u'_\alpha w'}$ or $\frac{\partial E_t}{\partial_z}$. Hence, addition of the (negative) buoyancy term does not necessarily imply any rise in the horizontal diffusion coefficient (at least, unless a thorough examination of all the terms is performed).

This conclusion proves to be correct in the light of Prych's empirical observations (1970) on horizontal diffusion in stratified and unstratified media. It appears that after an initial period of the gravitational spread of a plume in a stratified reservoir the intensity of horizontal turbulence remains unchanged in comparison with the unstratified case (Fig. 3.19).

Nevertheless, certain empirical data appears inconsistent with this standpoint. On the one hand we are confronted with be opinion (that has existed after Parr since 1936) on intensification of horizontal diffusion due to limited vertical spread in stratified media. This belief is continued through the formula

$$A_1 = A_1^\circ \left(1 + \gamma \frac{g\, Ex^2}{v^2}\right) \tag{3.64}$$

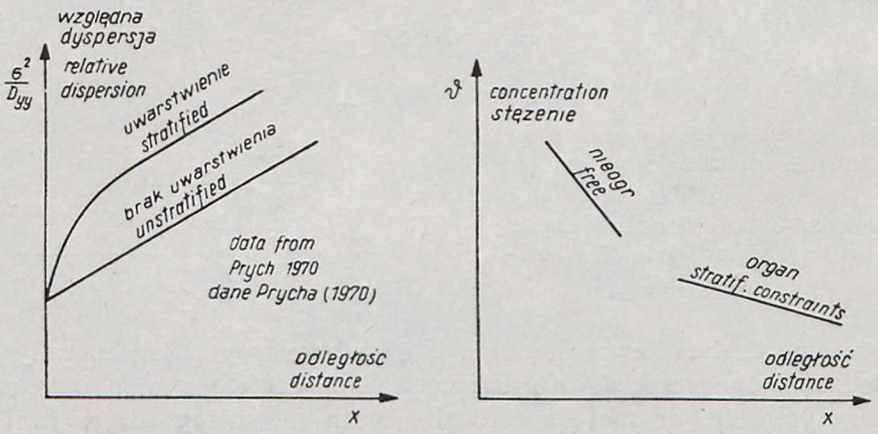

Fig. 3.19. The effect of stratification on horizontal dispersion
Rys. 3.19. Wpływ uwarstwienia na rozpraszanie poziome

derived by Riley in 1951. The parametr γ is equal to $1.8.\ 10^{-11}$, x is the distance between 2 measuring stations, and the stability parameter E is egual to $\frac{1}{\varrho}\,\frac{\partial\,\varrho}{\partial\,z}$. The same effect is essentially demonstrated by Ozmidov's correction to the 4/3 law in Fig. 3.6. For lower relative depths $\frac{H}{l}$ the power factor n approaches 4/3, which imposes a limit coupled with

very shallow or strongly stratified waters. This finding is contradicted, however, by other investigators' data, as discussed earlier in this chapter. In most field investigations one observes smaller decreases of concen-

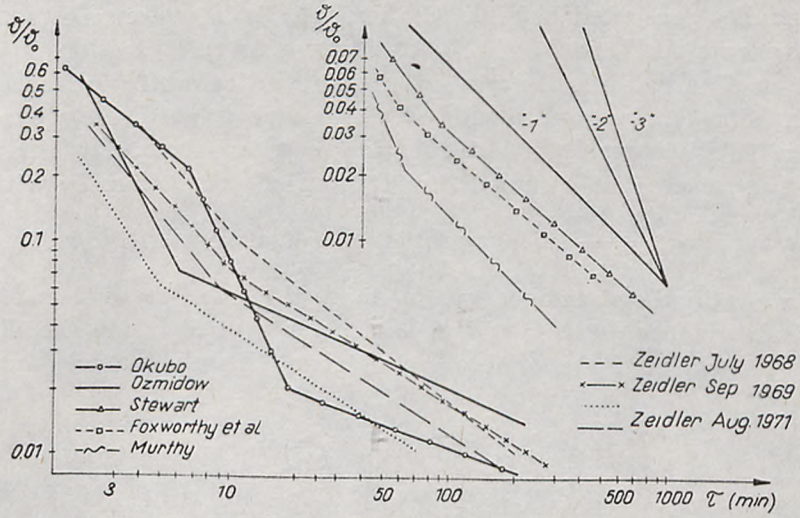

Fig. 3.20. Typical concentration decrease vs time for instantaneons source
Rys. 3.20. Charakterystyczny spadek stężenia w czasie dla chwilowego źródła

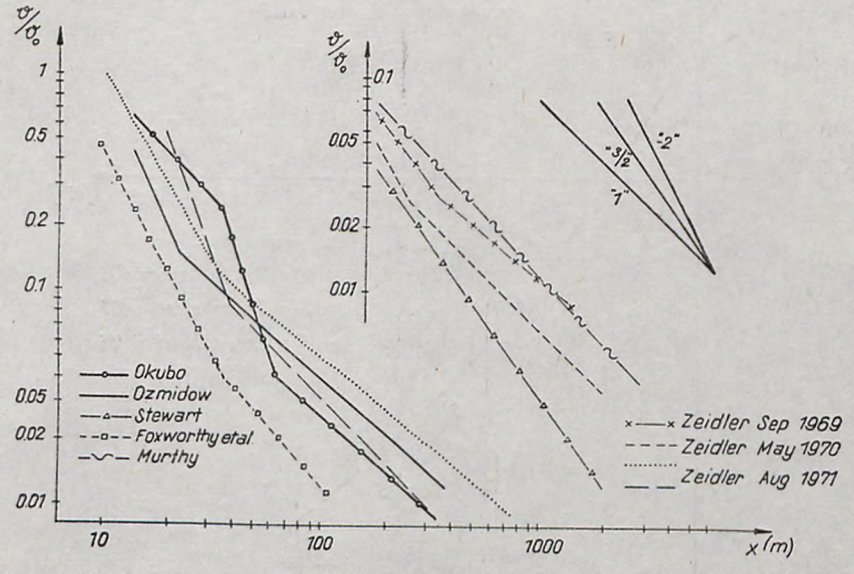

Fig. 3.21. Typical concentration fall vs distance for continuous point source
Ryc. 3.21. Charakterystyczny spadek stężenia z odległością dla ciągłego źródła punktowego

tration after longer times for either plumes or patches (Fig. 3.20, 3.21). This fact indicates that once a constraint has occurred over depth, the horizontal diffusion does not intensify enough to overcome the effect of weakened (or arrested) vertical diffusion. On the basis of the data from many studies presented in Figs. 3.20 and 3.21 it is reasonable to assume that horizontal diffusion is fairly insensitive to stratification.

Let us finally discuss variation of the vertical diffusion coefficient in both homogeneous and stratified media. We have already expressed this coefficient in terms of stratification (compare Eq. 3.55). Under this kind of approach it is assumed that D_{zz} varied proportionally with time and thus $K_{zz} = \frac{\Delta D_{zz}}{2t}$ is enough to characterize vertical diffusion in either a stratified or homogeneous medium. However, there is insufficient empirical evidence on the vertical homogeneity of diffusion (i.e. $D_{zz} \sim t$). On the contrary, the available data (even though scarce) show the

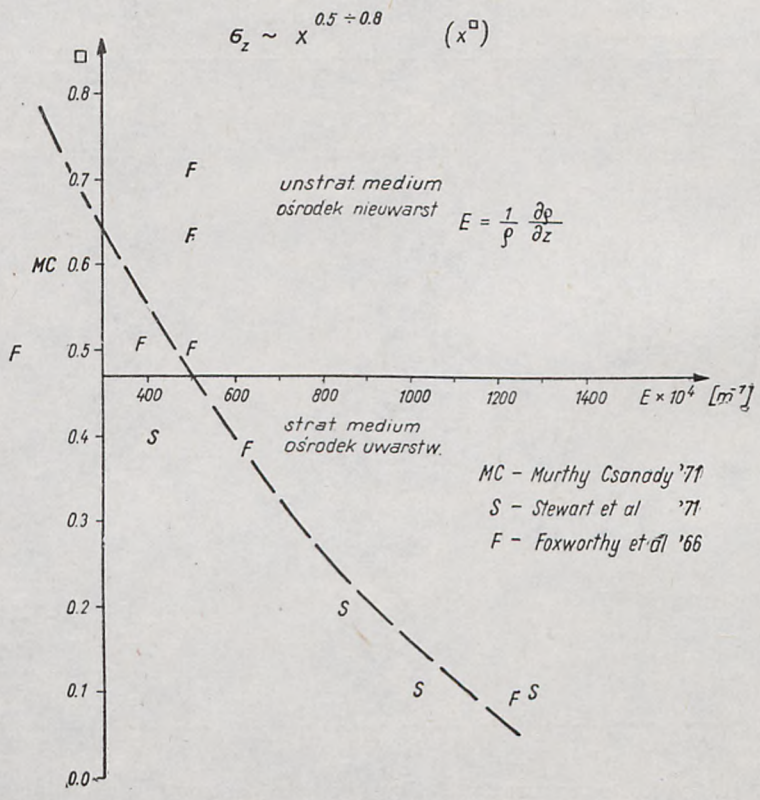

Fig. 3.22. Dependence of vertical diffusion on the stability E

Rys. 3.22. Zależność pionowej dyfuzji od stateczności E

decreasing exponent of the proportionality $D_{zz} \sim t^{\alpha}$ with higher stratification (Fig. 3.22). While ranging from 1.0 to 1.6 in homogeneous media, the factor α in strongly stratified water bodies approaches zero, i.e. turbulent eddies of significant size are unable to overcome buoyancy and vertical diffusion does not occur practically after some time elapses or a certain turbulence scale comes into question. Both concepts, i.e. stratification dependent and independent exponents are not quite antagonistic, as shown in Fig. 3.23. By enforcing time proportionality

$$D_{zz} = A\, l^{\alpha} = 2\,\frac{A}{2}\, u^{\alpha}\, t^{\alpha-1} \cdot t = 2\,K(t) \cdot t \qquad (3.65)$$

one includes the power variation into the time- (or turbulent-scale, which is governed by density stability) dependent diffusion coefficient. As follows from Eq. 4.6, K decrases with the density gradient (Ri), and also with time in stratified media, where $\alpha < 1$ and $\lim_{t\to\infty} K(t) = 0$ for longer times, i.e. bigger turbulence scale. The stronger the stratification, the bigger (relatively speaking) the turbulence scale for which vertical diffusion is impeded.

It is appropriate to mention that Fig. 3.22 shows the variation of absolute values of D_{zz} (and thus K_z), while the change with depth is still depicted in Figs. 3.15 and 3.16.

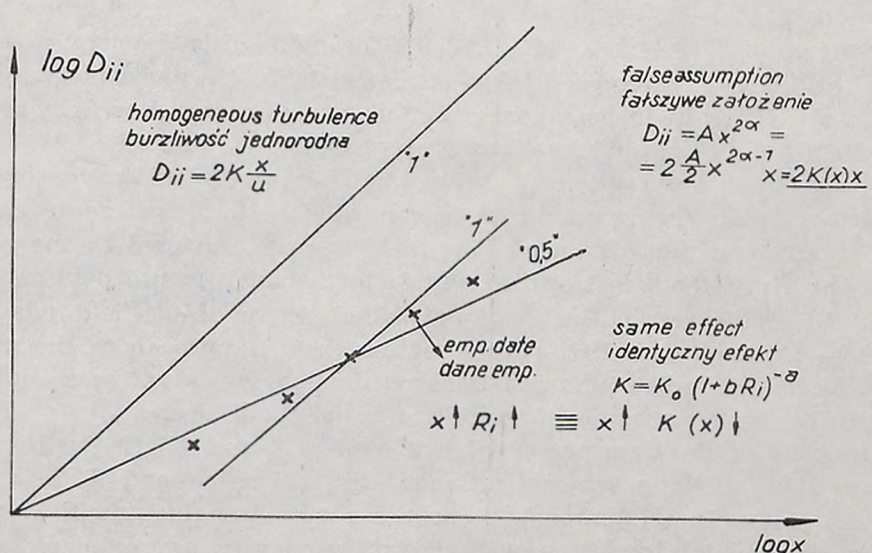

Fig. 3.23. Fictitious equivalence of the effects of turbulence scale and Ri on D_{ii} (x)

Rys. 3.23. Pozorna równoważność wpływu skali turbulencji i Ri na D_{ii} (x)

3.5. Choice of proper diffusion models for coastal conditions

From the preceding paragraphs it follows that both horizontal and turbulent diffusion vary within quite wide ranges. For example, D_x and D_y depend on time (or a length scale) as powers with exponent n_i which varies from 1 to over 2 (3 in a rough sea). This dependence is slightly different for the vertical diffusion (because of the density effects); for which the se exponents range from 0 to almost 2. These figures may be used in estimating the longitudinal decrease of plume concentration, which is of primary practical concern. Let us consider some of the most representative theoretical models presented in Par. 3.2 and combine them with the empirical findings discussed hitherto for continuous release:

$$\begin{array}{llll} u = \text{const} & K_y = \text{const} & \vartheta \sim x^{-1/2}\, x^{0 \div -0.8} = x^{-0.5 \div -1.3}, \\ u = \text{const} & K_y = K_1 . Y & \vartheta \sim x^{-1}\, x^{0 \div -0.8} = x^{-1.0 \div -1.8}, \\ u = u_1 Y & K_y = \text{const} & \vartheta \sim x^{-2/3}\, x^{0 \div -0.8} = x^{-0.67 \div -1.47}, \\ u = u_1 Y^{1/7} & K_y = K_1 . Y^{6/7} & \vartheta \sim x^{-8/9}\, x^{0 \div -8} = x^{-0.9 \div 1.7}. \end{array} \qquad (3.66)$$

It can thus be seen that the longitudinal decrease varies quite considerably, with the power factor ranging from —0.5 to —1.8, depending much on vertical density distribution ($0 \div -0{,}8$). Therefore a universal factor cannot be determined, although some schematization is possible. For example, in such coastal regions where constant depth and density can be assumed, the four sets of u, K give the exponents equal respectively to —1, —1.5, —1.17, and —1.4 for initial three-dimensional regions or —0.5, —1.0, —0.67, and 0.9 for more distant regions, where vertical diffusion is impeded. Moreover, model No. 4 is more adequate for longshore flows in inshore zones. Let us examine the above figures in the light of the field observations presented in Figs. 3.20 and 3.21.

From most observations it turns out that the "—1" power law is almost adequate for common inshore conditions with almost neutral stratification at greater distances. This law is fairly universal in the sense that is reflects the effect of different factors (model 2 vs model 4) which yield the same result. Such a longitudinal decay of far-field jets can thus be assumed as a first-approximation design approach to the problem. More detailed recommendations outlined herein must be accounted for in the further analysis of specific external conditions.

In view of the data presented in Chapters 2 and 3 it is justified to accept the following schematization of the advection and diffusion in coastal zones. In the immediate inshore region (roughly identical with the surf zone) the longshore-current profiles may be approximated with power functions. The exponents of 1/7 (for velocity) and 6/7 (for diffusion coefficient) found by the Author can characterize this zone in weak

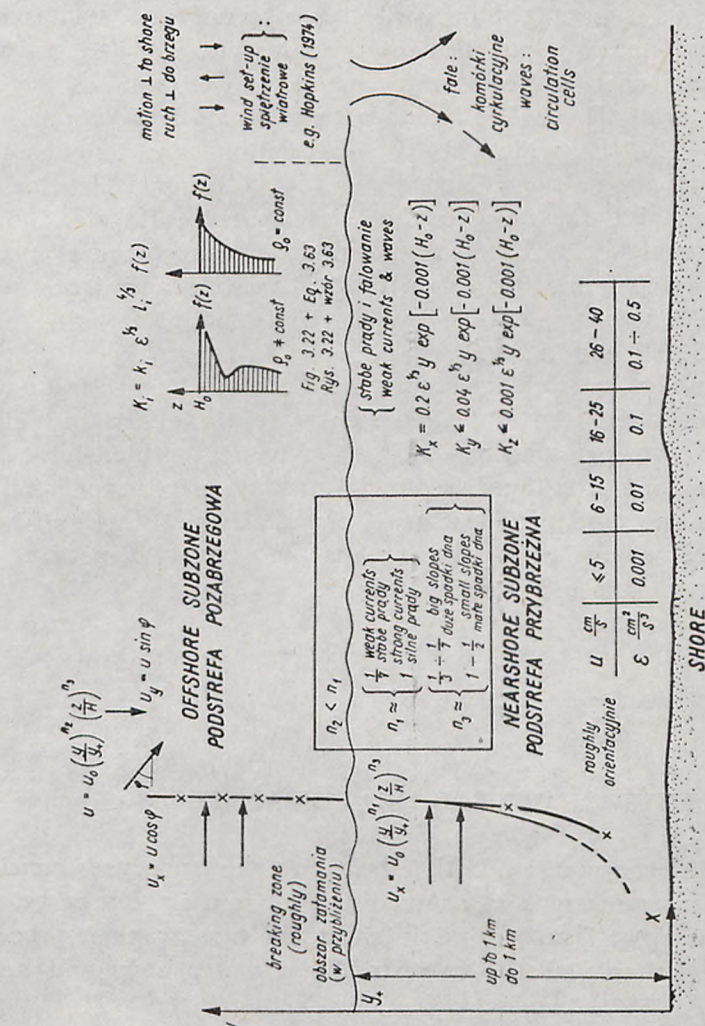

Fig. 3.24. Schematization of the coastal zone

Rys. 3.24. Schematyzacja strefy brzegowej

motions (the inherent longitudinal decrease is —0.9 for vertically-confined media, the most probable situation, or —1.7 under very rare conditions of high relative depths and considerable energy inflow from outside). This conclusion might be well true not only for wind-driven and wave-induced currents, but also for deep-sea currents (e.g. inetrial) entering a coastal zone. The case of perpendicular or oblique jet incidence must me treated individually; no general analytical guidance can be given because of the wide variety of situations apt to encounter. Beyond the nearshore subzone (surf zone) the pollution characteristics seem more predictable for more or less determinable flow and depth conditions. The model with horizontally-homogeneous currents and the vertical diffusion depending upon density stratification and depth seems most acceptable. The proposed schematization of pollution patterns in coastal zones is illustrated in Fig. 3.24.

It should finally be mentioned that the deterministic framework presented herein (where the advection fields are stationary and plane-homogeneneous) constitutes an approximation to the problem of coastal pollution. The marine situations assumed "steady" in common analyses incorporate inherent random deviations from steady patterns and hence add to a safety margin in designing marine waste disposals. The stochastic aspects are discussed in Chapter 10. *

Chapter 4

ENVIRONMENTAL HEAT TRANSFER

It has already been mentioned that heated water undergoes considerable thermal transformations at some distance from its discharge. The purpose of this chapter is to outline, in short, the heat transfer processes that control the behaviour of both an ambient water body and heated water discharge.

Notation and definitions for heat transfer components are given in Fig. 4.1. We shall now discuss them term by term following Harleman, 1972.

Incident solar radiation is the short wave radiation incident to the earth's atmosphere outside, coming primarily from the sun, which arrives at the earth's surface partly as direct radiation and partly as diffuse radiation. If direct measurements of the solar radiation

* See also the Author's paper in Journal of the Waterways, Harbors and Coastal Engineering Div, Amer. Soc. Civ. Eng., vol. 102, No. WWZ, 1976.

are not available, the following formula recommended by Kennedy (1949) may be used

$$\Phi_s = \frac{\Phi_{so}}{r^2} \sin \alpha_s \, a_t^m (1 - 0.65 \, C^2) \tag{4.1}$$

with Φ_{so} — solar constant of 10,305 BTU/ft² · day,
α_s — solar altitude,
r — normalized radius of the earth's orbit
(approximately $r = 1 + 0.017 \cos \left[\frac{2\pi}{365} (186\text{-}D) \right]$),
a_t — atmospheric transmission coefficient,
m — optical air mass,
C — cloudiness as a fraction of sky covered,

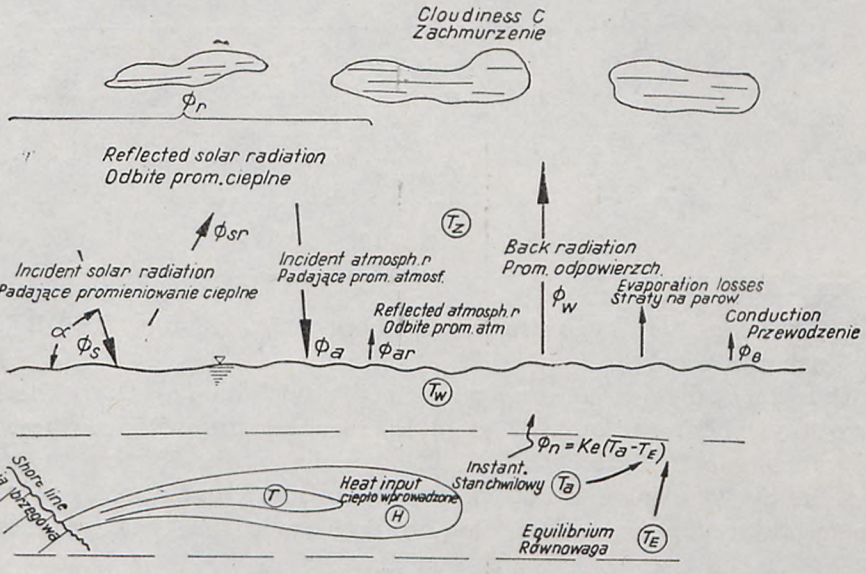

Fig. 4.1. Heat budget components
Rys. 4.1. Składowe bilansu cieplnego

D — the number of the day of the year (i.e. December 29 = day 363).

The atmospheric transmission coefficient a_t is usually taken to be a constant for a particular locality. Kennedy (1949) on the basis of 2-year data gives the value of 0.91. Hamon et al. (1954) found a_t to vary over the year from 0.7 in June to 0.85 in December. Kennedy (1949) recommends obtaining a_t by fitting Eq. 4.1. to data from the nearest available weather station.

The optical air mass can be computed from Kasten's (1949) formula to the local mean barometric pressure at altitude z in meters above sea level

$$m = \frac{1}{\sin \alpha_s + a\,(\alpha + b)^{-c}} \left[\frac{288 - 0.00652}{288}\right]^{5.256} \tag{4.2}$$

with $a = 0.15$, $b = 3.885$, and $c = 1.253$.

The reflected solar radiation Φ_{sr} can be expressed as a fraction of the incident radiation by Anderson's empirical formula

$$\frac{\Phi_{sr}}{\Phi_s} = A\,\alpha^B \tag{4.3}$$

with α_s in degrees, and the constants A and B as functions of cloudiness C as below.

Cloudiness C	0 Clear		0—0.5 Scattered		0.6—0.9 Broken		1.0 Overcast	
Constants	A	B	A	B	A	B	A	B
	1.18	-0.77	2.20	-0.97	0.95	-0.75	0.35	-1.45

The average monthly reflection is about 600 to 2000 or 8000 BTU/ft²/day (instantaneously).

The incident atmospheric radiation Φ_a is the longwave atmospheric radiation (3 to 100 μ) reaching the water surface. Typical values are 2000 to 3000 BTU/ft² day, i.e. about 50 percent greater than the average solar radiation. The atmospheric radiation is primarily due to water vapour, carbon dioxide, and ozone. The basic equation is

$$\Phi_a = \varepsilon\,\sigma\,T^4_z, \tag{4.4}$$

where ε is the average emittance of the atmosphere,

σ — Stefan Boltzman constant,
T_z — air temperature (absolute).

The reflected atmospheric radiation Φ_{ar} has been commonly assumed to be 3 percent of the incident atmospheric radiation.

The back radiation from the water surface is a longwave radiation, which is usually the largest single item in the energy budget

$$\Phi_w = 4.10^{-8}\,(T_w + 460)^4\,\frac{\text{BTU}}{\text{ft}^2/\text{day}}, \tag{4.5}$$

where T_w is the water surface temperature (°F). A simple linearized form of Eq. 4.5 with an accuracy of 30 $\frac{\text{BTU}}{\text{ft}^2/\text{day}}$ within a temperature range of 35 to 90°F is

$$\Phi_w = 1{,}600 + 23\, T_s. \tag{4.6}$$

Evaporation losses Φ_e are proportional to the mass of evaporated water. The vapour mass transport rate E_m is

$$E_m = f(W_z)\,(e_w - e_z), \tag{4.7}$$

where $f(W_z)$ is wind speed function,

e_w — saturation vapour pressure of water at temperature T_w,

e_z — vapour pressure at height z.

Hences Φ_e may be calculated by

$$\Phi_e = E_m \cdot L = \varrho\, f(W_z) \cdot (e_w - e_z)\, L, \tag{4.8}$$

where L is the latent heat of vaporization of water

$$L = 1087 - 0.54\, T_s. \tag{4.9}$$

The wind function $f(W_z)$ usually takes the form

$$f(W_z) = a + b\, W_z \tag{4.10}$$

in which the values of a and b have been determined by many investigators with little agreement. Therefore the best formula for Φ_e may be chosen as the simple one

$$\Phi_e = 17.2 \cdot W_z\,(e_w - e_z). \tag{4.11}$$

Conduction losses Φ_c (or sensible heat transfer losses) are customarily considered simultaneously with evaporation since the conduction process is considered proportional to the evaporation process in the following way:

$$\Phi_c = R \cdot \Phi_e = c \left| \frac{T_w - T_z}{e_w - e_z} \right| \Phi_e, \tag{4.12}$$

where R is the Bowen ratio, and $c = 0.255$ mm Hg/°F.

By using the formulae given above one may finally arrive at the following relationship

$$\Phi_n = \Phi_r - \{4 \cdot 10^{-8} (T_w + 460)^4 + 17.2\, W_z\, [(e_w - e_z) + 0.255\, (T_w - T_z)]\}, \tag{4.13}$$

where all the incident and reflected radiation terms are grouped in a

net radiation term Φ_r, which is a function of meteorological variables, while the remaining terms depend in part upon the water surface temperature.

In many cases it is not necessary to calculate natural ambient water temperatures; the interest is rather in the rise above ambient due to a man-made heat source, such as a power plant. Analysis in such cases may be conducted in terms of the equilibrium temperature, T_e, and the surface heat exchange coefficient K_e, which provide the following heat estimates:

$$\Phi_n = -K_e (T_{am} - T_E). \tag{4.14}$$

T_E is that water surface temperature which, for a given set of meteorological conditions, makes the back radiation, evaporation, and conduction losses exactly equal to the radiation inputs, that is, the net heat exchange Φ_n is zero. Hence T_E is the temperature, towards which every water body on the site will tend. The surface heat exchange is defined to give the incremental change of net heat exchange induced by an incremental change of water surface temperature.

Chapter 5

INITIAL MIXING AND DIFFUSION PROCESSES. JETS AND PLUMES

5.1. Introduction and definitions

It is customary to define "jets" as the diverging flow of one medium in another fluid due to momentum applied at the nozzle and buoyancy. The more specific term "plume" is used to desribe flows arising when buoyancy is supplied continuously.

The following groups of factors can be distinguished which affect the state of the submerged jets and plumes dealt with in this chapter:

1. characteristics of the jet itself (type and direction of discharge, momentum versus buoyancy, etc.),
2. thermal and density conditions of a recipient,
3. motion of a recipient,
4. initial and boundary conditions.

The influence of the respective factors is delineated in Fig. 5.1. Under given conditions one usually strives to achieve maximum mixing or dilution on the passage of the jet to the surface. Only some combi-

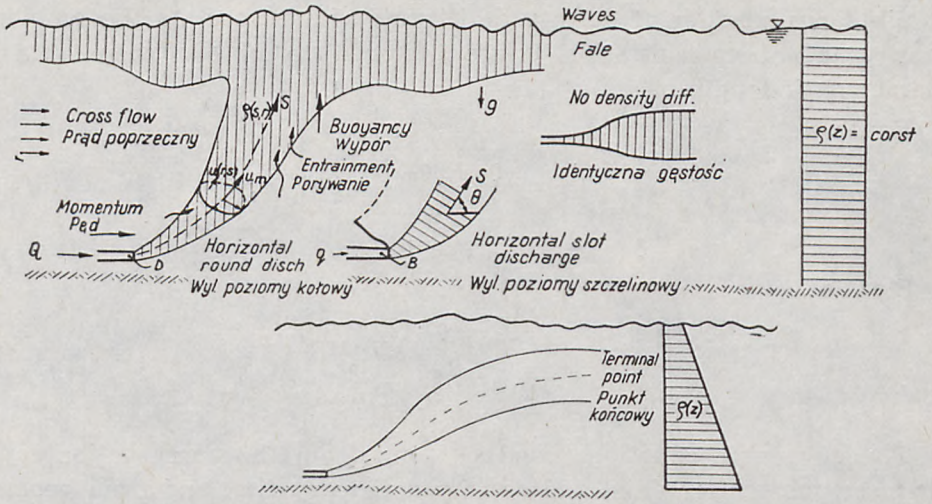

Fig. 5.1. Submerged round and slot jets under marine conditions

Rys. 5.1. Zatopione strugi kołowe i szczelinowe w warunkach morskich

nations of the factors shown in Fig. 5.1 have been explored, and these are discussed on further pages.

5.2. Round jets and slot jets in stagnant ambient fluid of uniform density

General theoretical models have been derived and verified experimentally for this case with a few exceptions for slot jets when the models proposed have not been checked adequately by experiment.

The entrainment or change of volume flux across the jet is assumed proportional to a characteristic velocity along the jet axis u and a characteristic length b, for the round jet. Although other methods for handling entrainment have been proposed, experimental evidence suggests this method is to be preferred (Morton, 1971)

Round Jet

$$\frac{dQ}{ds} = 2\pi\alpha bu,$$

Slot Jet

$$\frac{dq}{ds} = 2\alpha u. \tag{5.1}$$

The velocity profiles are assumed to be Gaussian, i.e., local velocity is related to a centerline value and the standard deviation:

Round Jet

$$u(s, r) = u_m(s)\, e^{-r^2/b^2},$$

Slot Jet

$$u(s, n) = u_m(s)\, e^{-n^2/b^2}. \tag{5.2}$$

where n is measured perpendicularly to s.

Similarly, profiles of density deficiency with respect to the ambient density and of concentration ϑ are assumed to be Gaussian with a characteristic length b.

Round Jet

$$\frac{\varrho_o - \varrho\,(s, r)}{\varrho_o} = \frac{\varrho_o - \varrho_m\,(s)}{\varrho_o} \cdot e^{-r^2/\lambda^2 b^2}, \tag{5.3}$$

$$\vartheta\,(s, r) = \vartheta_m\,(s)\, e^{-r^2/\lambda^2 b^2}.$$

Slot Jet

$$\frac{\varrho_o - \varrho\,(s, n)}{\varrho_o} = \frac{\varrho_o - \varrho_m\,(s)}{\varrho_o} \cdot e^{-n^2/\lambda^2 . b^2}, \tag{5.4}$$

$$\vartheta\,(s, n) = \vartheta_m\,(s) \cdot e^{-n^2/\lambda^2 . b^2},$$

The governing equations can be found from the conservation laws for mass, momentum flux, and density deficiency flux and from geometrical relations. We shall write them down in the integral form only for the round jet.

The continuity equation, assuming small variations in density and the entrainment relation, can be written as

$$\frac{d}{ds}\int_o^\infty 2\,\pi\, u \cdot r\,dr = 2\,\pi\,\alpha\, bu. \tag{5.5}$$

As the pressure field is assumed to be hydrostatic and no force acts in the horizontal direction, the x-momentum flux is conserved:

$$\frac{d}{ds}\int_o^\infty 2\,\pi\,\varrho\, u^2 \cdot \cos\Theta\, r\,dr = 0. \tag{5.6}$$

The force due to buoyancy must balance the rate of change of y-momentum flux

$$\frac{d}{ds}\int_o^\infty 2\,\pi\,\varrho\, u^2 \cdot \sin\Theta\, r\,dr = g\int_o^\infty 2\,\pi\,(\varrho_o - \varrho^*)\, r\,dr. \tag{5.7}$$

Since heat must be conserved and a linear temperature-density relationship is assumed, conservation of density deficiency flux is necessary

$$\frac{d}{ds}\int_o^\infty 2\,\pi\, u\,(\varrho_o - \varrho)\, r\,dr = 0, \tag{5.8}$$

$$\frac{d}{ds}\int_o^\infty 2\,\pi\, u \cdot \vartheta\, r\,dr = 0. \tag{5.9}$$

After simplification by integration and substitution one obtains the following governing equations for a round jet:

$$\frac{d}{ds}(u_m b^2) = 2\alpha ub, \tag{5.10}$$

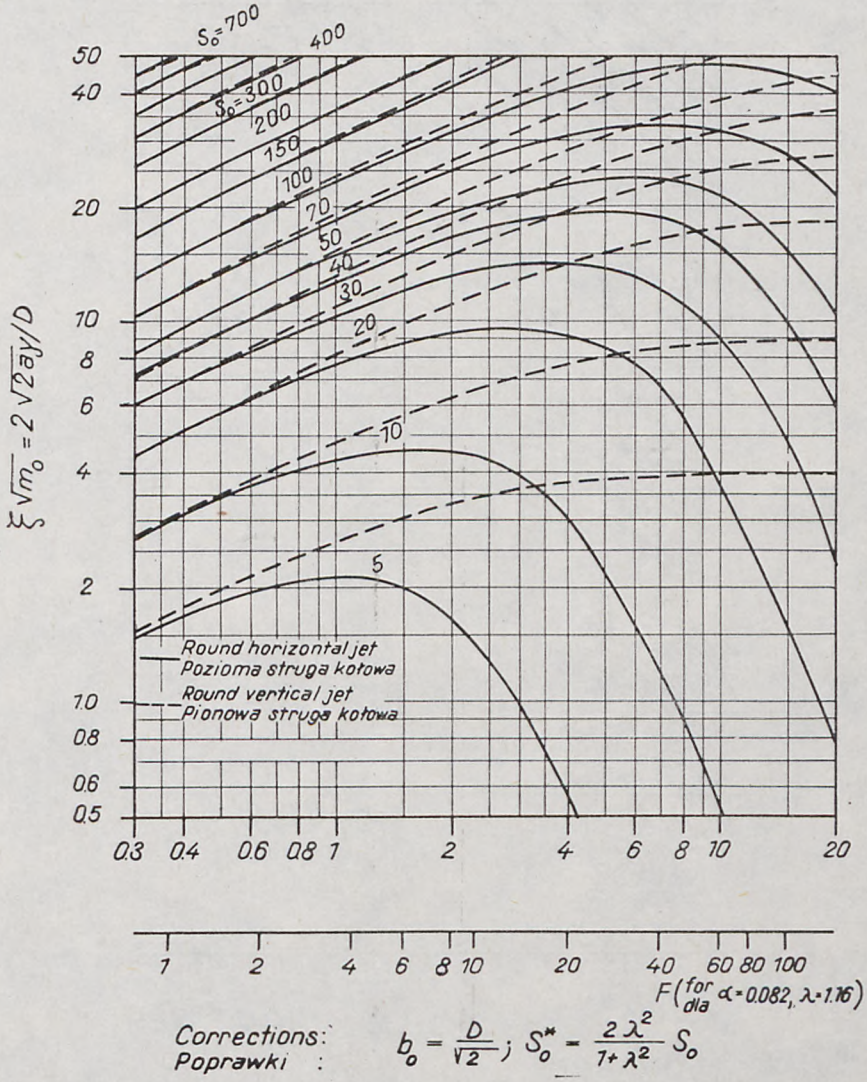

Fig. 5.2. Dilution of round buoyant jets in stagnant uniform environments, Fan and Brooks, 1969

Ryc. 5.2. Rozcieńczenie w kołowych strugach z wyporem w ośrodku o stałej gęstości Fan and Brooks, 1969

$$\frac{d}{ds}\left(\frac{u_m^2 \cdot b^2}{2} \cdot \cos\Theta\right) = 0, \tag{5.11}$$

$$\frac{d}{ds}\left(\frac{u_m^2 \cdot b^2}{2} \cdot \sin\Theta\right) = g\lambda^2 b^2 \frac{\varrho_o - \varrho_m}{\varrho_o}, \tag{5.12}$$

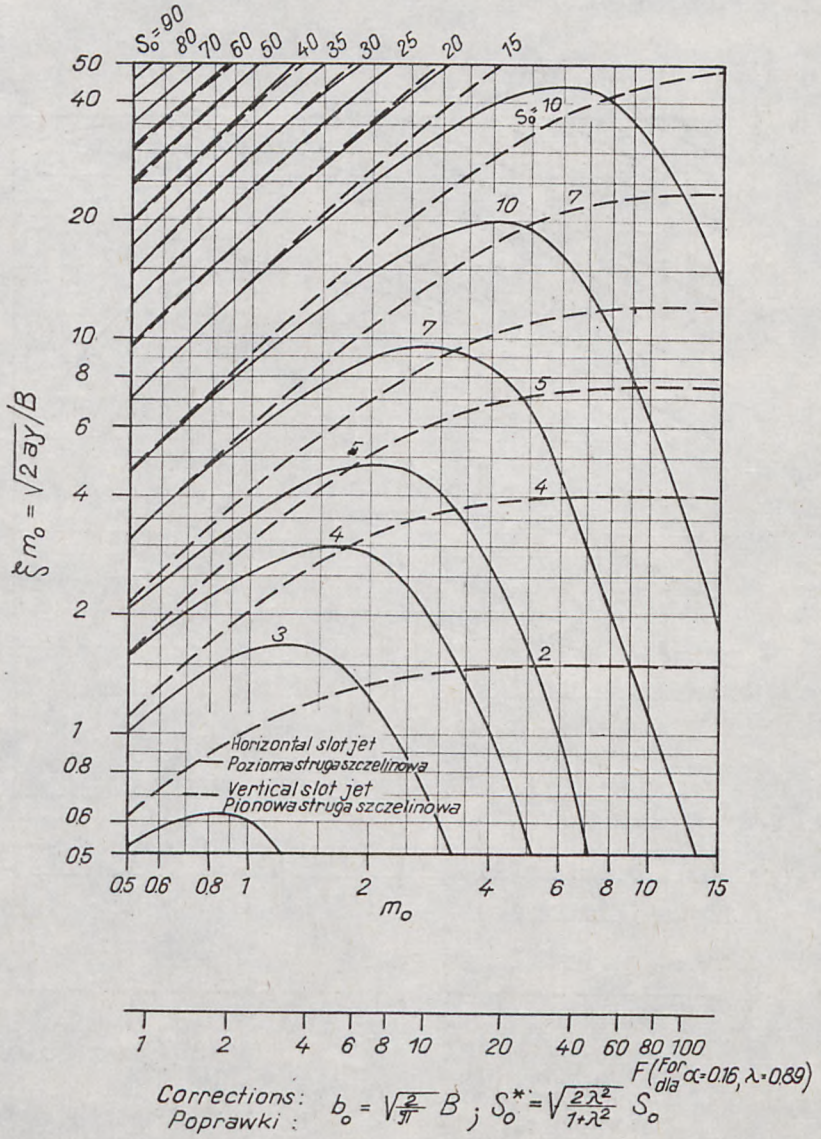

Fig. 5.3. Dilution of slot buoyant jets in stagnant uniform environments, Fan and Brooks, 1969

Rys. 5.3. Rozcieńczenie w szczelinowych strugach z wyporem w ośrodku o stałej gęstości, Fan and Brooks, 1969

$$\frac{d}{ds}\left[ub^2(\varrho_o - \varrho_m)\right] = 0, \tag{5.13}$$

$$\frac{d(\vartheta\, ub^2)}{ds} = 0. \tag{5.14}$$

Solutions to these sets of ordinary differential equations may not be found in closed analytical form, but they can be obtained readily by numerical integration with a digital computer. A convenient way to solve the equations consists in using normalized quantities, such as the densimetric Froude number:

$$F = \frac{V_o}{\sqrt{\frac{\varrho_o - \varrho_1}{\varrho_o} g D}}, \qquad F = \frac{V_o}{\sqrt{\frac{\varrho_o - \varrho_1}{\varrho_o} g B}} \tag{5.15}$$

For the large jet densimetric Froude number ($F \to \infty$), the jet behaves as a simple momentum jet, while for small F ($F \to 0$), the jet resembles a simple plume (a source of buoyancy only).

On the basis of numerical solutions found by Fan and Brooks (1969) and recently summarized by Shirazi and Davis (1971) one is able to present the trajectories and centerline solution ratios in the jets at any distance s from the outlet. A characteristic result is that the larger the Froude number, the longer the jet trajectory of a horizontally discharged jet and the wider a jet at any given elevation. The jet centerline dilution ratios S_o are given if Figs. 5.2 and 5.3. From these drawings it follows that mixing at any level increases as the jet densimetric Froude number increases. Increased dilution brought about by the change over from a single jet to a slot (multiport) may be seen for a fixed discharge on comparing Figs. 5.2 and 5.3. At the fixed elevation above the outlet, many jets of smaller diameter have larger S_o values bacause Y/D and F are larger.

Finally, it should be noted that the initial core zone of any jet is not subject to dilution even though some mixing occurs. According to different investigators, the length of the core zone varies about 6 D and 5 B. Therefore, the corrections introduced in Figs. 5.2 and 5.3 must be accounted for.

5.3. Interference of single jets in a stagnant uniform recipient

Common designs include diffuser pipes, which initially discharge single jets. As the jets grow, they interact with each other and merge into an effective slot jet (Fig. 5.4).

The intersection point of vertical jets may be found from geometrical considerations for a simple momentum discharge; the distance s = 3.1 L is shown in Fig. 5.4.

Koh and Fan (1970) present another possible definition of transition based on equal entrainment of round and slot jets, but their calculations of buoyant jet behaviour indicate little difference. Experimental studies

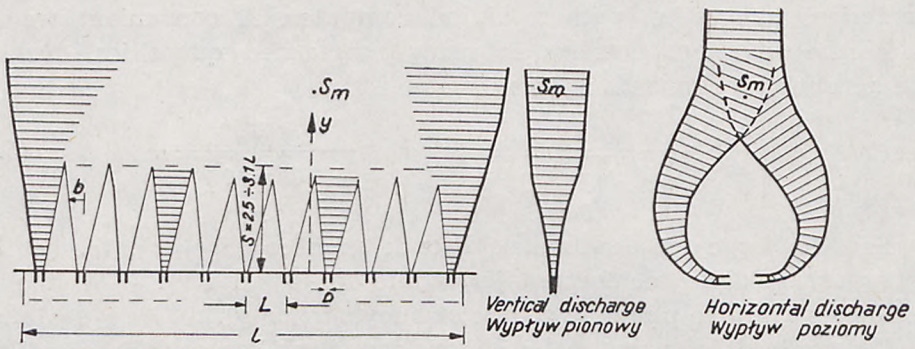

Fig. 5.4. Merging of single jets

Rys. 5.4. Łączenie się strug pojedynczych

of the merging of round buoyant jets by Liseth (1970) show that by distances of s/ = 2.5 from the source the round jets have lost their round character and merged to a two-dimensional (or slot) jet. Limited experiments by Larsen and Hecker (1972) indicate similar results.

In analyses of discharges from multiple-port diffusers, round jet calculations are used from the point of discharge to the merging point. The calculation is then for a slot jet whose length along the diffuser is L, and the port spacing is l = L/n — l, where n is the number of individual round jets. To shift the calculation from round jets to a slot jet, the mass flux, momentum flux, and density deficiency (or excess temperature) flux must be the same for round and slot jets at the transition. This continuity requires that the relationships in Fig. 5.4 hold.

The analysis of the slot jet is then carried out for temperature, a slight discontinuity in centerline temperature difference occurs in transition. Total heat is still conserved for heated water discharges.

The possibility of slot jets from either side of a diffuser merging into one plume was studied experimentally by Liseth (1970). Jets discharged horizontally from both sides of a diffuser tend to merge above the diffuser, although trajectories of similar jets discharged from only one side of that diffuser indicate no tendency to move over the diffuser. The smaller the densimetric Froude number of the initial round jets, the nearer to the diffuser the merging occurs. Upon merging, the diluting

capacity of the plume is greatly reduced as effectively one side of each slot jet not longer entrains ambient water. Liseth's (1970) experimental results for a wide range of conditions under which merging occurs are given in Fig. 5.5.

5.4. Non-uniform density of recipient waters

5.4.1. Linear stratification of the recipient waters

The choice of a linear density profile in the receiving water is reasonable because nearly linear density profiles are not uncommon in nature and the development of general results is possible for this case. The

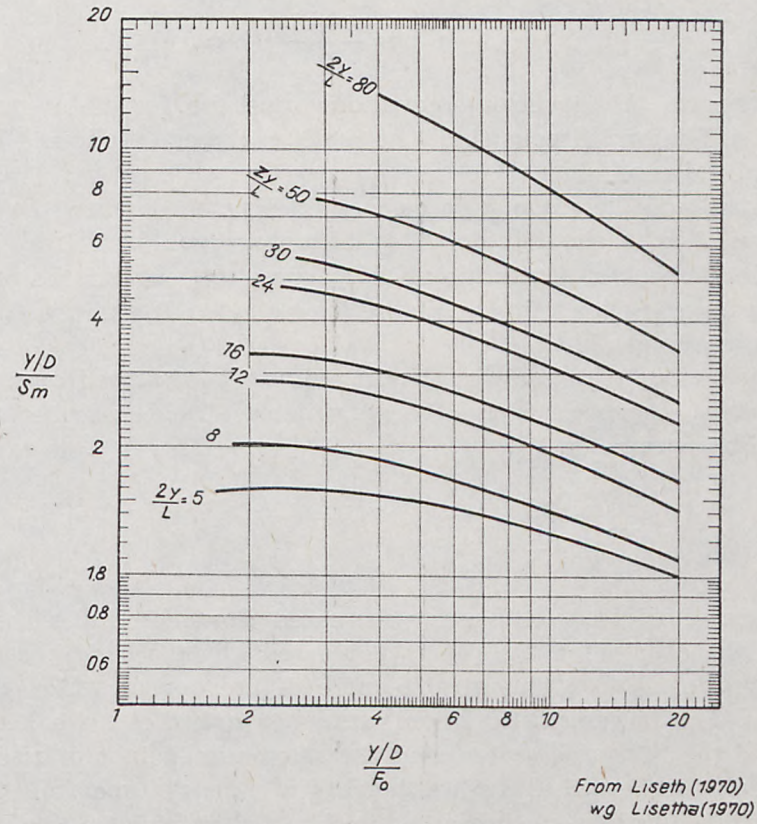

Fig. 5.5. Experimental observations of minimum dilution along the centre of merging buoyant jets from a manifold in stagnant receiving water of uniform density

Rys. 5.5. Wyniki pomiarów minimalnego rozcieńczenia wzdłuż osi łączących się strug w nieruchomej wodzie o stałej gęstości

basic definitions and assumptionts given in Section 5.2 hold, except that the ambient density ϱ_a varies linearly with depth z. Buoyant jets have the opportunity to entrain water of varying density from the environment and may in fact reach a terminal elevation below the water surface. The variation in the ambient density is accounted for in the z-momentum flux equation for a round jet as

$$\frac{d}{ds}\left(\frac{u_m^2 \cdot b^2}{2} \sin\Theta\right) = g\,\lambda^2 \cdot b^2\,\frac{\varrho_a - \varrho_m}{\varrho_o} \tag{5.16}$$

and in the density deficiency flux equation as

$$\frac{d}{ds}\int_o^\infty 2\pi u\,(\varrho_o - \varrho)\,r\,dr = \alpha\, ub\,\lambda^2\,(\varrho_o - \varrho_a), \tag{5.17}$$

which can be reduced to

$$\frac{d}{ds}\left[u_m\, b^2 \cdot (\varrho_a - \varrho_m\right] = \frac{1+\lambda^2}{\lambda^2} \cdot b^2 u_m\,\frac{d\,\varrho_a}{ds}. \tag{5.18}$$

Solutions to the governing equations must be found by numerical integration. Fan and Brooks (1969) normalized the equations and presented generalized results.

The maximum height of rise of the jet is reached when the vertical momentum flux becomes zero. This condition manifests itself by the vertical component of centerline velocity going to zero and the jet width becoming large. Beyond this point the jet spreads out and the governing equations no longer hold.

The behaviour of a buoyant jet in a linearly stratified environment is completely characterized by the densimetric Froude number and the stratification parameter

$$\mathcal{T} = \frac{\varrho_o - \varrho_1}{D\left(-\frac{d\,\varrho_a}{dz}\right)} \quad \text{or} \quad \mathcal{T} = \frac{\varrho_o - \varrho_1}{B\left(-\frac{d\,\varrho_a}{dz}\right)}. \tag{5.19}$$

The jet trajectories show that for increased Froude number the maximum height of rise of the jet is decreased. This occurs because the higher Froude number jet entrains more of the denser water at lower elevations. The larger stratification parameter indicates a weaker stratification of the receiving water, and the maximum height of rise of the jet is greatly increased. Terminal heights of rise, volume flux parameters, and thus dilutions are presented in Figs. 5.6 and 5.7.

It should be noted that the dilution ratio gives only the dilution of a constituent which is in the discharge and constant in the receiving water. If the ambient stratification is due to temperature and the dis-

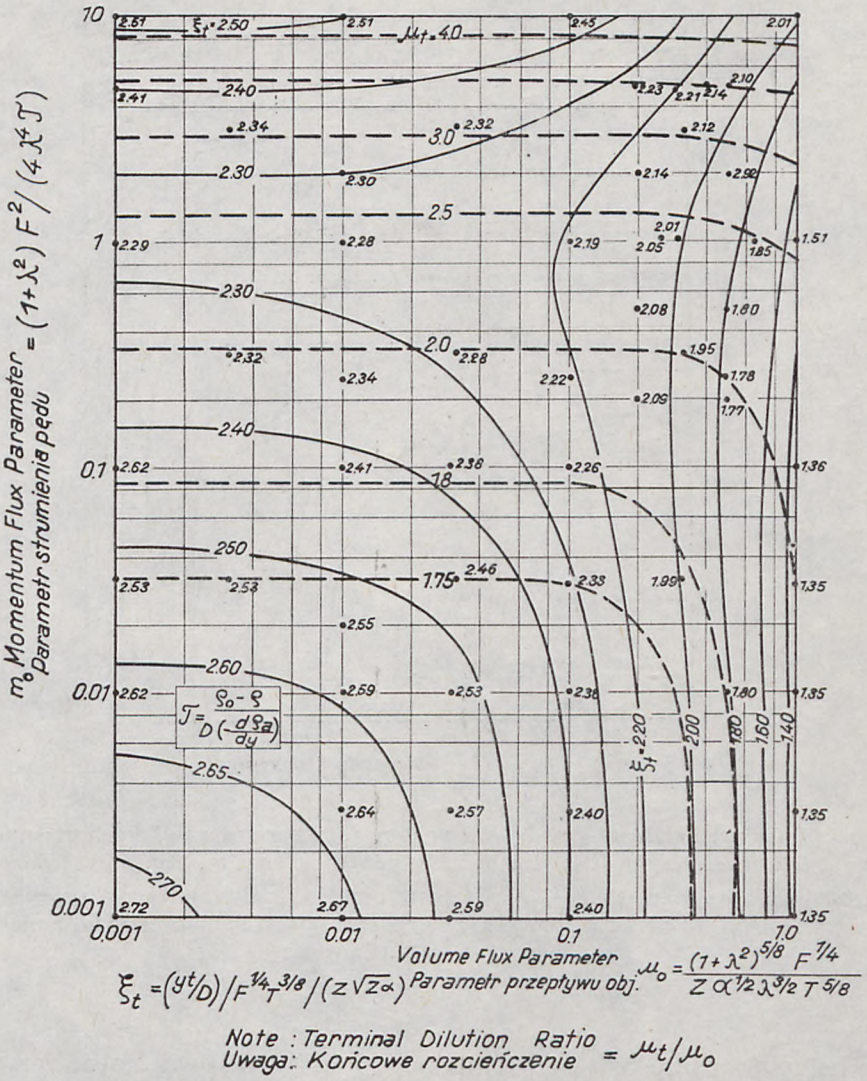

Fig. 5.6. Terminal height of rise ξ_t and volume flux parameter μ_t for vertical round buoyant jets in environments with linearly-stratified density, Fan and Brooks, 1969

Rys. 5.6. Końcowe wzniesienie ξ_t i parametr objętościowego natężenia przepływu μ_t dla pionowych kołowych strug z wyporem w ośrodkach z liniowo zmienną gęstością Fan and Brooks, 1969

charge is heated water, the excess temperature in the jet is not given by S_o, but through the density deficiency flux and the linear relation assumed between density and temperature. Detailed solutions and experimental results are given by Fan (1967) and Fan and Brooks (1969).

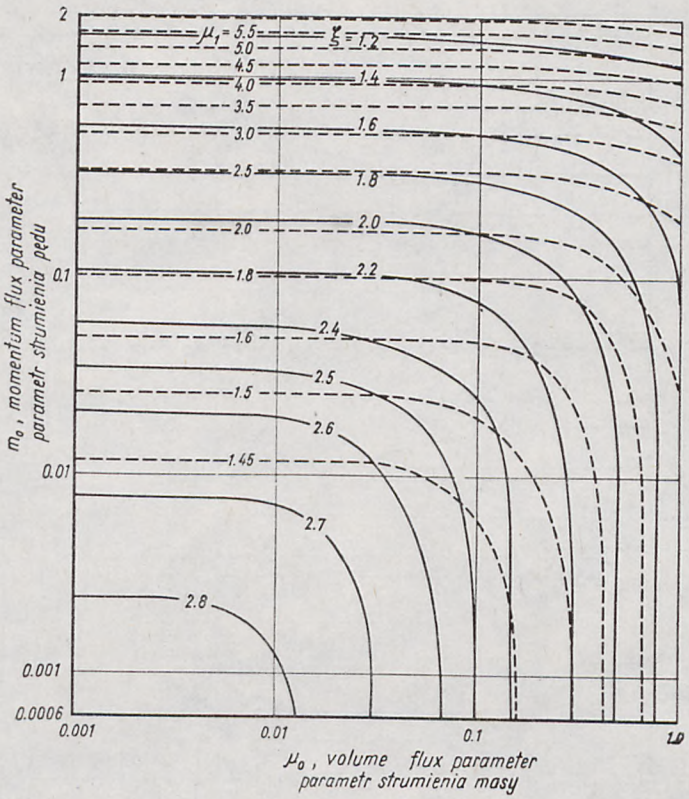

Fig. 5.7. Terminal height of rise ξ_t and volume flux parameter μ_t for horizontal slot buoyant jets in environments with linearly-stratified density, Fan and Brooks, 1969

Rys. 5.7. Końcowe wzniesienie ξ_t i parametr objętościowego natężenia przepływu μ_t dla poziomych strug szczelinowych z wyporem w ośrodku o liniowo zmiennej gęstości, Fan and Brooks, 1969

The relationship between temperature and density is linear for small temperature differences, but nonlinear for large differences. The above jet analyses cease to hold for temperature differences of 10°C or greater in the range of 10°C to 30°C, and give incorrect maximum heights of rise. This error may be readily avoided by conserving excess temperature flux instead of density deficiency flux:

$$\frac{d}{ds}\left[u_m b^2 \cdot (T_a - T_m)\right] = \frac{1+\lambda^2}{\lambda^2} b^2 \cdot u_m \cdot \frac{dT_a}{ds} \tag{5.20}$$

for round jets and

$$(\varrho_a - \varrho) = \varrho\,(T_a) - \varrho\,(T). \tag{5.21}$$

5.4.2. Arbitrary stratification of the ambient liquid

In the presence of thermocline structures, the density profiles are not linear. Description of buoyant jet behaviour in an arbitrary density profile is readily accomplished in a numerical sense, but generalized solutions are not possible as in the cases of uniform and linearly stratified environment. This means that the solutions are uniquely tied to the density profile assumed. The gradient of the ambient density in the density deficiency flux equations is no longer a constant, but varies with depth. Since the solution to the governing equations requires numerical integration, this may be carried out with the local density gradient continually adjusted according to the arbitrary ambient density profile. A computer program to find solutions for round jets in arbitrary ambient density profiles is given with examples by Ditmars (1969). Programs to solve this problem for round and slot jets are also given by Koh and Fan (1970) and in EPA publications by Shirazi and Davis (1971) and Baumgartner et al. (1971). Calculations for ambient density profiles which have rapid changes in gradient (i.e., thermoclines) often show that the jet is trapped below or in this region. However, no general conclusions can be reached and each case must be calculated individually.

5.5. Buoyant jets in recipients with currents and waves

The waste or heated water can be discharged at any angle to the ambient current, although considerable interest has been given to the cases of co-flowing (parallel to ambient current) and cross stream (perpendicular to ambient current) discharges. A good review of analyses and experimental data for round buoyant jets in flowing environments is given by Hirst (1971). Most of the analyses follow the integral approach outlined previously for buoyant jets in stagnant environments with the inclusion of either a drag coefficient to account for the pressure variations around the bend jets or additional entrainment coefficients to account for the entrainment of ambient flow momentum. Many of the analyses have been fitted to experimental data and thus their coefficients are not universal constants but vary over a range of discharge and flow conditions. Hirst's attempt (1971) in this respect falls far short of good agreement with other data.

Thus, at present, no analysis seems to be available to give a faithful prediction of the jet behaviour in a flowing environment. However, the body of experimental data is fairly large and gives a good insight into the behaviour of the buoyant jet.

A simple dimensional analysis shows that the governing parameters for a round buoyant jet into a flowing environment of uniform density are the angle of discharge relative to the current, the densimetric Froude number, and the ratio $k = V_o/V_{am}$. The larger the k, the more the jet behaves as if in a stagnant environment. For a small k, the jet is swept down current and the dilution is inhibited. Experiments by Fan (1967) show that this effect is accentuated as the jet densimetric Froude number increases. The stratification case was studied by Hirst (1971).

In the case of a slot jet it extends laterally across the flowing environment and interacts more with the ambient current than the round jet around which the ambient current can flow.

Cederwall (1971) presented experimental data on buoyant slot jet discharges in such a way as to distinguish the various regimes of flow that can occur (Fig. 5.8).

The Author has also endeavoured to give further insight into buoyant slot discharges in recipients with currents and waves. On the basis of momentum and mass conservation equations together with geometrical considerations the laws of jet centerline concentration are given for the wide range of the governing parameters shown in Fig. 5.9 along with the laboratory layout. The formulae presented in the drawing and the data furnished clearly delineate the tendency of concentration changes.

A diagram similar to Fig. 5.8 was elaborated by the Author for his studies on the effect of waves on slot jets (Zeidler 1971). Wave parameters analogous to those in Fig. 5.8 were found to control the jet regimes under wave conditions (see Fig. 5.10). The photo-electric equipment and a camera used in those studies made it possible to determine both velocity and concentration along jet centerline in different wave phases. The resulting formulae for distinct jets are

$$\frac{u_m}{u_o} = C_1 \left(\frac{D}{s}\right)^{\frac{a}{2}} \left[1 + C_2 F_o^{-2} \left(\frac{s}{D}\right)^{3/2}\right]^{1/3} \tag{5.22}$$

$$\text{and } \frac{\vartheta_m}{u_o} = C_3 \left(\frac{D}{s}\right)^{1-\frac{a}{2}} \left[1 + C_4 F_o^{-2} \left(\frac{s}{D}\right)^{3/2}\right]^{-1/3}, \tag{5.23}$$

where $a = 35 \cdot 10^{-3} \left(\frac{h^2}{gT^2H}\right)^{-0.12}$.

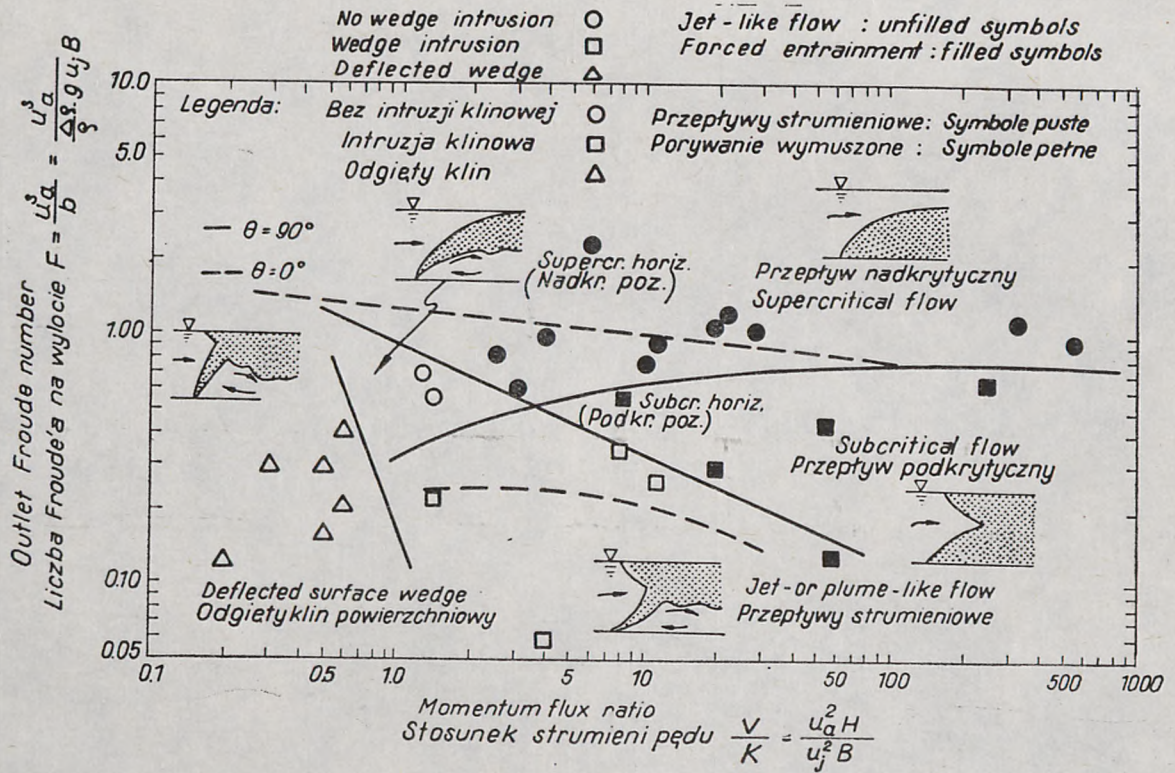

Fig. 5.8. Observed flow regimes for vertical and horizontal (in parantheses and broken) buoyant slot jets in a cross stream. Forced entrainment: the typical buoyant jet flow pattern breaks up and there is efficient mixing close to the source, Cederwall, 1971

Rys. 5.8. Reżimy przepływu dla pionowych i poziomych (w nawiasach i przerywane linie) strug z wyporem w prądzie poprzecznym. Porywanie wymuszone: struktura strumieniowa zanika i przy wylocie następuje wydatne mieszanie, Cederwall, 1971

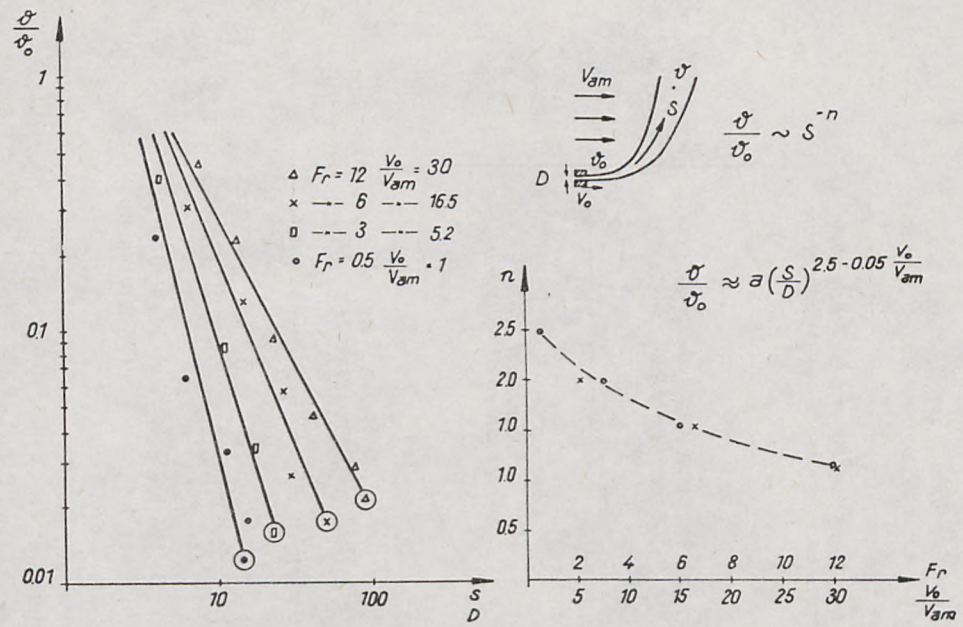

Fig. 5.9. Jet center-line concentration vs velocity ratio $\frac{V_o}{V_{am}}$

Rys. 5.9. Zależność osiowego stężenia strumienia od względnej prędkości $\frac{V_o}{V_{am}}$

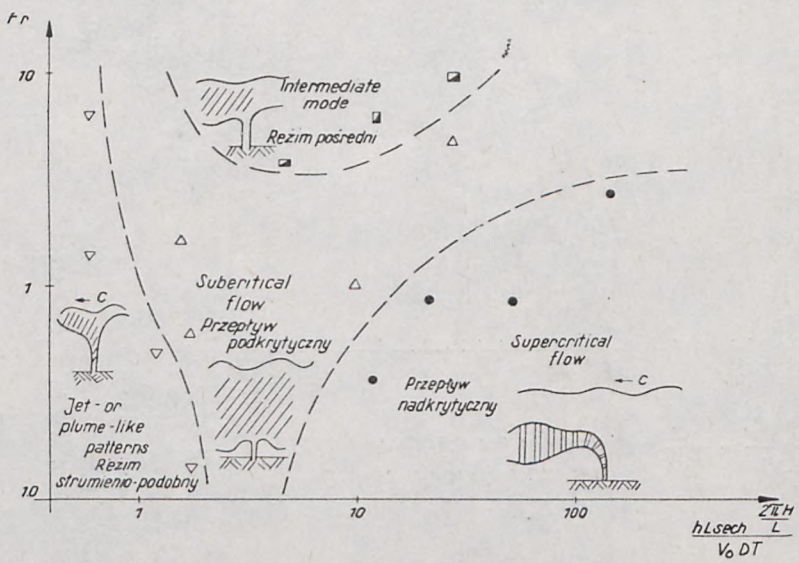

Fig. 5.10. Jet modes under ambient wave conditions

Rys. 5.10. Reżimy strumieni przy falowaniu ośrodka

5.6. Jets in shallow waters

Recipients are often shallow with respect to jet discharge outlets (this is the case as regards the Baltic Sea). Interaction of such jets with the bottom and free surface result in complex flow patterns, for which the most reasonable analytical approach consists in assuming constant depth- and length-averaged concentrations downstream a discharge diffuser (and in fact observed in experiments). Such a uniform mixing is a natural consequence of the occurence of the subcritical regimes of Figs. 5.8 and 5.10.

Adams (1972) presents an analysis of such slot diffuser structures which takes advantages of their well-mixed natures. Of the two cases presented in Fig. 5.11 let us first consider a current co-flowing with the discharged jet. By writing the one-dimensional conservation equation for momentum between sections 1 and 4, neglecting forces on the lateral boundaries and friction on the bottom, assuming frictionless Bernaulli equations between sections 1 and 2 and sections 3 and 4 for the pressure change across the diffuser, and by using the momentum equation between sections 2 and 3 for energy dissipation, one obtains u_4 and Q_1, which finally yields the following dilution

$$\frac{\vartheta_o}{\vartheta_m} = \frac{Q_1}{Q_o} = \frac{1}{2}\frac{V_a \cdot l \cdot H}{V_o a_o n} + \frac{1}{2}\left[\left(\frac{V_a l H}{V_o a_o n}\right)^2 + \frac{2 l H}{a_o n}\right]^{1/2}. \qquad (5.24)$$

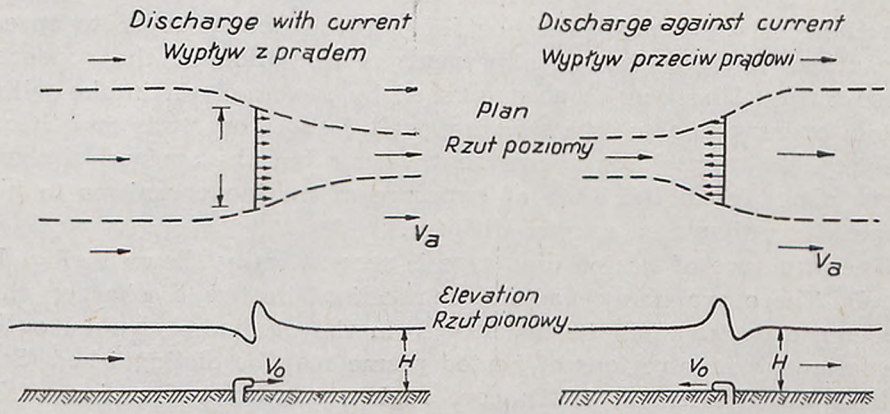

Fig. 5.11. Discharge in flowing shallow water Adams 1972
Rys. 5.11. Wypływ w płynącym ośrodku płytkowodnym Adams 1972

The case of the current aligned against the diffuser discharge can be viewed in a similar manner and is characterized by

$$\frac{\vartheta_o}{\vartheta_m} = \frac{1}{2}\frac{V_a l H}{V_o a_o n} + \frac{1}{2}\left[\left(\frac{V_a l H}{V_o a_o n}\right)^2 - \frac{2 l H}{a_o n}\right]^{\frac{1}{2}}. \qquad (5.25)$$

Discharges into time-ranging ambient cross currents exhibit maximum temperature rises at the times of minimum current velocities. Increasing port spacing in general reduces maximum temperatures.

Cases of unsteady and weak ambient currents over shallow receiving water are not readily amenable to analysis and experimental work is necessary. Diffuser structures discharging perpendicular to a steady cross current or into stagnant water exhibit re-entrainment of waste- or heated water (Harleman et al. 1972).

Chapter 6

SURFACE DISCHARGES OF HEATED WATER

By combining good engineering design with proper assessment of biological effects, once-through cooling will long remain a viable mechanism for heat dissipation in major rivers, reservoirs, large lakes and coastal waters. As pointed out in Chapter 1, in contrast to submerged diffusers, for surface discharge mixing is avoided and the heated water is "floated" onto the receiving water in a relatively thin surface layer. Heat dissipation to the atmosphere is at a maximum rate and there are no temperature changes at or near the bottom of the receiving water. Simultaneously, because of the ability of the heated layer to spread, precautions must be taken to prevent recirculation at the condenser water intake. This can be accomplished by means of an intake with a bottom opening known as a skimmer wall. Laboratory tests and theoretical considerations have shown that very often the surface discharge brings about much less time of exposure of marine organisms to high temperatures than a submerged diffuser.

The structure of heated discharge is schematically shown in Fig. 1.2, Alt. B. There are many factors controlling heated discharge; their importance varies with the distance from the discharge channel outlet. The following four regions of heated plume may be distinguished (Stolzenbach and Harleman, 1971): core region, entrainment region, stable region, and far field region. There is no significant surface heat loss in the core region, where all parameters change slightly. In the entrainment region, the jet spreads downward by turbulent processes. The lateral growth is dominated by gravitational spreading at a much greater rate than the vertical turbulent spread. Local densimetric Froude numbers in this region decrease rapidly and the dilution rises

sharply as a result of entrainment. Surface heat loss is still negligible in this region.

Vertical entrainment in the stable region is inhibited by vertical stability as indicated by the local densimetric Froude number which is of the order of one or less. The jet depth continues to decrease because of lateral spreading. The small jet depths reduce the lateral entrainment, the dilution and centerline temperature remaining relatively constant in this region. The centerline velocity, however, drops sharply as a cosequence of the large lateral spread. The surface temperature pattern is dominated by a wide constant temperature stable region.

The heat loss region marks the end of the stable region. The lateral spread is sufficiently large to allow significant surface heat transfer and the temperature begins to fall again. Once surface heat loss has begun to be important, the rate of temperature decrease is very rapid and in conjunction with the low centerline velocity the discharge may no longer be considered as a jet.

The far field region is dominated by ambient convective and diffusive processes. Moreover, if ambient flow velocities are large, the far field region may begin before the stable region has formed. The excess discharge heat is ultimately lost to the atmosphere in the far field.

From Koh's analysis (1971a) it can be seen that the flow field in a horizontal buoyant jet at the surface can be very different from that in either an ordinary nonbuoyant jet or submerged buoyant jet. For the case when no heat loss occurs at the water surface, no steady-state solution is possible. The source will be inundated sooner or later. A steady state can be found only for non zero heat exchange.

Accordingly, at some distance from the source, when the local Richardson number reaches a critical value, the jet ceases to expand and the phenomenon resembles a two-layered stratified flow. From that point on, the flow can no longer be classified as a free turbulent flow but may be divided into the zone of flow establishment, the supercritical region, where the flow is basically a jet with decreasing entrainment rate, the internal hydraulic jump and the subcritical region, where interfacial shear on surface heat exchange plays a dominant role. The last two zones may be absent if the surface heat exchange coefficient K_e is sufficiently large. In that case the flow field is similar to that in an ordinary jet. If K_c is sufficiently small, the source becomes inundated and it is only the last zone that exists.

It may be argued (Pedersen 1972) that the assumption of shear τ_i transferred to the bottom is unacceptable and thus the whole concept of the entrainment process occurring only at supercritical flow should be

modified. This seems to be supported by empirical evidence and, according to Stolzenbach and Harleman (1971), the prediction of internal hydraulic jumps is probably not of importance in the case of three-dimensional discharges, mainly due to the lateral spreading of warm water. Koh's assumptions are also contradicted by the fact that in a self-similar flow the coefficient of surface heat exchange must be constant. On the other hand, Stefan at al. (1971 confirm findings of Koh for the two-dimensional case. The mixing zone near the outlet may be a buoyant half-jet followed by an internal hydraulic jump, a free internal hydraulic jump or a submerged outlet flow. Stefan et al. derive the conditions for the occurrence of these flows and the associated entrainment ratios. Hence, definite determination of whether internal hydraulic jump occurs in the three-dimensional (axisymmetric) case is a matter of the future.

The basic set of the equations governing the surface heated discharge consists of three Navier-Stokes equations (for x, y, and z-momentum) together with the equation of mass conservation, heat conservation, and thermal expansion. All of them are considered for the turbulent state, when additional term appear because of turbulent fluctuations. These equations must be analysed as to the order of magnitude of respective terms; various assumptions may be made, and space integration over the jet is required to arrive at the final set. Before turning to this set let us examine the major factors that play a role in its selection.

Among them, entrainment poses most problems. For non-buoyant jets, the entrainment coefficient α is generally taken as constant for horizontal and vertical entrainment. Morton et al. (1963) first applied the idea represented by Eq. 5.1; Abraham (1963) and (1965) pointed out that the values of α for simple jets and simple plumes were different (0.057 vs 0.082). He proposed a variable α to account for variable growth of horizontal and vertical jets. Fan and Brook's (1965) results for constant $\alpha = 0.082$ agree well with their experimental findings and Abraham's analysis. However, in the light of Fan's work (1967), for vertical jets in stratified environments, the prediction of terminal heights of rise by using $\alpha = 0.057$ seemed to give better results. Naturally, the dependence of vertical entrainment on stratification, as given by Ellison and Turner (1959)

$$\frac{\alpha_{zs}}{\alpha_z} = \exp\left[-5\,\frac{g\dfrac{\Delta\varrho_c}{\varrho}H}{u_c^2}\right] \tag{6.1}$$

still holds. For round buoyant jets in uniform environments the solution for jet trajectories by using $\alpha = 0.082$ agreed better with observed jet flows than Abraham's solutions.

Fan (1967) analyzed the problem of a buoyant jet in a uniform cross stream by assuming an entrainment mechanism based upon the vectorial difference between the characteristic jet velocity and the ambient velocity. The coefficient α varied from 0.4 to 0.5 in the ten cases studied where the Froude jet number ranged from 10 to 80 and for the velocity ratio (jet-current) of 4 to 16.

From Motz and Benedict's tests (1972) it follows that geometry is apparently the major factor in determining α, which decreases with decraasing values of ambient flow width to initial jet width. Three values of 0.16, one of 0.44, and one of 0.44 were found for α in five field runs. On the other hand, no correlation between the entrainment coefficient, α, and the velocity ratio was found in a rectangular flume (2.0-ft wide and 1.0-ft deep). The mean value of α did, however, decrease with the outlet angle β_o' although it might have been due to the proximity of the wall — which restricted entrainment at the inner edge of the jet.

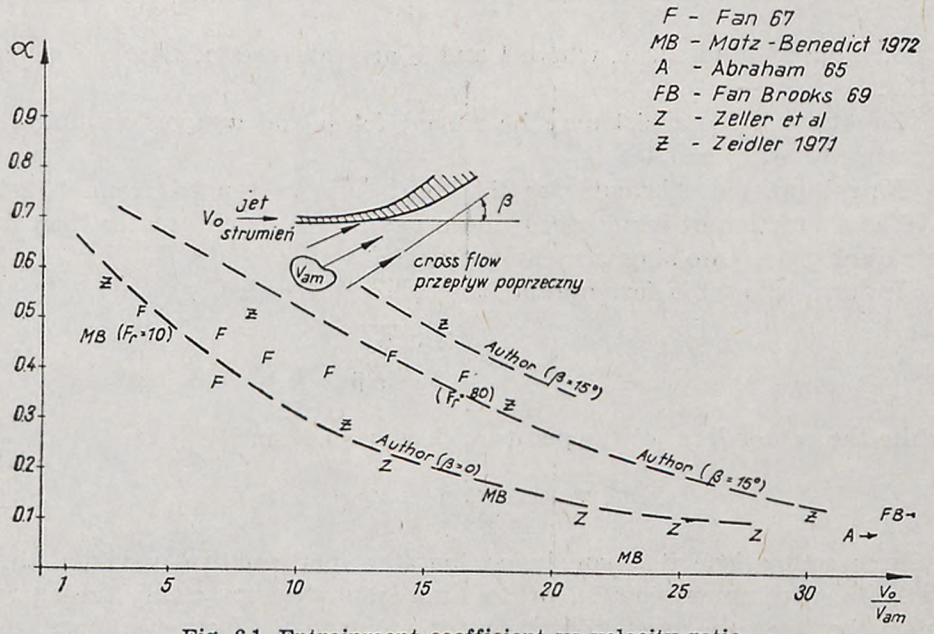

Fig. 6.1. Entrainment coefficient vs velocity ratio

Rys. 6.1. Współczynnik porywania α dla przepływu poprzecznego

The Author has added to the above exploration of α by measuring velocities and concentrations for round and slot surface jets flowing with and against ambient water in a rectangular channel. The observed values of α are shown in Fig. 6.1 and compared with other data. They expose considerable dependence on both jet width and resulting velocity.

Moreover, the character of this relationship is quite similar to that of submerged jets.

As to the pressure term in the Navier-Stokes equations, Tamai et al. (1969) show that it reaches 3 percent within the range of distances $\frac{x}{h_o}$ between 0 and 50.

In the case of a cross flow which deflects the jet at angle to shore line, expressions for α can be obtained from the mass and momentum conservation relations (Zeller et al. 1971).
In the equations

$$\alpha = \frac{I_1}{4}\left(\frac{db}{ds} - b \operatorname{ctg}\beta \cdot \frac{d\beta}{ds}\right), \tag{6.2}$$

$$\alpha = -\frac{V_o I_2 \cdot b_o^{1/2}}{2 V_L} \frac{b^{1/2}}{(\sin\beta)^{3/2}} \frac{d\beta}{ds}. \tag{6.3}$$

α is a function of the rates of spread $\frac{db}{ds}$ and curvature $\frac{d\beta}{ds}$ of the jet for negligible wind shear, where I and I_2 are integrals of flow characteristics.

Equations 6.2 and 6.3 may be solved for β and α upon assuming a certain rate of spread.

Entrainment coefficients for the field surveys ranged from 0.07 to 0.78 as a function of wind speed; these values are much greater than for jets discharging into stagnant environments.

In terms of such a formulation, the center-line velocity is

$$V_{sm} = \frac{V_o \sqrt{b_o}}{\sqrt{b \cdot \sin\beta}} \tag{6.4}$$

while the center-line jet temperature decrease becomes

$$T_{sm} = \frac{Q_o}{Q}(T_o - T_m). \tag{6.5}$$

From comparison it is concluded that the mathematical model with a variable entrainment coefficient does not improve appreciably the agreement between the predicted characteristics and field observations.

Furthermore, Stolzenbach, and Harleman (1971) found that cross flow deflects the surface jet but does not change the dispersion characteristics. substantially. However, this has not been confirmed by another set of experiments performed by the Author in a laboratory channel. As shown in Fig. 6.2, the lateral spread of the surface jet deflected by cross-flow is quite pronounced in comparison with the stagnant recipient. The empirical curve fitted in Fig. 6.2 may be used as

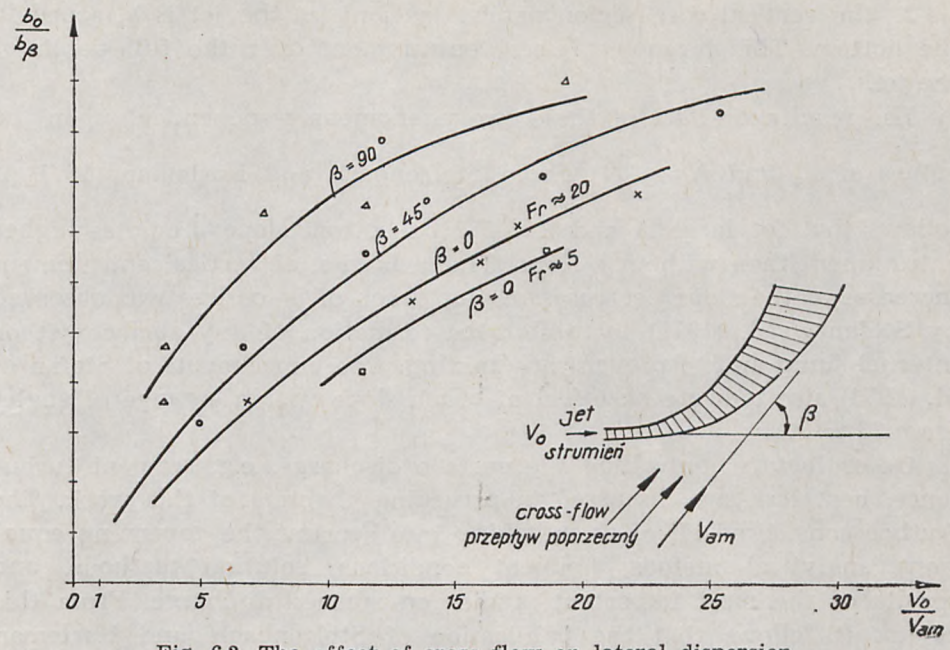

Fig. 6.2. The effect of cross flow on lateral dispersion

Rys. 6.2. Wpływ przepływu poprzecznego na rozproszenie poprzeczne

a guideline in choosing the best analytical model for the effect of a cross flow. Motz and Benedict established that a realistic value of the drag coefficent C_D, in the case of cross flow acting against be surface discharge is about 0.5.

Temperature and velocity distributions in a surface plume are most often assumed to remain basically structured as in a turbulent jet. Abramovich (1963) introduced $(1 - X_i^{3/2})^2$ and $(1 - X_i^{3/2})$ for velocity and concentration profiles, respectively, in both lateral and vertical direction. The internal mechanism of surface discharges was observed in a series of studies by Tamai (1969). Tamai et al. (1969), Jen et al. (1969), and Dornhelm et al. (1970). They point out that the surface distribution of temperature is not desribed by Gaussian curves. Considerable velocity and temperature fluctuations of the order of 10 (for velocity at $\frac{x}{D} = 10$, $F_o = 3.2$, and $Re = 12{,}600$) were measured.

Bottom slope has two counteracting effects upon the jet:

1. Vertical entrainment is inhibited by the presence of a solid boundary,

2. the vertical core region persists as long as the jet is attached to the bottom. This promotes lateral entrainment over the full depth of the jet.

The resultant effect of these two phenomena is dependent upon the values of F_o and $A = \frac{h_o}{b_o}$. From Stolzenbach and Harleman (1971) it follows that for large A and low F_o the bottom slope promotes higher entrainment than without a slope. The reduction of vertical entrainment increases as the slope decreases. A flat beach of 5° or less was observed by Stefan et al. (1971) to inhibit the formation of any surface jet or internal jump and to prevent any mixing. The experiments of Stefan et al. (1971) also indicate no effect of beach slope within a range of angles from 23 to 90°.

Other factors controlling the surface discharge, e.g. ambient turbulence, heat loss, are discussed in preceding chapters of this work. The Author considered all of them taking into account the governing equations, analytical metods, ambient conditions, solution methods, and results of the most important studies on surface discharge. From this review it follows that the publication of Stolzenbach and Harleman

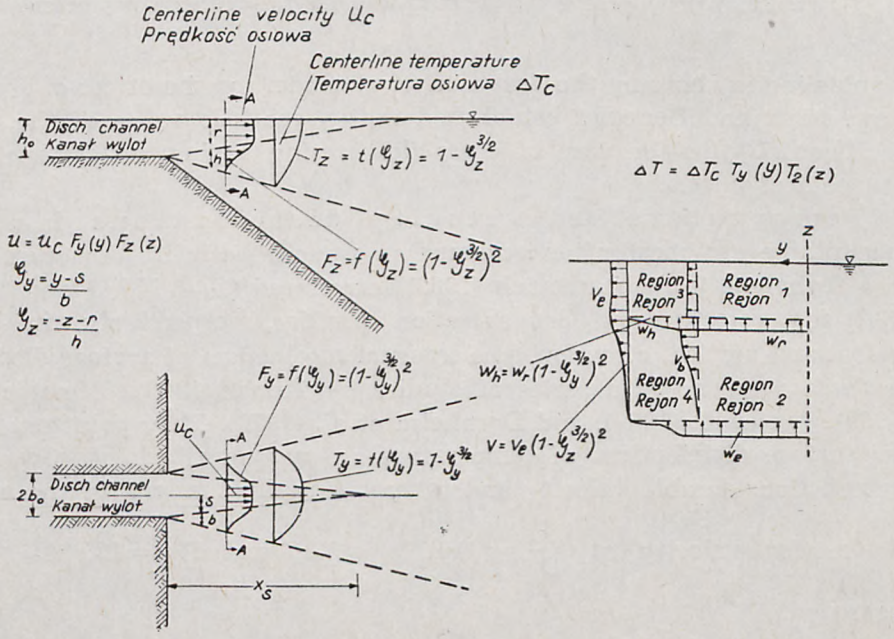

Fig. 6.3. The structure of surface jet proposed by Stolzenbach and Harleman (1971)
Rys. 6.3. Struktura strugi powierzchniowej proponowana przez Stolzenbacha i Harlemana (1971)

(1971) provides the deepest insight into the phenomenon and gives the best analytical and experimental description. The jet structure and the velocity and temperature distributions assumed in that study are shown in Fig. 6.3. In the case of cross flow the basic equations consist of a set for continuity, momentum, jet heat, jet bending, and jet position in all the four regions discussed above. Some characteristic results can be seen in Fig. 6.4.

In dimensionless form the temperature field can read

$$\frac{T - T_a}{T_o - T_a} = f\left(F_o, A, \frac{K_e}{\varrho C U_o}, \frac{V}{u_o}\right). \tag{6.6}$$

The theoretical lower limit for F_o is 1.0 since for lower values a stagnant wedge of ambient water will intrude into the discharge channel, forcing a value of $F_o = 1.0$ at the exit section.

The solution of the basic equations proceeds by computer-aided inte-

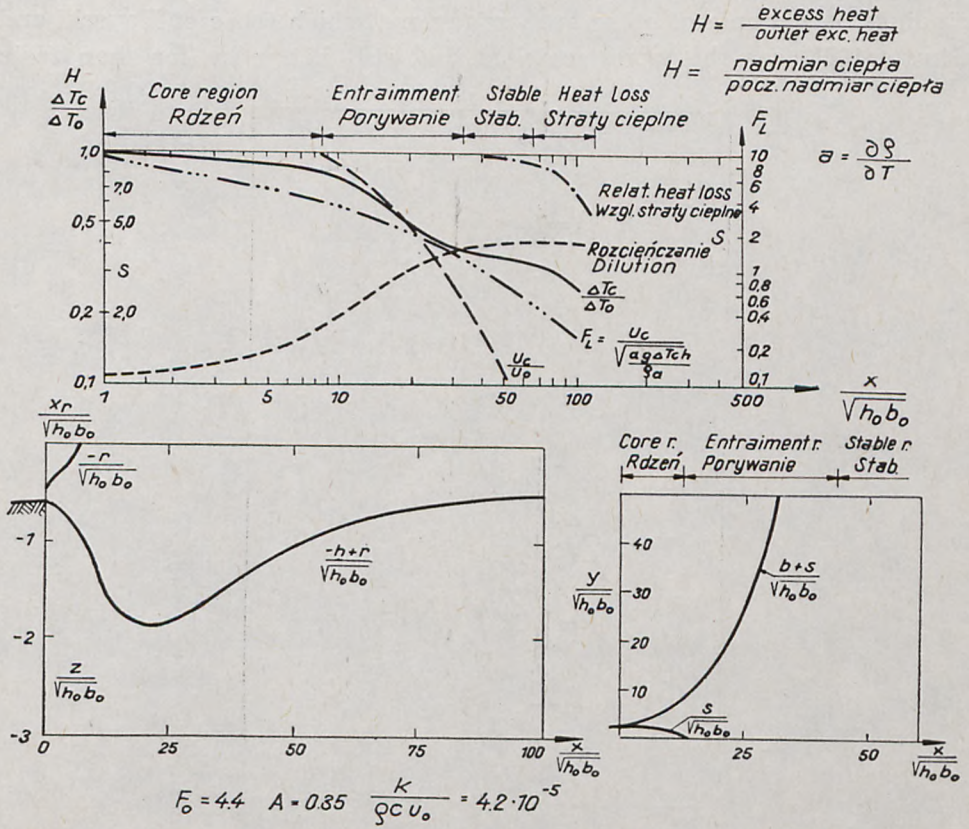

Fig. 6.4. Results of Stolzenbach and Harleman's (1971) theoretical calculations

Rys. 6.4. Wyniki teoretycznych obliczeń Stolzenbacha i Harlemana (1971)

gration of the equations over the jet cross-sections. Some alterations have been introduced to the resulting program by the Author because of the improvements, mainly for ambient turbulence, discussed in this study. The resulting set of integrated equations yields values for u_c, T_c, r, s, h, b, F_L, x_r, and H for all x. This set may not be solved by exact methods, but obviously a numerical solution to the resulting equation can be developed by means of a fourth order Runge-Kutta integration technique.

As an asymptotic case, the boyant terms for large F_o are small and the centerline temperature is given by

$$\frac{T_c - T_a}{T_o - T_a} = \frac{10.7 \cdot \sqrt{h_o b_o}}{x}; \quad F_o > 15 \tag{6.7}$$

in agreement with quite a few empirical data for slightly buoyant jets.

It should be noted that the Stolzenbach-Harleman method proves to be best among others as it not only matches well the evidence of their own laboratory tests, but also describes quite satisfactorily empirical findings of a couple of other authors (among which those of Hayashi and Shuto (1968) are the worst matched, but still better by far than their

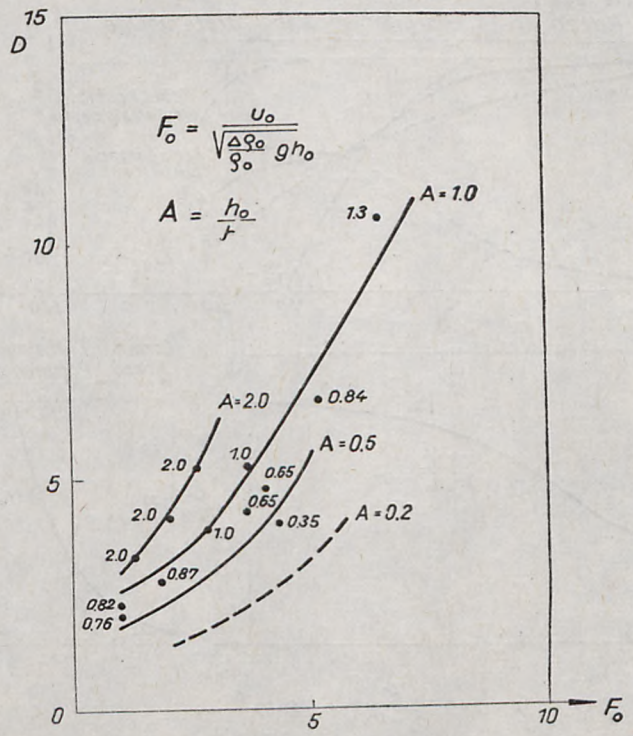

Fig. 6.5. Dilution in the stable region (after Stolzenbach and Harleman, 1971)
Rys. 6.5. Rozcieńczenie w strefie stabilizacji (wg Stolzenbacha i Harlemana, 1971)

original theory). Some dilution data of Stolzenbach and Harleman are presented in Fig. 6.4 together with the Author's results obtained indirectly for smaller aspect ratios.

Results of a number of works are given as quite simple formulae for velocities and temperatures. The empirical data of Tamai et al. (1969) indicate the decrease of $\frac{T - T_a}{T_o - T_a}$ proportional to $\left(\frac{x}{D}\right)^2$, thus being in agreement with Hayashi and Shuto's formula (1967) rather than with those given by Jen et al. (1966). The latter found that for values of $\frac{x}{D} <<$ about 100 the surface temperature along the centerline of a warm water jet discharging horizontally at the water surface can be expressed as

$$\frac{T_c - T_a}{T_o - T_a} = 7.0 \frac{D}{x} \tag{6.8}$$

for $18 < E_o < 180$ and $8{,}300 < Re < 21{,}000$.

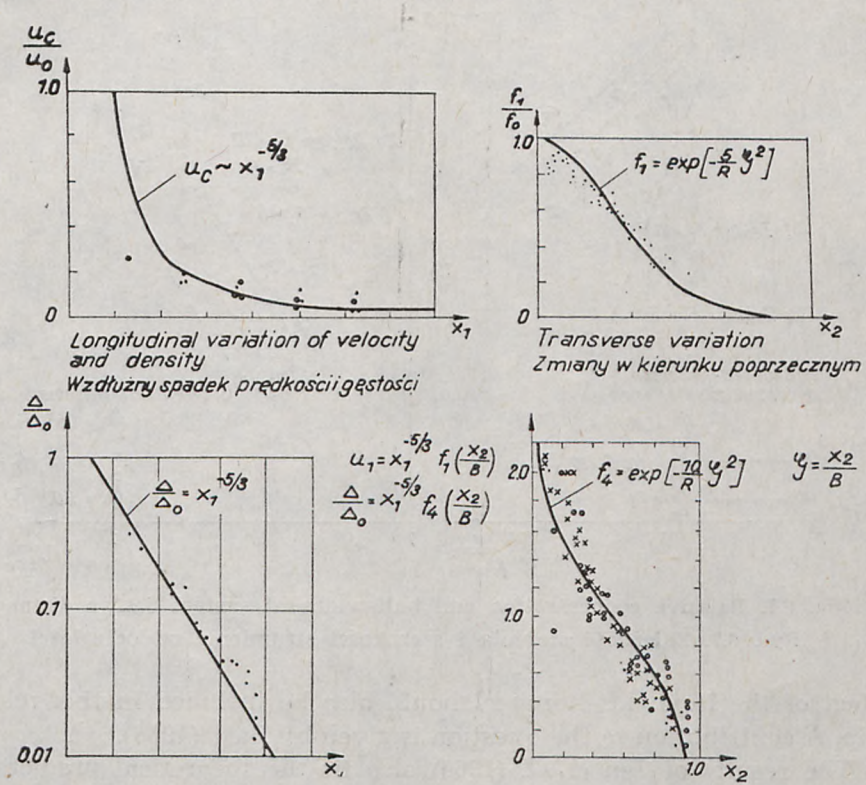

Fig. 6.6. Surface jet velocity and density variation (Engelund-Pedersen 1972)
Rys. 6.6. Zmiany prędkości i gęstości strugi powierzchniowej

The lateral distribution is exponential

$$\frac{T - T_a}{T_c - T_a} = \exp\left[-3 F_o^{1/2} \left(\frac{y}{x}\right)^2\right]. \tag{6.9}$$

As the process is rather a highly irregular one, considerable variations must be expected from the mean values predicted by use of this formula. This is especially true for $\frac{X}{D_o} > 100$.

The half-width y_c was found to vary linearly with x. An analogous result, $\frac{y}{D} = C_1 \cdot \frac{x}{D F_o^{1/4}} - C_2$, was observed by Wood and Wilkinson (1966), and was again confirmed by Tamai et al. (1969), with a wider spread due to buoyancy. As has been pointed out by Tamai et al., the

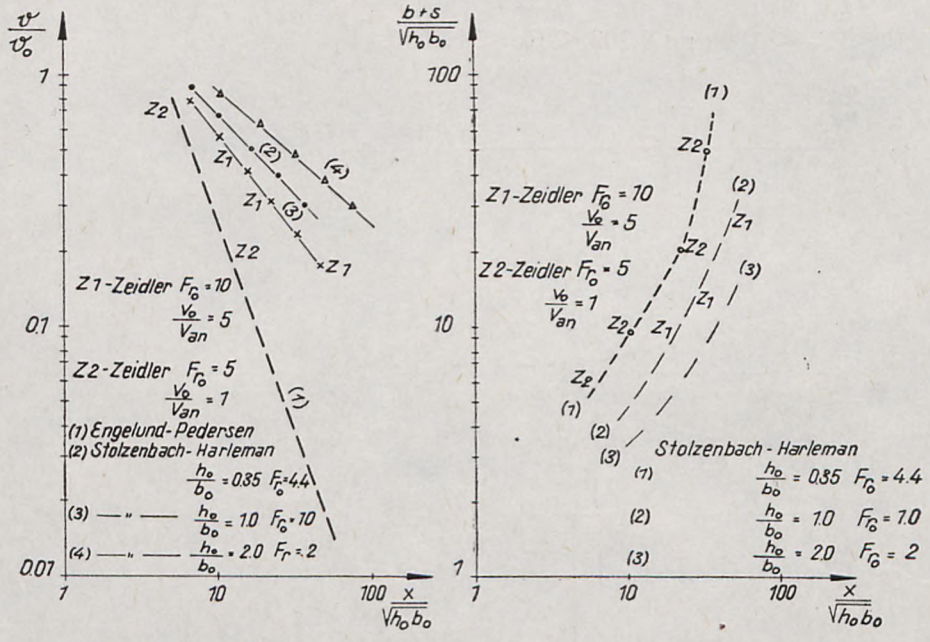

Fig. 6.7. Relative concentration and half-width of surface jet vs distance
Rys. 6.7. Zależność stężenia i szerokości strumienia od odległości

effect of the Reynolds number should also be included in this relationship. A contribution to the question is given by Barr (1966).

The results of Jen et al. (1966) also fit the theoretical pradiction of surface jet for all Richardson numbers by Engelund and Pedersen 1972).

They derived the following relationship

$$u_1 = x^{-5/3} \exp\left[-\frac{5}{R} \cdot \frac{y^2}{B^2}\right] \tag{6.10}$$

$$\frac{T}{T_o} = x^{-5/3} \exp\left[-\frac{10}{R} \cdot \frac{y^2}{B^2}\right], \tag{6.10.1}$$

where $R = 0.15\ Ri \cdot x^{-8/3}$. The agreement between empirical and theoretical findings is shown in Fig. 6.5.

Some results obtained by the Author in this area are compiled in Fig. 6.6 along with other data discussed herein.

In addition to the above, it must be stated that the density in estuarine and coastal waters is affected by both temperature and salinity, which may result in the sinking of heated water.

Chapter 7

EXPERIMENTAL TECHNIQUES

This chapter contains a brief discussion of the techniques which aid empirical investigations, both field and model, conducted in the area discussed. As may be seen from the accompanying chapters, empirical studies are still required to explore different aspects of advection, diffusion, heat transfer, initial dilution, biology and chemistry of the recipients, etc. Among them, advection and diffusion patterns focus most attention of researchers, both for general exploratory purposes in the construction of universal theories and to expose specific characteristics of a given area (as many factors and coefficients remain unknown and must be determined experimentally). However, we shall deal only with those techniques which are most directly coupled with the design of marine discharges of wastes and heated water and thus the standard oceanographic equipment will not be presented. The primary purpose of this chapter is to describe the techniques used by the Author (against the background of others' procedures and instrumentation), to analyse the errors involved and to make pertinent comparisons. Fig. 7.1 attempts to compile the tracers used in the investigation of currents as well as dispersion and the detection methods. Chemical tracers include such properties as oxygen demand, pH, amount of elements, etc. and may be

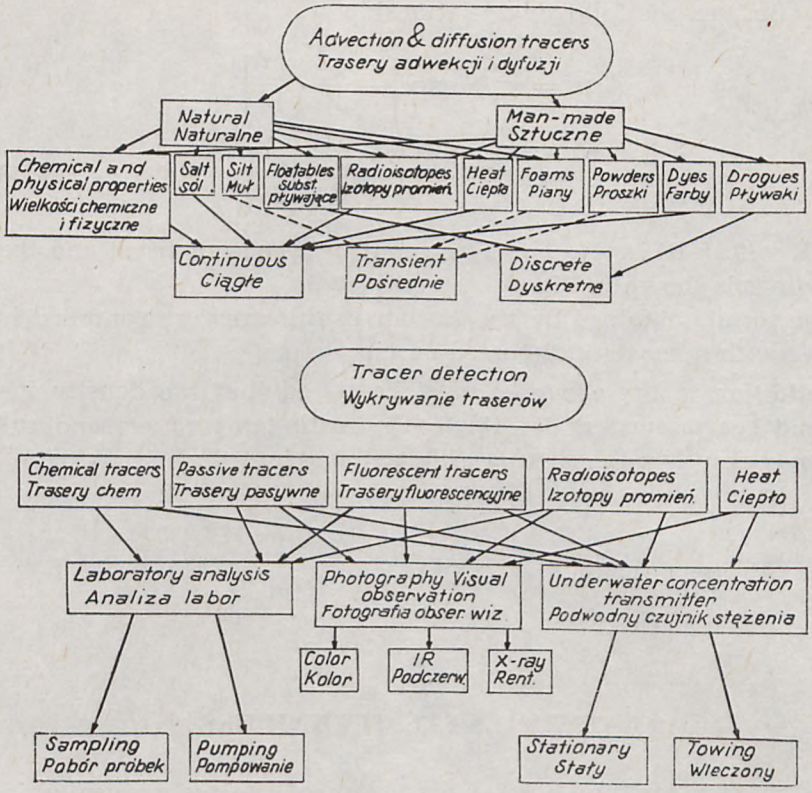

Fig. 7.1. Advection and diffusion tracers and their detection

Rys. 7.1. Trasery adwekcji i dyfuzji i ich wykrywanie

detected similarly to analogous physical properties, as conductivity. Passive tracers (floatables, non-fluorescent) are such, which do not affect the dynamics of the recipients and at the same time are not qualified to fall into other categories. The other terms are self-explanatory.

A comprehensive discussion of passive tracers (with some reference to dyes) is given by Waldichuk (1967). Therefore only some of them will be mentioned along with examples of the Author's solutions.

Coastal droques used by the Author are shown in Fig. 7.2. Both types do not differ much as to the representation of water motion, which is averaged over the surface layer, without any significant effect of wind on the marking flag especially for lower winds. It is recommended to apply groups of floats amounting to about 40—50. This number is sufficient to ensure reasonable statistical characteristics of diffusion and does not cause too much handling effort.

For a normal distribution of Lagrangian co-ordinates the confidence

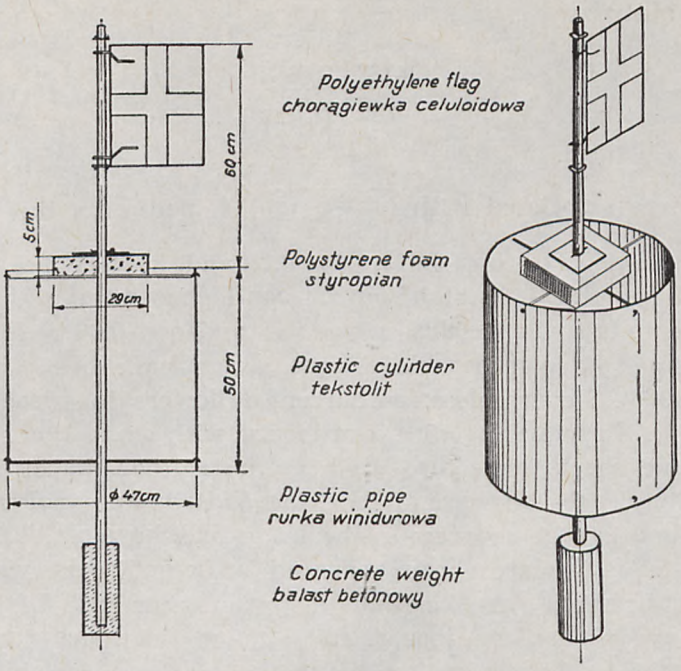

Fig. 7.2. Surface drogues used by the author
Rys. 7.2. Pływaki powierzchniowe stosowane przez autora

level of the standard deviation $\tilde{\sigma}$ is given by

$$\alpha = P\{\gamma_1 \tilde{\sigma} < \tilde{\sigma} < \gamma_2 \tilde{\sigma}\} = P\left\{\frac{\sqrt{k}}{1+q} < \chi < \frac{\sqrt{k}}{1-q}\right\} = \int_{\frac{k}{1+q}}^{\frac{k}{1-q}} P_k(\chi)\, d\chi \qquad (7.1)$$

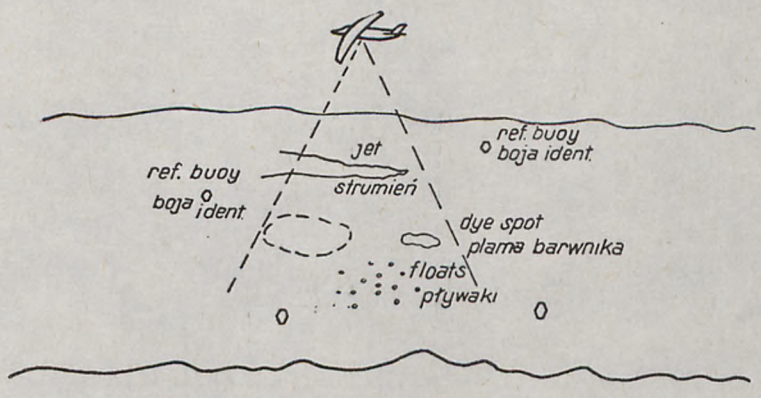

Fig. 7.3. Aerial photographs of tracers
Rys. 7.3. Zdjęcia lotnicze traserów

with the probability

$$P_k(\chi) = \frac{\chi^{k-1} e^{-\frac{\chi^2}{2}}}{2^{\frac{k-2}{2}} \Gamma\left(\frac{k}{2}\right)} \tag{7.2}$$

and $q = \frac{\varepsilon}{\tilde{\sigma}}$ for ε associated with $(\tilde{\sigma} - \varepsilon, \tilde{\sigma} + \varepsilon)$ and k as the number of droques less one. For $\alpha = 0.913$, $q = 0.2$, and $k = 40$ one obtains $\gamma_1 = 0.847$ and $\gamma_2 = 1.228$, i.e. fairly wide confidence intervals. This is, however, difficult to avoid because $\alpha = 0.941$ and $q = 0.06$ require $k = 500$. Other sources of considerable droque errors have been indicated by Terhune (1968). Nevertheless, as current followers the droques are not as bad as for dispersion studies. Hardboard with small floats, paper, and polyethylene sheets were also used by the Author. Paper is inexpensive and simple to dispense, while hardboard and polyethylene remain intact and can be recovered. The latter are, however, hazardous to navigation. 50-cm squares have appeared sufficient to be visible on aerial photographs taken over the whole dispersion area (Fig. 7.3). Unlike the flag-marked droques, hardboard and similar floatables cannot be observed geodetically. This is an irrelevant feature in the case of labora-

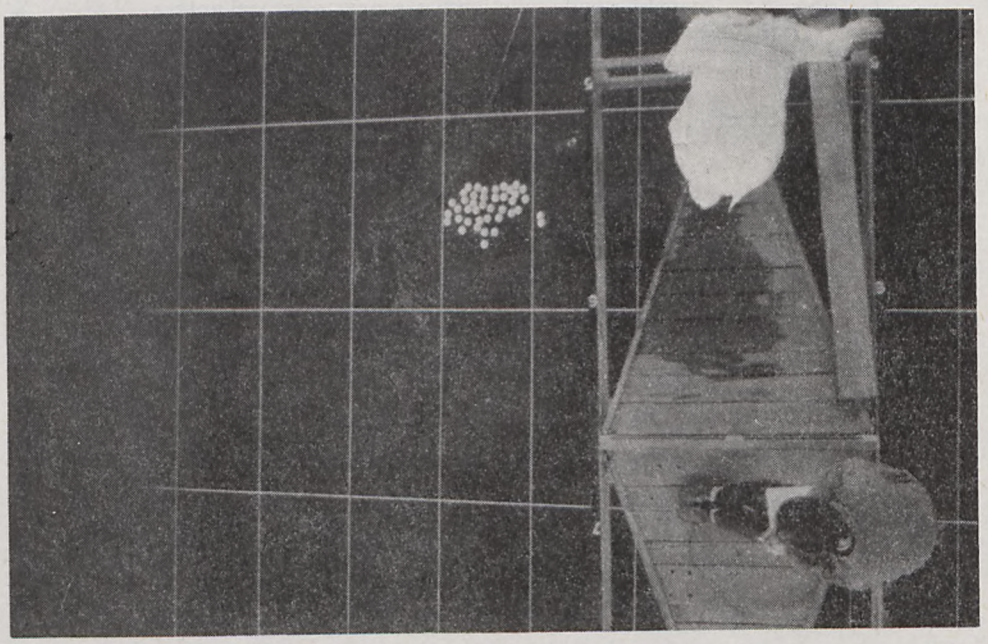

Fig. 7.4. Ping-pong tracers in laboratory

Rys. 7.4. Trasery ping-pongowe w laboratorium

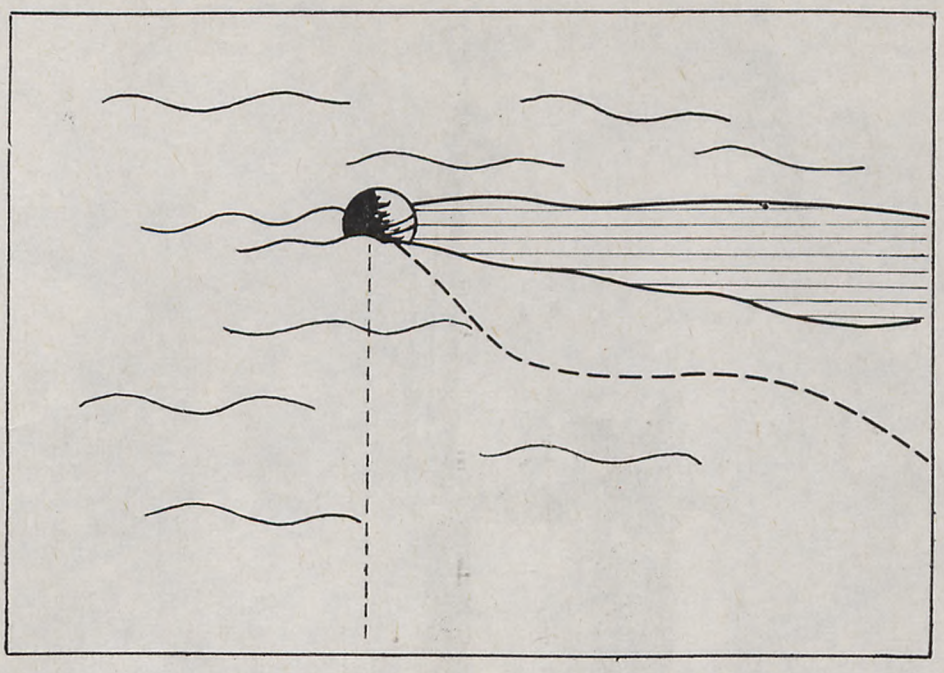

Fig. 7.5.a. Continuors discharge of tracer: buoy
Rys. 7.5.a. Ciągły zrzut trasera: boja

tory studies. Fig. 7.4 present an instantaneous layout of a group of pin-pong balls partially filled with water (in order to avoid their sticking), which proved helpful in the Author's investigation of wave-induced dispersion.

Ordinary non-fluorescent dyes are inconvenient because they are suitable mainly for short time-lapse aerial photography. It is much more promising to rely on fluorescent tracers, which can be detected in small concentriations. A comprehensive account of fluorescent dyes has been given by Feuerstein and Selleck (1963), Diachishin (1963), Ozmidov (1970), and many others. Rhodamine B and uranine turn out to be the most suitable because of their detection level, photochemical decay, difference from seawater fluorescence, cost, adhesion to suspended particles, handling possibilities, etc. Fluorescent tracers may be released as either continuous discharges (the Authores field and laboratory studies — Fig. 7.5) or point sources (field — Fig. 7.6).

In a series of the Author's studies on the biochemical decay of municipal wastes (Chapter 9) it was established that dissolved oxygen data may be used as dispersion indicators for short times up to 5 hours. In contrast to fluorescent tracers, D.O. varies within one order of magni-

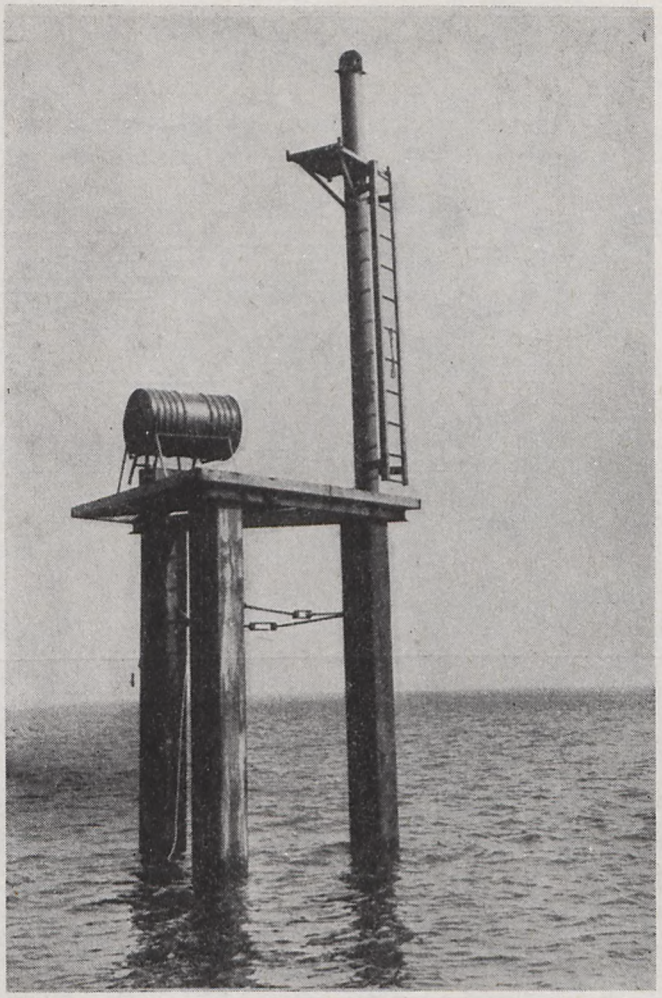

Fig. 7.5.b. Continuous discharge of tracer: dolphin
Rys. 7.5.b. Ciągły zrzut trasera: dalba

tude, which yields data fairly insensitive to ambient changes. This is also true for conductivity, pH, contents of different marine elements, salinity, etc. (IGW report 1968). Hence, chemical and physical properties of this kind seem to be suitable only in a limited sense for mapping advection (compare Palmer 1972); some promises are indicated by Wilde (1971).

An appropriate radiotracer must have good contrast against the marine background and an optimum half-life, its concentration cannot be toxic to marine organisms, and its sorption by suspensions and bottom

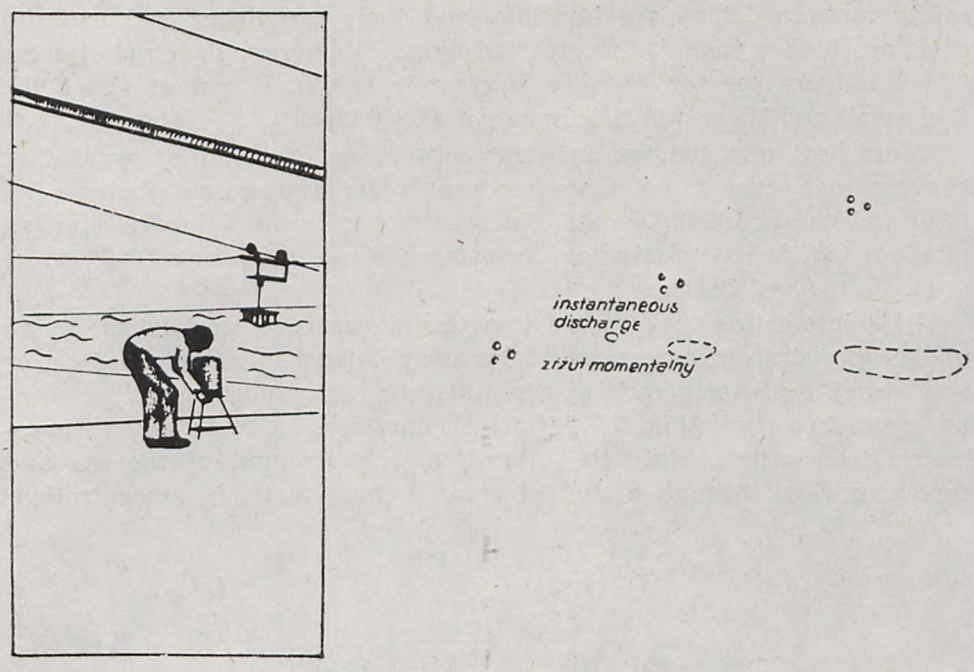

Fig. 7.6. Instantaneous discharge of tracers with overhead container

Rys. 7.6. Chwilowy zrzut traserów z kolejki linowej

must be limited; naturally, a good tracer should be inexpensive and commercially available. The most common radioisotope used in marine diffusion studies is bromine Br-82 (NH_4Br). Radioisotopes require special

safety measures, they are invisible, and their equipment and material costs are higher than for fluorescent dyes. Bibliography on radiotracers is voluminous, see for instance Harremoës (1967), Barret et al. (1968), Cederwall and Hansen (1968), Bonde et al. (1967).

Most heat and temperature transmitters and techniques are rather conventional, except for more modern infrared airborne photopraghy (see e.g. Weiss, 1970). Nonetheless, aerial photography has become an efficient tool in coastal studies (for reference see Waldichuk 1967, James et al. 1971, Assof 1971).

It is interesting to compare two techniques of tracer detection: an underwater transmitter versus laboratory analysis (either onshore or shipborne). Both techniques can be illustrated for fluorescent dyes scanned from two ships (Fig. 7.7), of which one tows an underwater fluorometric transmitter, while the other pumps water out of the sea and forces its flow through a studied area. In both methods concentrations

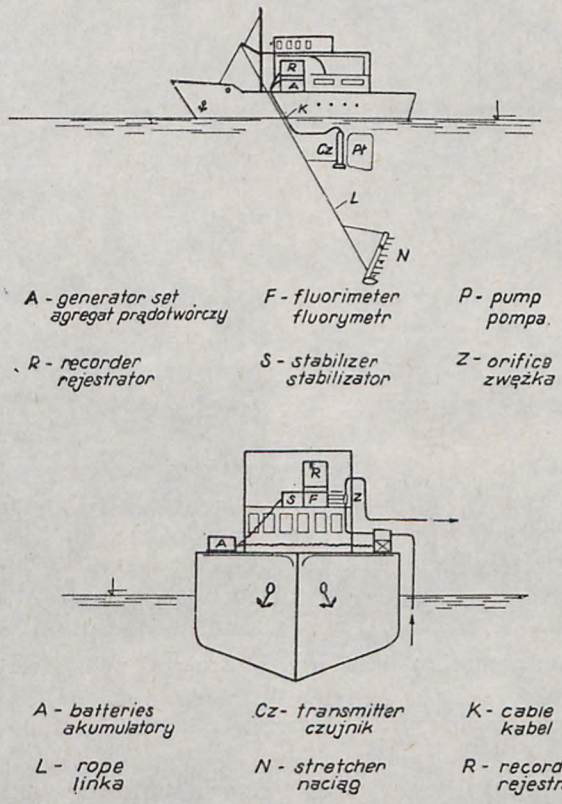

Fig. 7.7. Towed-transmitter and pumping techniques for fluorescent tracers

Rys. 7.7. Metody wleczonego czujnika i pompowania dla traserów fluorescencyjnych

are recorded aboard. The Author has found that the pumping technique was more suitable in his micro- and mesoscale coastal measurements (Ceglarski et al. 1972) as it does not involve excessive mixing due to the large size of the underwater transmitter equipment consisting of transmitter housing (about 1 m long as for Karabashev's 1966), stabilizers, ropes, etc. The suction nozzle of the pumping hose attached to a small streamlined weight or to a vertical column enabled the Author to measure concentrations from a motor boat in depths as shallow as 0.5 m.

Sampling on site is not recommended (unless suitable probes and instruments for continuous scanning are available, but even so pumping should be preferred to sampling), but it may be used on a laboratory scale (Fig. 7.8), although scanning with a continuous-operation pumping

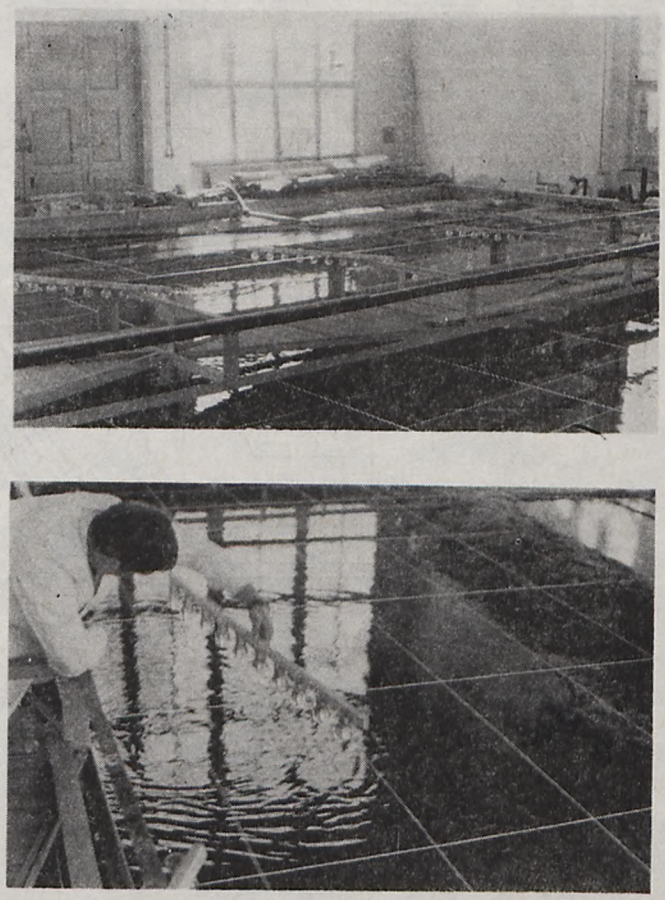

Fig. 7.8. Manual sampling
Rys. 7.8. Ręczny pobór próbek

system ending with a syringe needle (Fig. 7.9) is more accurate and adequate. Details of the fluorescent techniques used by the Author may be found in Zeidler et al. (1970). Ceglarski et al. (1972), and other papers by the Author.

Some promise in remote sensing of the concentration of fluorescent solutions is offered by aerial photography coupled with subsequent photodensitometric measurements on films, see Ichiye and Plutchak (1966). This method requires higher dye concentrations and good atmospheric conditions.

Some complications in waste—oriented diffusion studies are connected with the decay of both wastes and tracers due to various factors (biochemical, photochemical, radioactive, etc.). An ideal case would arise

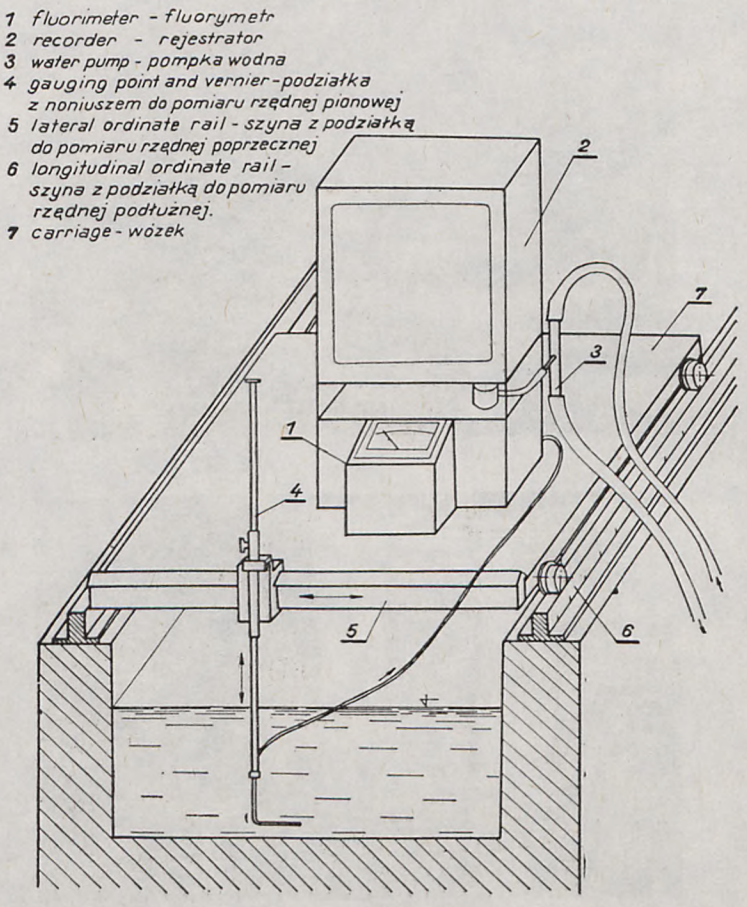

Fig. 7.9. Continuous sampling
Rys. 7.9. Ciągły pobór próbek

if a tracer had a half-life period identical with that of wastes. Since this requirement is rarely satisfied, an efficient research alternative is provided by the use of two disparate tracers of different half-lives T_{p1} and T_{p2}, being released continuously at rates of Q and Q_2. From the concentrations observed at a given point

$$\vartheta_1' = \vartheta_1 \exp\left(-\frac{\tau \ln 2}{T_{p1}}\right), \tag{7.3}$$

$$\vartheta_2' = \vartheta_2 \exp\left(-\frac{\tau \ln 2}{T_{p2}}\right) \tag{7.4}$$

and from

$$\frac{\vartheta_1}{Q_1} = \frac{\vartheta_2}{Q_2} \tag{7.5}$$

it follows

$$\tau = \frac{T_{p1} \cdot T_{p2}}{(T_{p1} - T_{p2}) \cdot \ln 2} \cdot \ln \frac{\vartheta_1' Q_2}{\vartheta_2' Q_1}, \tag{7.6}$$

where τ is the residence time of water elements travelling from the injection point to the point of detection as defined by

$$\vartheta'(T) = e^{-\frac{\tau \ln 2}{T}} \int_0^T f(t)\, dt = \vartheta(T)\, e^{-\frac{\tau \ln 2}{T_p}} \tag{7.7}$$

with the function f (t) that characterizes the random flow between the above points; no prime at ϑ denotes concentration of a non-decaying agent. Henceforth, Eq. 7.6 allows one to identify the (diffusive) advection of other substances.

Various aspects of markers, dyes, tracer studies, and marine monitoring may also be found in Welsh (1967), Crickmore (1972), Ellis (1972), and many others. Hints as to evaluation of heat exchange coefficients are given by Hindley and Miner (1972). An automatic multi-sensor electrochemical monitor for sea water measurements has been presented by Wilde (1971). The back scattering laser-Doppler technique conceived by Jurisch (1973) bears prospects of current measurements from above the water surface, without the necessity of either penetrating the water stratum or observation through glass walls, as for forward-scattering. Similar to other measurements, the ones presented in this paper may also be facilitated through the use of fast and efficient data-collecting and processing systems, computer packages, etc. (see e.g. Gunther and Bugliarello, 1973).

Chapter 8

PHYSICAL MODELLING OF WASTE- AND HEATED-WATER DISCHARGES

The need for model investigations on physical (hydraulic) models is well understood, though sometimes questioned as to the possibility of substitution by using computer-aided mathematical models. In the case of waste disposals and thermal discharges, especially into the marine environment, there are many factors involved and it would be very difficult to include all of them in the analysis without the aid of physical models. A significant advantage of the latter comes particularly from their use as a tool to study various phenomena, and not only to consider special cases connected with a given project.

The most common complexity necessitating a model study is irregular geometry. Such cases usually have concentration or temperature distributions which are highly three-dimensional and irregular; analytical methods may not be applicable to these problems.

The factors governing the discussed phenomena have been considered in previous chapters, and this discussion is thus limited to the modelling effects.

A hydraulic model should provide similarity of prototype phenomena over their widest range. Geometric similarity requires that corresponding dimensions maintain the same proportions in the prototype and its model. For kinematic similarity corresponding distances must be passed by fluid during corresponding times. Finally, the dynamic similarity brings about the correspondence of forces. Further modelling requirements arise when movable bed and sediment motion are considered. In the case of waste disposal and thermal discharges one has to account additionally for the laws of turbulent diffusion and heat transfer.

The modelling laws can be developed by various techniques: the dimensional analysis, the use of empirical formulae, and the application of differential equations describing a phenomenon. The best way consists in using differential equations, if known (their existence does not imply the existence of solutions, since numerous complications are often involved, such as complex boundery conditions etc.). For the motion of density homogeneous liquids with free surface, the above methods produce a number of similarity criteria, among which the fundamental two are

$$F = \frac{u}{\sqrt{gH}}, \qquad Re = \frac{uL}{\nu} \tag{8.1}$$

Table 8.1 shows how these two criteria may contribute to our study, while the following text provides deeper insight into the modelling criteria.

Table 8.1

Fundamental similarity requirements

	Geom. distortion	F	Re	Roughness
Jet diffusion — near field	not acceptable	if gravity dependent	$Re_o \gtrsim 2.500$	immaterial
Buoyant plume	not acceptable	densimetric	$Re_o > Re_{cr}$	immaterial
Convective spread	often needed	densimetric	$Re\,dens > Re_{cr}$	immaterial
Ambient motion	permissible	yes	$Re \gtrsim 600$	needed to give corr. head loss
Ambient turbulence	not acceptable	yes	yes	needed at bottom

The temperature distribution induced by a heated discharge (or equivalent concentration of passive matter) has to be discussed in terms of a near field and a far field region (compare other chapters for definitions). In general, the near field and far field temperature distributions are interrelated, and consideration of one implies treatment of the other. Temperature and concentration in the near field ambient water may itself be a function of the manner in which heat or other pollutants accumulate in the far field.

For the near field it may be demonstrated that all types of turbulent jets must be modelled with undistorted scales because the turbulent mixing region will not be distorted in the model, regardless of the geometric distortion.

The far-field case is controlled by surface cooling, interfacial stresses of a thermally stratified flow, and diffusion phenomena. Hardly ever can these factors be reduced to the Ackers (1969) approximation. He states that heat loss is proportional to area x time x temperature difference assuming that the same "climate" exists in the model shed as in the prototype. The temperature drop is proportional to mass divided by heat loss. Hence, if the lower index denotes scale ratio, one has

$$(\Delta T)_r = \frac{(\text{Mass})_r}{l_{xr}^2 \cdot t_r \cdot T_r}. \tag{8.2}$$

But to produce equal temperatures in model and prototype, we also need to produce equal temperature drops.

Using the same fluid, $(\text{Mass})_r = t_{zr} \cdot l_{xr}^2$ and in a Froude model $t_r = l_{xr} \cdot l_{zr}^{-1/2}$. Inserting in the above, putting $(\Delta T)_r = T_r = 1$, we thus require the distortion

$$l_{xr} = l_r^{3/2}. \tag{8.3}$$

This distortion prevents the accurate simulation of turbulence. Moreover, interfacial stresses must be represented in a proper way.

In the case of two-layered, thermally-stratified flows in open channels the theoretical analysis may be carried out by treating the upper and lower layers as channel flows (Harleman, Stolzenbach, 1964). The resulting differential equations require an undistorted model. However, for given Froude numbers and upper-to-lower flow rate ratios, one obtains

$$\frac{dh_l}{dx} = N\left(f, f_i, \frac{h_l}{h_u + h_l}\right)$$

and the model law for interfacial depths becomes

$$N_r = l_{zr} : l_{xr} \tag{8.5}$$

which requires the specification of the friction factors f and f_i. The bottom friction factor f may usually be estimated from the established open channel resistance equation. The assumption of a smooth interface and normal friction laws yields a good estimate of the friction factor f_i. In a distorted model ($l_{zr} > l_{xr}$) the model "friction" must be increased, so that $N_r > 1.0$.

For the turbulent diffusion, from Eq. 3.1 it follows that the model of a three-dimensional turbulent flow must be undistorted ($l_{xr} = l_{yr} = l_{zr}$) and conform to

$$\frac{u_r l_r}{K'_r} = 1.0 \tag{8.6}$$

This condition can be satisfied in many three-dimensional free turbulent flows (with eddy diffusivities $K' \sim ul$).

Unfortunately, this is not true in channel flows where, as previously mentioned, distortion is usually necessary for practical reasons. As shown by Holley, Harleman and Fisher (1970) these distorted models overemphasize longitudinal dispersive effects of an injected contaminant due to the distortion of the velocity distribution as shown in Fig. 8.1.

For a distorted model to reproduce the dispersion of a cloud correctly it is necessary, that

$$K_r = \frac{l_{xr}^2}{T_r} = l_{xr}\, l_{zr}^{1/2} \tag{8.7}$$

In steady channel flows a distorted hydraulic model magnifies the dispersive effects of vertical velocity gradients and diminishes the effects of transverse gradients. Cases in which the two tendencies cancel to produce proper modelling seem unlikely, and thus, in general, distorted models of steady flows should not be used to model dispersion.

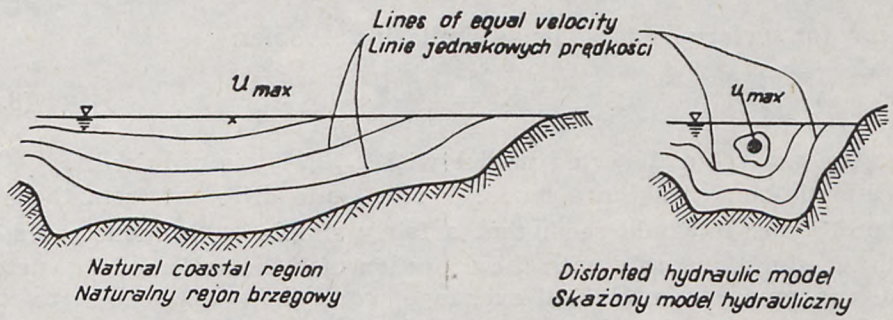

Fig. 8.1. The effect of model distortion on velocity field
Rys. 8.1. Wpływ skażenia modelu na pole prędkości

For oscillatory flows, as found in estuaries, the dispersive effects of vertical gradients are magnified in the model just as for steady flow. The dispersive effects of transverse gradients may be magnified, diminished, or correctly modelled, depending on the value of the prototype dimensionless time scale. Figure 8.2 depicts the relationship between the transverse cross-sectional mixing time scale and the dispersion coefficient ratio.

In very wide estuaries the dispersive effects of both transverse and vertical velocity gradients are magnified; hence, dispersion will occur faster in the model than in the prototype. In narrow estuaries dispersion due to transverse gradients may be properly modelled, but dispersion in the model is usually caused primarily by vertical gradients, and the overall result is magnified.

The treatment of surface heat exchange similitude in thermal models may be much simplified by use of the equilibrium temperature and surface heat exchange coefficient concepts. As a consequence of Eq. 4.14, the forced temperature rise $T_F = T - T_a$ obeys the equation

$$\frac{v}{Q}\frac{d\Delta T_F}{dt} = \frac{\mathcal{H}}{\varrho c Q} - \Delta T_F\left(1 + \frac{K_E A}{\varrho c Q}\right) \tag{8.8}$$

where $\mathcal{H}$ — artificial heat input , v — volume of water body, A — its area.

The model law which will insure that $\Delta T_F/\Delta T_p$ is the same in the model and prototype, is:

$$K_r \cdot l_{xr} \cdot l_{yr} = Q_r \tag{8.9}$$

Assuming that the model also obeys a densimetric Froude law $\left(\frac{\Delta \varrho}{\varrho}\right)_r = 1.0$, and that:

$$Q_r = u_r\, l_{zr}\, l_{yr} = l_{zr}^{3/2} \cdot l_{yr} \tag{8.10}$$

the law for surface heat exchange similarity becomes:

$$K_r = \frac{l_{zr}^{3/2}}{l_{xr}} \tag{8.11}$$

Thus, in general a distorted model with $l_{zr} \neq l_{xr}$ is required.

Climatic conditions on a model can be quite different from those in the prototype. It would seem that a fairly simple experiment could be conduced simultaneously with the operation of a thermal model to determine the environmental heat-exchange coefficient applicable to the model. Modifications could then be made either to the model scale or to the model results.

To generalize the above considerations it should be emphasized that by using criteria 8.3 and 8.11 for surface heat exchange and 8.7 for turbulent diffusion one assumes that near field processes are negligibile. However, surface cooling and ambient turbulence may not be modelled simultaneously, because laws 8.7 and 8.11 are antagonistic. A summary of other modelling requirements is given below to add further details.

For all buoyant jet models:

$$u_r = \left[\frac{\Delta \varrho}{\varrho}\right]_r l_{zr}^{1/2}. \tag{8.12}$$

For near field jet and turbulent mixing regions:

$$l_{xr} = l_{yr} = l_{zr}. \tag{8.13}$$

For two-layer flows:

$$N_r = l_{zr} : l_{xr}. \tag{8.14}$$

For ambient heat or other waste transport:

In open channel flow: $l_{xr} = l_{yr} = l_{zr}$. (8.15)

In diffusion regions:

Three dimensional $l_{xr} = l_{yr} = l_{zr} = \alpha_r^6 \left[\frac{\Delta \varrho}{\varrho}\right]_r^{-3}$, (8.16)

(α = coefficient in $K' = \alpha \cdot l^{4/3}$)

Two dimensional $l_{xr} = l_{yr} = l_{zr}^{3/2}\ \alpha_r^{-3} \left(\frac{\Delta \varrho}{\varrho}\right)_r^{3/2}$. (8.17)

For surface heat loss:

$$K_r = \frac{l_{zr}^{3/2}\left[\frac{\Delta \varrho}{\varrho}\right]_r^{1/2}}{l_{xr}}. \tag{8.18}$$

It is clear that a single model may not in general replicate all portions of the concentration distribution because the model similitude requirements are in conflict. It is usual practice to limit the model application to one of the above physical mechanisms and to build more than one model if more than one process is important.

Assuming that $K_r = 1.0$ and thus $\frac{l_{xr}}{l_{zr}} = l_{zr}^{1/2}$ the values of $\frac{l_{xr}}{l_{zr}\, l_{xr}^{1/3}}$ and $N_r\, l_{zr}/l_{xr}$ greater than unity result in exaggeration of temperature loss and friction effects, respectively, and in a subsequent exaggeration of interfacial height change. The best value of l_{zr} is that which gives $N_r\, l_{zr}/l_{xr}$ closest to, but greater than unity, so that the model never underrestimates interfacial changes.

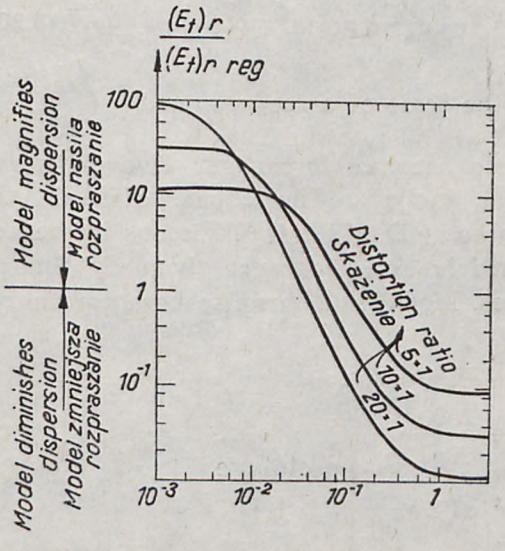

Fig. 8.2. The effect of model distortion on dispersion due to transverse velocity gradients (x-axis)

Rys. 8.2. Wpływ skażenia modelu na rozpraszanie związane z poprzeczny i gradientami prędkości (oś x)
Fisher and Holley, 1971

As mentioned above, the condition $K_r = 1$ requires a distorted model. However, proper modelling of beach slope and channel geometry effects is associated with an undistorted model. Any distortion would make S_x and h_o/b_o larger in the model. This contradiction must be by-passed by a compromise solution. Considering the natural advantages of distorted

models it is logical to build a distorted model and attempt to interpret the effects of differences in S_x and h_o/b_o on the concentration (temperature) distribution. A further phase consists in studies of the far field on a distorted model and subsequent comparison of the distortion effects mentioned.

An important feature of the thermal discharge processes is the spread of buoyant surface discharge. By using the method of synthesis for quite a general case of unsteady spread, Sharp (1971) found the following set of dimensionless ratios governing the process:

$$f\left(\frac{L\,(g')^{1/5}}{Q^{2/5}},\ \frac{T\,(g')^{3/5}}{Q^{1/5}},\ \frac{Q\,(g')^{1/3}}{\nu^{5/3}},\ \frac{D\,(g')^{1/5}}{Q^{2/5}}\right) = 0, \tag{8.19}$$

where $g' = g\,\frac{\Delta\varrho}{\varrho}$.

Experiments provide results in the form of a correlation between times and distances travelled for specific values of $Q\,(g')^{1/3} \cdot \nu^{-5/3}$ shown by Sharp (1971). The information contained in these diagrams can be used to form a logical basis for hydraulic model design. The most obvious criteria are that, for correct reproduction of the rate of spread, the model outfall must be designed on a standard Froudian basis, i.e.

$$\left.\frac{D\,(g')^{1/5}}{Q^{2/5}}\right|\text{model} = \left.\frac{D\,(g')^{1/5}}{Q^{2/5}}\right|\text{prototype} \tag{8.20}$$

There is a danger of reducing the scale of a model $\left(\text{and } \frac{Q\,(g')^{1/3}}{\nu^{5/3}}\right)$ to the extent that viscous influence becomes important. Two different minima may be obtained from this analysis. The choice of scale to be used depends on a prototype value of $D\,(g')^{1/5} : Q^{2/5}$. Viscous influence must be avoided in hydraulic models and diagrams given by Sharp provide a method of choosing scales. Model size can also be accordingly reduced by distortion.

According to Ackers (1969) the inequality

$$\left(\frac{l_{zr}}{l_{xr}}\right)^{5/2} \cdot l_{xr}^{3/2} > \left.\frac{150}{\left[\frac{\sqrt{g\,\frac{\Delta\varrho}{\varrho}} \cdot H^{5/2}}{L\nu}\right]}\right|\text{prototype} \tag{8.21}$$

can be used to deduce the minimum l_{xr} vertical exaggeration that satisfies the convective spread criterion, although there may be good reasons for using a lesser exaggeration after checking that the error involved in convective spread to some critical position is small.

Only a few comparison studies of the model and prototype data are

available. Among them, Hindley et al. (1971) state that winds, waves, and changing bottom topography affect a prototype but not a model.

The model-prototype comparisons given by Ackers (1969) show that reasonably good agreement is possible, although there remains the problem of the representation of initial mixing zones in vertically exaggerated models. In general, adjustments for levels and cross flow are independent, but correct only for some selected time points of cyclic (e. g. tidal) changes. Measurements of velocities, levels, ambient temperature, and the pattern and temperature of cooling water emerging from an existing station should all be obtained simultaneously and, ideally, instantaneously.

In the light of the discussion presented herein it seems that only under exceptional conditions can prototype diffusion phenomena be reproduced in the model without exaggeration, as in studies by Higuchi and Iwagaki (1968). In fact, the problem of model representation of marine discharges has many facets.

Chapter 9

BIOLOGICAL, BIOCHEMICAL, SEDIMENTOLOGICAL, STRUCTURAL, AND RELATED PROBLEMS

This chapter is devoted to the problems that do not come under the other chapters, but are important with respect to ultimate design of waste and heated-water discharge. Biological problems arise directly as biochemical and other factors affect the nonhydromechanical decay of wastes and also have indirect influence on the impact of heated water and wastes on the marine life. Sediment motion is not explicitly tied with the design of wastes spreading, but turns out to be an essential factor of most plants. Since construction and other engineering problems may also stand alone (and are not specific for waste discharge and water intake facilities), the main body of this chapter will deal with basic aspects of the biology of waste- and heated-water discharges.

Aside from radioactive and toxic or non-recycling substances (such as DDT, which is systematically aggregated in animal and human tissues), which should not be disposed of at all in the sea, there are municipal and industrial wastes, which affect the environment in two manners. They contain nutrients, such as mineral salts and organic particles, which feed the marine life chain. However, at the same time the aerobic bacteria develop on nutrients and use oxygen for respiration purposes. This,

in turn, disables other organisms to develop; the oxygen deficit is as harmful as toxic matter accompanying the nutrients in the discharged wastes. Besides, pathogenic organisms grow on wastes (Coliforms are used to indicate the number of these organisms).

Marine self-purification consists of three main processes:

a) dilution due to advection and turbulent diffusion,

b) biochemical aerobic mineralisation, and

c) deposition, i.e. metabolic transformations (by micro- and macro--organisms), adsorption, and sedimentation. There is a large variety of chemical, biological, and bacteriological indicators of marine pollution. If a considerable amount of organic matter collects somewhere, oxygen

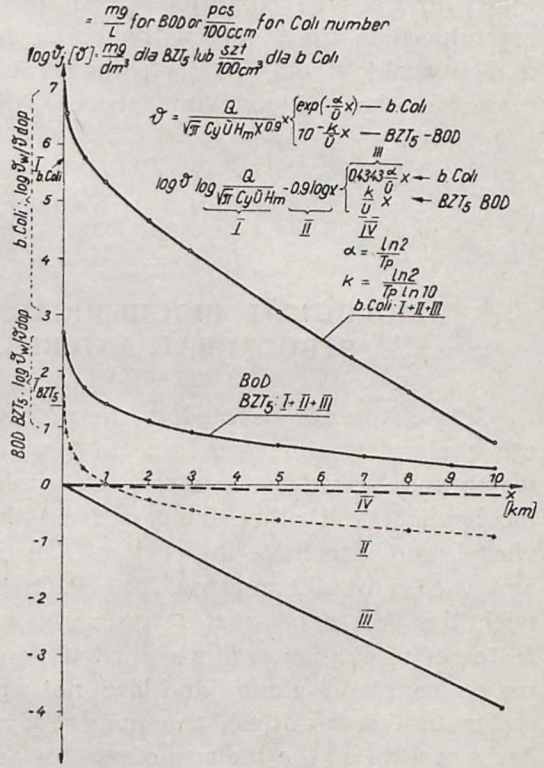

Fig. 9.1. The effects of hydromechanical, biological, and biochemical factors on decay of pollutants

Rys. 9.1. Wpływ czynników hydromechanicznych i biochemicznych na spadek stężenia ścieków

becomes used up and only saprogenic and sulphuric bacteria remain. Hydrogen sulphide, ammonia, nitrites, and other toxic substances characterize the amount of waste as well as biochemical oxygen demand (BOD), oxidizing capacity, Coli number, and others.

While designing marine waste discharge facilities an engineer is not necessarily obliged to take into account all the processes discussed above

since in most cases he must conform to some legal requirements as to the permissible levels of contamination, etc. However, it is highly recommended that the designer be aware of the purity (or pollution) conditions he faces and of the environmental consequences of the steps he undertakes. The same is the case with thermal pollution due to discharges of heated water. On the one hand, the excessive heat may be utilized in the growth of some species, but on the other hand the oxygen deficit bars the growth of other species, high temperatures may simply cause boiling up, and de-icing of large areas in winter may also bring about situations as unpleasant as those due to other infringements of the natural equilibrium. As it is less relevant to the subject of this study, the thermal impact on the environment will not be discussed; some references may be found in the list of bibliographical sources.

The biochemical aerobic mineralisation is an efficient factor helping the diffusion processes in decreasing waste concentrations. This fact is illustrated in Fig. 9.1, where the two most common and representative indicators of the biological and biochemical decay, Coli number and BOD, are compared against hydromechanical effects for the chosen exponent of 0.9. The diagram shows the essential role of non-hydromechanical factors at farther distances from the waste collector outlet. Hence, accurate determination of α and k seems to be of paramount importance. From bibliographical sources (Zeidler et al. 1969) it appears that k is equal to about 0.1 day^{-1} (at 20°C) and depends exponentially on temperature as $k/K_o = \exp(1.046\ T/T_o)$. The coefficient α is much higher, so that $T_p = \frac{\ln 2}{\alpha}$ is equal to 2 hours on average. However, some authors indicate $T_p = 0.75$ h (Bonde 1967, Pearson et al. 1966) and even $T_p = 0.2$ h (Thomas 1964).

In view of the above discrepancies and for the weight of the biochemical and biological decay the Author undertok a series of experiments at an existing sewage outfall in Puck Bay. The biological and biochemical decay was assessed by substracting the rhodamine-traced hydromechanical effects from the overall decrease in Coli number determined by ample sampling over a large area. The coefficient α found in the experiments of 1970 is presented in Fig. 9.2. It may be observed that α is higher at short distances from the outfall, i.e. the half-life period extends with increasing distances (or increasing marine residence time of wastes). The respective times are $T_p \cong 0.5$ hour up to about 350 m from the outfall or some two-hour residence time versus $T_p \cong 1.5$ hour at greater dinstances or longer residence times (the tests we e conducted up to 1000 m from the outfall, or six-hour residence).

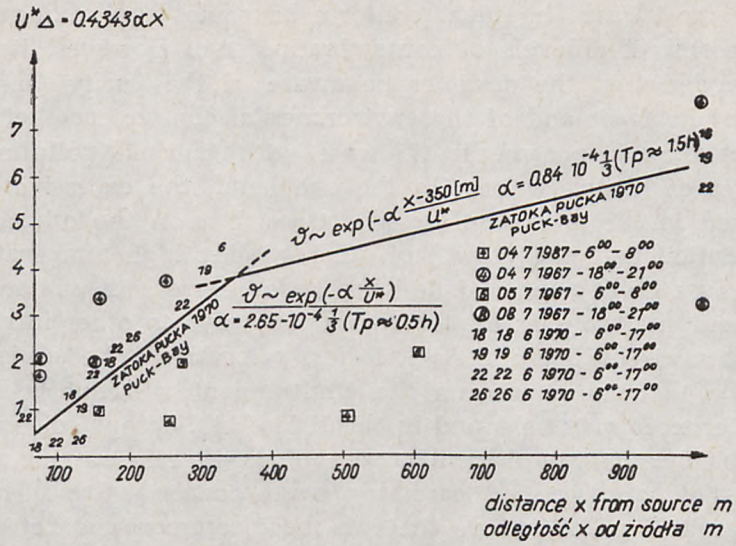

Fig. 9.2. Coli number decay due to biochemical and biological factors
Rys. 9.2. Spadek liczby bakterii Coli spowodowany przez czynniki pozahydromechaniczne

The same trend was observed in 1967. Some light on these results is shed by Aubert et al. (1969), Pramer (1969), and Mitchell and Morris (1969), who indicate that the rate of bacterial decay increases with the increasing number of bacteria. For higher concentrations the antibiotic effect of plankton due to waste nutrients might be stronger than the growth of bacteria. In further elucidating these phenomena much attention should be devoted to biological factors; the physical and chemical factors (such as radiation, temperature, salinity, pH etc. etc.) do not seem to be the governing ones as the bacterial behaviour is quite different in sterile water.

It is interesting to note that similar regional self-purification patterns have been exposed by Bronfman (1974) in his study of pollution due to oil products and detergents. The observations of Pomeroy (1959), however rough and descriptive, also confirm the Author's finding of increased mortality of Coli at sewage outlets.

That the marine environment is lethal to Coliforms has also been proved by Harremoës (1970). The effect of various factors on Coliforms in the dark and daylight was studied by Pike et al. (1969) and Gameson and Saxon (1968), while the sample storage conditions and time were investigated by Lonsane (1968). It is fairly commonly accepted that Coliforms are unsatisfactory indicators of marine pollution (e.g. Savage and Hanes, 1971) and must be aided by other parameters. Nevertheless,

the Coliform variation shown by the Author describes at least qualitatively the marine patterns of waste disappearance and self-purification..

The existence of movable bottom and sediments in the recipients of waste and heated water further complicates the discharge design. Any structure projecting into the sea brings about changing accretion and erosion patterns. Appropriate construction technology and solutions must be foreseen for discharge channel outlets and cooling-water intake towers, pipes, piers, etc. Serious problems arise for underwater pipelines, which add substantially to the total costs of a plant. All these sediment motion and beach erosion questions are dealt with in pertinent literature. Similarly, sedimentation and settling basins do not pose questions limited exclusively to the subject of this study. Some answers may be found in Sarikaya's paper of 1973.

There are also many interesting aspects of internal hydraulics for the discharge and intake structures. They are extensively discussed by Rawn et al. (1960) and more recently by French (1972), Vigander (1970), Silvester and Patarapanich (1972), Parkhurst (1967), Nece (1966) and many others. Although bibliography pertaining to other engineering problems of waste and heated-water discharge is voluminous, many particulars must often be solved individually for a given project.

Chapter 10

STOCHASTIC APPROACH TO THE PROBLEM

10.1. General

In previous chapters the problem of waste- and heated-water discharges has been discussed in terms of deterministic models in which the external diffusion-controllling conditions have been assumed as non-random. Nevertheless, diffusion is still inherent in those models on the microscale level (the presence of turbulent eddies which do not change advection patterns of the homogeneous velocity field). Therefore such models can be called quasi-deterministic. Upon reasonable assumptions about the flow field U (X, t) and the diffusion coefficient K_{ij} (X, t) it is possible to predict the spread of pollutants under a variety of external conditions (each condition being homogeneous). However, such conditions are not fully adequate to reality, because the water bodies in which

waste and heated water spreads also undergo random motion. * Nonetheless, quasi-deterministic models are very useful, because aside from their independent validity, the may be used components of stochastic models.

A couple of techniques can be employed in analyzing random fields, but only some of them suit the purposes of this study. We examine the following ways of approach:

1. The Fourier (or integral) transforms applied to the equation of turbulent diffusion analyzed within the quasi-deterministic model,
2. the purely probalistic, most complete, description through multidimensional probability density functions,
3. the application of characteristic functionals,
4. a step-by-step procedure based on the quasi-deterministic approach dealt with in subsequent steps of approximated random fields. Variational analysis may be used to bolster the step-by-step procedure.

10.2. Integral transforms

Integral transformations seem to be the most natural way of expanding the quasi-deterministic situations with non-random advection fields into the realm of random situations which might happen under natural conditions. In a very rough manner, for a quasi-deterministic model one eventually comes to the concentration

$$\vartheta = f(X_i, t, K_{ii}, U_i, \alpha_i \ldots), \tag{10.1}$$

where the decay exponents α_i vanish for conservative matter. The other independent variables of Eq. 10.1 being non-random, it is the flow veloxity U_i which must be represented as the integral of random components

$$U(t) = \int_{-\infty}^{+\infty} e^{i\omega t} \cdot d\,\mathcal{F}_u(\omega). \tag{10.2}$$

The problem of finding the mean concertration for a mean velocity remains unchanged.

* Scales of turbulent motion are not clearly defined. It may be assumed that microscale fluctuations have periods shorter than 0.5s, fine scales stretch from 0.5 to 50s, mesoscales from 50s to 5 hours, and macroscales are all longer. Microscales and mesoscales are distinquished in this study to emphasize their weak interaction, but they can include the adjacent subregion of the fine scales. In Monin's classification (cf. Ozmidov, 1974), the upper limit of fine scales sometimes approaches tens of minutes (hundreds of meters), while the mesoscales may reach the magnitude of one day (kilometers).

The final goal of the Fourier transformation in this aspect is to determine the spectral density

$$S_v(\omega) = \mathcal{F}(X_i, K_{ii}, S_u; \omega), \tag{10.3}$$

where

$$S_v(\omega) = \int_{-\infty}^{+\infty} R_v(\tau)\, e^{i\omega\tau}\, d\tau \tag{10.4}$$

and

$$R_v(\tau) = \frac{1}{2\pi} \int_{-\infty}^{+\infty} S_\vartheta(\omega)\, e^{i\omega\tau}\, d\omega. \tag{10.5}$$

Coming back once again to the fundamental equation

$$(i, j = 1, 2, 3)\ \frac{\partial \vartheta}{\partial t} + \frac{\partial (\vartheta u_i)}{\partial x_i} + \alpha\vartheta = \frac{\partial}{\partial x_i} K_{ij} \frac{\partial \vartheta}{\partial x_j} \tag{10.6}$$

one may rewrite it for the correlations between two points A and B

$$\frac{\partial}{\partial \tau} R_{vv}(\tau) + \overline{u_i}\ \frac{\partial}{\partial x_i} R_{vv}(\tau) + \alpha R_{vv}(\tau) + \frac{\partial}{\partial x_i} \overline{\vartheta} R_{\vartheta . u_i}(\tau) +$$

$$+ \frac{\partial}{\partial x_i} R_{v,vu_i}(\tau) = 0 \tag{10.7}$$

with the correlations

$$R_{vv}(\tau) = \overline{\vartheta'_A \cdot \vartheta'_B}, \tag{10.8}$$

$$R_{vu_i}(\tau) = \overline{\vartheta'_A \cdot u'_{iB}}, \tag{10.9}$$

$$R_{v,vu_i}(\tau) = \overline{\vartheta'_B \cdot \vartheta'_A \cdot u'_{iA}}, \tag{10.10}$$

$$\tau = t_A - t_B.$$

After performing respective transformations

$$R_{vv}(\tau) = \frac{1}{\pi} \int_0^\infty e^{i\omega\tau} S_v(\omega)\, d\omega, \tag{10.11.1}$$

$$R_{v,u_i}(\tau) = \frac{1}{\pi} \int_0^\infty e^{i\omega\tau} S_{vu_i}(\omega)\, d\omega, \tag{10.11.2}$$

$$\frac{\partial}{\partial x_i} R_{v,vu_i}(\tau) = Q_{vv}(\tau) = \frac{1}{\pi} \int_0^\infty e^{i\omega\tau} M_{vv}(\omega)\, d\omega, \tag{10.11.3}$$

$$Q_{vvu_i}(\tau) = \frac{\partial}{\partial x_i} R_{vu_i}(\tau). \tag{10.11.4}$$

The spectral equivalent of Eq. 10.7 becomes

$$j\,\omega\,S_v(\omega) + \overline{u_i}\frac{\partial}{\partial x_i}S_v(\omega) + \alpha\,S_v(\omega) + \frac{\partial}{\partial x_i}\overline{\vartheta}\,S_{vu_i}(\omega) + M_{vv}(\omega) = 0. \quad (10.12)$$

Making use of the ideas of Heisenberg and Tehen (Aitsam 1969) one obtains from Eq. 10.12

$$S_v(\omega) = S_v^{\circ}(\omega)\exp(-\chi x)\left[\cos\frac{\omega}{\overline{u}}x + \overline{u}\frac{\chi}{\omega}\sin\frac{\omega}{\overline{u}}x\right], \quad (10.13)$$

where

$$S_v^{\circ}(\omega) = S_v(\chi = 0, \omega),$$

$$\chi = \frac{\omega^2}{\overline{u}^2}\beta\int_0^{\infty}\sqrt{\frac{S_u(\omega)}{\omega^3}}\,d\omega,$$

β — dimensionless coefficient.

An apparent feature of solution in the form of Eq. 10.13 is its comparative character i.e. determination of $S_v(\omega)$ in terms of $S^{\circ}_v(\omega)$. The latter result also does not cover the case of space variability of velocities and eddy diffusivities.

Let us now return to solution 3.40, obtained in Chapter 3 for „regular" pattern of spreading of pollutants, i.e. plane — parallel advection (with possible shears) and fine turbulence contributing to diffusion, but not to displacement of whole „portions" of pollutants. Eq. 3.40 can simply be presented as a product of two factors

$$\vartheta^{(P)}t) = f_1(x, y, z).\exp[-f_2(x, y)\cdot u_{x_o}(t)] \quad 10.14)$$

of which the latter allows for the effect of water velocity on the concentration at a certain point P (x, y, z). Should this velocity be random, the concentration will also become random, according to Eq. 10.14.

Let us present the random function $u_{xo}(t)$ as a series with random amplitudes Φ_k and random frequencies ω_k

$$u_{xo}(t) = \sum_k \Phi_k\,e^{i\omega_k t} \quad (10.15)$$

Substituting Eq. 10.15 for u_{xo} in Eq. 10.14 and expanding $\exp(j\omega_k t)$ in the Maclaurin series gives

$$\vartheta^{(P)}t) = f_1\exp\{-f_2[\sum_k \Phi_k - t(\Phi_1\omega_1^1 + \Phi_2\omega_2^2 + \ldots.) + \frac{t^2}{2}(\Phi_1\omega_1^4 + \Phi_2\omega_2^4 + \ldots) - \frac{t^3}{6}(\Phi_1\omega_1^6 + \Phi_2\omega_2^6 + \ldots) + \ldots]\}. \quad (10.16)$$

If the basic energy of coastal turbulence is contained in fluctuations with periods of several minuter and longer, and when the time series has a length of several hours in the practical applications considered,

the sum in the square brackets of Eq. 10.16 converges quickly and it is enought to take into account only the first three (or even two) terms:

$$\vartheta^{(P)}(t) \simeq f_1 \exp\{-f_2[\sum_k \Phi_k - a^{(2)} t + a^{(4)} t^2 \ldots]\} \tag{10.17}$$

Expanding the exponential function in Eq. 10.17. in an analoqous Maclaurin series gives

$$\vartheta^{(P)}(t) \simeq f_1 e^{-f_2 \sum_k \Phi_k}\left[1 + (f_3 t - f_4 t^2) + (f_3 t - f_4 t^2)^2 \frac{f_3^2}{2} + (f_3 t - f_4 t^2)^3 \frac{f_3^3}{6} + \ldots\right] \tag{10.18}$$

where

$$f_3 = f_2 a^{(2)} = f_2 (\Phi_1 \omega_1^2 + \Phi_2 \omega_2^2 + \ldots) \tag{10.19}$$

$$f_4 = f_2 a^{(4)} = \frac{f_2}{2} (\Phi_1 \omega_1^4 + \Phi_2 \omega_2^4 + \ldots) \tag{10.20}$$

The Fourier transformation yields finally the relationship between the spectra of concentration and velocities:

$$S_\vartheta(\omega) = f_1(x, y, z) \exp\left[-f_2(x, y) \sum_k \Phi_k\right] \times$$

$$\times \{-f_3^2 \frac{1}{\omega^2} + (f_3^3 f_4 + \frac{f_3^6}{6}) \frac{6}{\omega^4} - \ldots\}. \tag{10.21}$$

Again, sufficient practical accuracy is ensured by the last two terms.

A tacit assumption made in the derivation of Eq. 10.21. is the stochastic similarity of velocities in the space between the source and point P. Considering also the approximations accepted one must not regard Eq. 10.21. as a general solution. Therefore, here we make use of other tools.

10.3. Characteristic functionals

The purely probabilistic description of fluid elements is outlined in Chapter 3. Characteristic functionals provide an even more general and concise tool than the multidimensional probability function discussed therein.

The simplest characteristic function is known as

$$\varphi(\Theta_k) = \int_{-\infty}^{+\infty} \exp(+ i \Theta_k u_k) p(u_k) d u_k \qquad (k = 1, 2 \ldots\ldots) \tag{10.22}$$

If instead of the discrete multidimensional variable u_k a continuous variable is considered as a function of the single parameter u (x), and if the function Θ (x) conforms with the requirement

$$u\,[\Theta\,(x)] = \int_a^b \Theta\,(x)\,u\,(x)\,d\,x \tag{10.23}$$

then one has

$$\Phi\,[\Theta\,(x)] = \overline{\exp\{iu\,[\Theta\,(x)]\}} = \overline{\exp i\int u\,(x)\,\Theta\,(x)\,d\,x} \tag{10.24}$$

with the bar dnoting the operation of averaging.

For a random function depending on four variables the characteristic functional is

$$\Phi\,[\Theta\,(x,t)] = \overline{\exp\left\{i\int\limits_{-\infty}^{+\infty}\iiint \Theta\,(x,t)\,u\,(x,t)\,d\,x_1\,d\,x_2\,d\,x_3\,d\,t\right\}}, \tag{10.25}$$

which finally, in the case of several random functions (as, e.g. concentration, O.D., B.O.D., temperature, velocities, etc., for our purposes), becomes

$$\Phi\,[\Theta_1(\vec{x},t),\Theta_2(\vec{x},t)\ldots\Theta_N(\vec{x},t)] = \overline{\exp\left[i\int\limits_{-\infty}^{+\infty}\iiint\sum_{k=1}^{N}\Theta_k(\vec{x},t)\,u_k(\vec{x},t)\,d\,\vec{x}\,d\,t\right]} \tag{10.26}$$

Since functionals allow one to determine any statistical moments of their variables, the approach to our problem by means of functionals is a universal one.

At this point we shall consider only the case of the characteristic functional $\Phi[\vec{\Theta}(\vec{x})\,t]$ of a concentration field $\vartheta(\vec{x})$ (or u in accordance with the above notation). The time derivative of Φ is

$$\frac{\partial\,\Phi}{\partial\,t} = i\left(\vec{\Theta}\,\frac{\partial\,\vartheta}{\partial\,t}\right)\exp\{i\,(\vec{\Theta}\,\vartheta)\}. \tag{10.27}$$

Substituting this into equation

$$\frac{\partial\,\vartheta}{\partial\,t} + u_\alpha\,\frac{\partial\,\vartheta}{\partial\,x_\alpha} = \frac{\partial}{\partial x_\alpha}\,K_{\alpha\beta}\,\frac{\partial\,\vartheta}{\partial\,x_\beta} \tag{10.28}$$

yields

$$\frac{\partial\,\Phi}{\partial\,t} = i\left(\Theta\left\{\frac{\partial}{\partial\,x_\alpha}\left[\overline{K_{\alpha\beta}\,\frac{\partial\,\vartheta}{\partial x_\beta}\,e^{i(\Theta\vartheta)}} - \overline{\vartheta\,u_\alpha\,e^{i(\Theta\vartheta)}}\right]\right\}\right). \tag{10.29}$$

By introducing variational derivatives

$$\mathcal{D}_j\,(M)\,\Phi = \frac{\delta}{\delta\,\Theta_j\,(M)\,d\,M} = \overline{i\,u_j\,(M)\exp\{i\,\vec{\Theta}\,\vec{u}\}}, \tag{10.30.1}$$

$$\mathcal{D}_j\cdot(M_1)\,\mathcal{D}_k\,(M_2)\,\Phi = -\overline{u_j\,(M_1)\,u_k\,(M_2)\exp\{i\,(\vec{\Theta}\,\vec{u})\}}\ \text{...etc.} \tag{10.30.2}$$

one has in lieu of Eq. 10.29:

$$\frac{\partial\,\Phi}{\partial\,t} = \Theta\left\{i\,\frac{\partial}{\partial\,x_\alpha}\left[K_{\alpha\beta}\,\frac{\partial}{\partial\,x_\beta}\mathcal{D}_\beta\,\Phi + i\,u_\alpha\,\mathcal{D}\,\Phi\right]\right\}. \tag{10.31}$$

This equation, like the Hopf equation for the fluid velocity field, may not be solved explicitly, because of the difficult mathematics involving variational derivatives. Therefore, the functional approach does not bear hopeful prospects until convenient mathematical tools are available. It seems that some solutions to Eq. 10.31 might be obtained by employing functional power series as either

$$\Phi = 1 + \sum_{n=1}^{\infty} \Phi_n \tag{10.32}$$

or

$$\Phi = e^{\widetilde{\Phi}_1 + \widetilde{\Phi}_2} (1 + \sum_{n=3}^{\infty} \widetilde{\Phi}_n) \tag{10.33}$$

with homogeneous power functionals Φ_k of k, as Hopf proposed for his equation. The solution may be sought as power series of the Reynolds number.

10.4. The step-by-step procedure

Aside from being incomplete in its description of the field of pollutants, any integral transformation can also be regarded as somehow inconsistent with the assumption of statistical inhomogeneity (both in time and space) of u (t) and ϑ (t), which must be taken up in the analysis of real conditions. Strictly speaking, the real concentration and velocity fields would be correctly represented in the integral form if their transforms displayed single peaks within more or less pronounced frequency bands. Since this is not the case for the sea (compare Ch. 3) where the turbulent energy outbreaks at different distant bands (and so might do other transforms), the integral transform approach seems to be appropriate in the analysis of individual ranges of turbulent scales, while being usatisfactory in the treatment of the whole random field of physical quantities in the sea. It is thus reasonable to assume jet-or patch-like patterns of polutants for small-scale turbulent eddies of higher frequencies, which cause relatively insignificant dilution of pollutants (e.g. in comparison with the near-field dilution), together with the dispersal of jets or patches as whole structures brought about by the turbulent eddies from an adjacent, range of energy-containing eddies of longer life. In other words, the growth of individual jets (or patches) may be conceptually divided into that due to the microscale turbulence and the dispersal of jets (or patches) caused by meso- and macroscale turbulence, which

results in much higher dispersion (Fig. 10.1). This concept of dual dispersion of pollutants is bolstered by results of empirical investigations for marine velocities within different frequency ranges. These results are depicted in Fig. 2.9 together with some theoretical generalization. The respective time scales of the external dispersion-controlling fields. (i.e. those of velocity and diffusion coefficient) must be thoroughly assessed with respect to characteristic times of a given inshore water body.

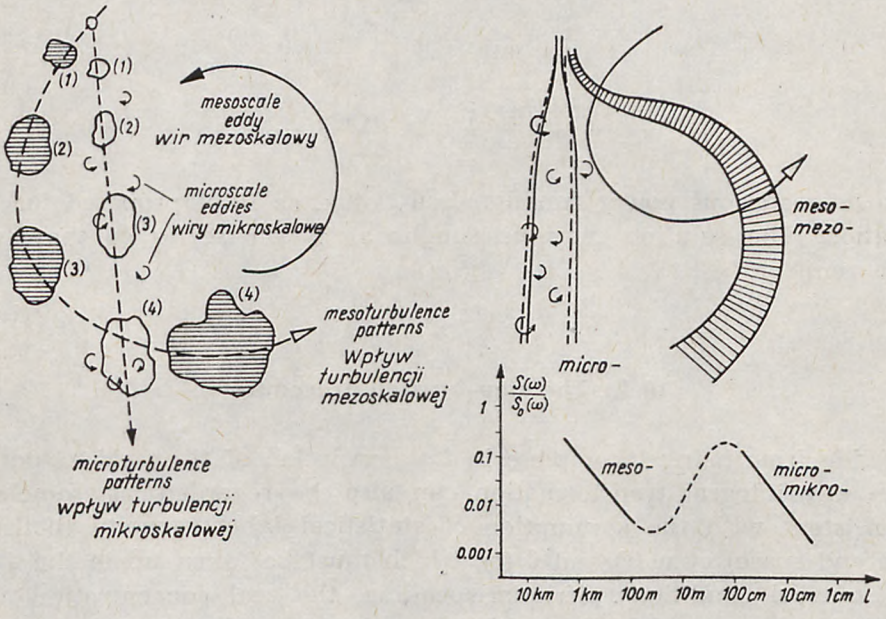

Fig. 10.1. The concept of dual dispersion

Rys. 10.1. Koncepcja podwójnego rozpraszania

While microscale turbulence is accounted for in terms of the equations of diffusive advection (whereas the latter takes place in an approximately steady direction) with additional effect of possible relative displacement of either patches or jets (still due to microscale turbulence), the meso- and macroscale turbulence must be considered in subsequent steps following a chosen time sequence of changes in the inshore zone. The recommended calculation procedure is thus as follows:

1. For known statistical characteristics of the water velocity in a given physical area stretching between a proposed outlet of pollutants and a protected zone (say, shore line) one assumes stationarity for a certain time longer than it follows from microscales, but shorter than that required to reach the protected boundary. The selected time corresponds

essentially to turbulent mesoscales. Such treatment allows individual, relatively large jets or patches to flow "unidirectionally" during a certain time and to change their flow conditions drastically after that time elapses.

2. For the sake of simplicity, let us now discuss continuous discharge of pollutants. During the next time interval, jet "No. 1" continues its spreading, but changes direction and is now treated as a genuine patch as if separated from the discharge outlet. Simultaneously another jet begins to flow from the discharge outlet and eventually forms a jet-like structure not necessarily identical with that of No. 1.

3. During subsequent time intervals new jets are produced and the older patches follow their own patterns. Between every two time instants of velocity change the patches are subject to diffusion. During the same time the whole velocity field (except specific areas close to shore) is assumed homogeneous; it also changes only at the end of each time interval.

4. The whole procedure is repeated until the number of time steps becomes representative in the statistics of shore pollution. For practical estimations it should be taken as about 20, if the ratio of the shortest time required for a discharged pollutant to reach a boundary zone (hereinafter referred to as the "shortest pollution time") to the selected time interval is about 5, and must be higher for higher ratios.

The procedure is illustrated in Fig. 10.2. A number of subroutines are included in the computer program for this procedure being prepared

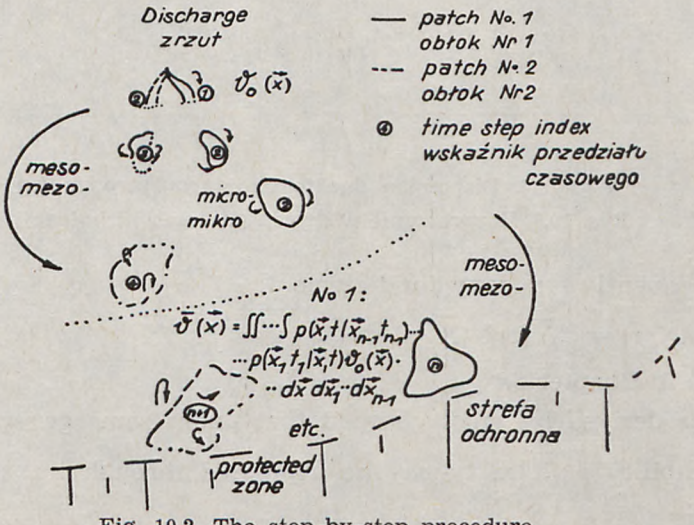

Fig. 10.2. The step-by-step procedure

Rys. 10.2. Metoda kolejnych kroków

by the Author. They allow for the initial spread of jet or plume, determination of jet boundaries, integration over jet portions, substitution of patches for jet portions, spread of patches, repeated virtual division of patches into smaler patches, tracking of all patches by their falling into a protected zone, and integration of all concentrations in this zone.

Let us reiterate that at any time t the concentration field (e.g. of patch No. 2 at the time denoted by "3") is

$$\vartheta(\vec{X}, t) = A[u_o(\vec{X}), t]\,\vartheta_o(\vec{X}) \tag{10.34}$$

with the random operator A of time t and velocity field $u_o(\vec{X})$. If one is interested in the mean concentration $\overline{\vartheta}(\vec{X}, t)$ as a function of initial $\overline{\vartheta}_o(\vec{X})$, then from averaging and using the concept of the delta function for a single fluid element one obtains

$$p(\vec{X}|\vec{x}, t) = \overline{A}(t)\,\delta(\vec{X} - \vec{x}) \tag{10.35}$$

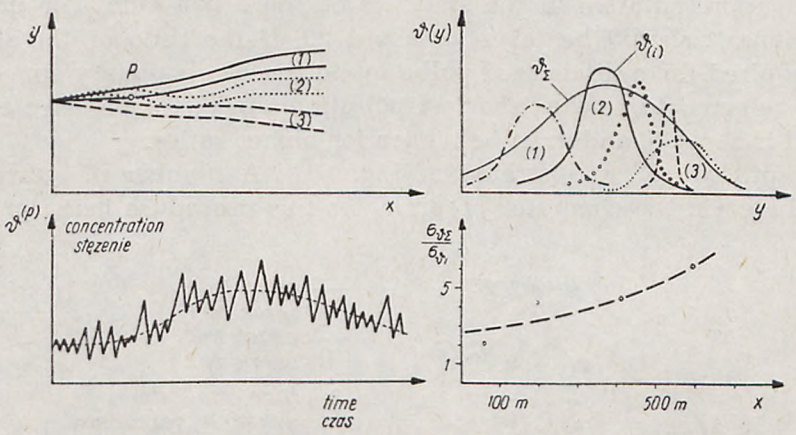

Fig. 10.3. Dispersion due to two turbulence bands
Rys. 10.3. Rozpraszanie w dwóch pasmach turbulencji

and consequently for many fluid elements

$$\overline{\vartheta(\vec{X}, t)} = \int \overline{A}(t)\,\delta(\vec{X} - \vec{x})\,\vartheta_o(\vec{x})\,d\vec{x} = \int p(\vec{X}|\vec{x}, t)\,\vartheta_o(\vec{x})\,d\vec{x} \tag{10.36}$$

as shown in Chapter 3.

It was derived by Smoluchowski that under some general conditions the probability $p(\vec{X}|\vec{x}, t)$ may be expressed through transitional probabilities

$$p(\vec{X}|\vec{x}, t) = \int p(\vec{X}, t|\vec{X}_1, t_1)\,p(\vec{X}_1, t_1|\vec{x}, t_o)\,d\vec{X}_1. \tag{10.37}$$

By extending this relationship to the whole class of patches analyzed herein one has

$$p(X|\vec{x}, \vec{t}) = p(X, \vec{t}|X_{n-1}, t_{n-1}) p(\vec{X}_{n-1}, t_{n-1}|\vec{X}_{n-2}, t_{n-2}) \ldots$$
$$\ldots p(\vec{X}_1, t_1|\vec{x}, t_o) \tag{10.38}$$

and consequently

$$\overline{\vartheta(\vec{X})} = \int\int \cdots \int p(\vec{X}, t|\vec{X}_{n-1}, t_{n-1})\, p(\vec{X}_{n-1}, t_{n-1}|\vec{X}_{n-2}, t_{n-2}) \cdots$$
$$\ldots p(\vec{X}_1 t_1|\vec{x}, t_o)\, \vartheta_o(\vec{x})\, d\vec{x}\, d\vec{X}_1 \ldots d\vec{X}_{n-1}. \tag{10.39}$$

Formula (10.39) provides a general possibility of finding $\overline{\vartheta(\vec{X})}$ for the probabilities which vary within inshore zones. Of practical interest is the case of renewal processes, when the transitional probabilities keep their form identical and unchanged from one time to another, i.e. when the intervals between successive events are independently and identically distributed:

$$p(t_1, t_2 \ldots t_{n-1}) = p_1(t_1)\, p_1(t_2 - t_1)\, p_1(t_3 - t_2) \ldots p_1(t_{n-1} - t_{n-2}). \tag{10.40}$$

If $p_1(t_1)$ is exponential, the processes is Markovian and can be identified as a homogeneous Poisson process.

In his experiments on turbulent diffusion in the coastal zone the Author found that the Gaussian distribution occurs at distances sufficiently far off shore, in the absence of considerable velocity shear.

The shortest pollution time may be estimated either by dividing a given distance by average velocity or by employing the variational calculus for a given distribution of velocities in space. Such a variational determination of the shortest pollution time may be of independent interest because of biological and biochemical factors, which take over the pollution control after longer times. In the case of heated water, such a determination allows one to establish the stretch of each dilution zone.

The time interval employed in the step-by-step procedure must always be taken from given spectral data for velocities. From empirical data presented in Fig. 2.11 and other sources it appears that a time step of several minutes may often be encountered in practical computations of coastal pollution.

An order of magnitude of the „additional" coastal dispersion due to the meso-scale factors is given by the Author's data presented in Fig. 10.3, where the dispersion characteristics of a single jet structure are compared against those from a superposition of jets over a longer period of time. Taken at different distances from the source, the ratios of single-jet width to multiple-jet „width" (more precisely, cross-section

variances) vary from five to ten. However, one should not forget that the computed figures correspond to the lower edge of the meso-scale band i.e. to fluctuations with periods of a few minutes, while the longer can induce much higher dispersion.

Chapter 11

SUMMARY AND CONCLUSIONS

In view of the world's increasing energy demand and high costs of complete wastewater purification, the marine disposal of waste- and heated water will long remain a reasonable solution. There appears an urgent necessity to provide engineers with a scientific basis which will enable them to design both submerged outlets and surface discharges (cf. Fig. 1.2).

Sea motion (currents, waves, etc.) controls the advection of waste- and heated water toward protected zones. The Autor's field and laboratory studies on inshore currents have made possible further schematization of inshore processes. Wind-driven currents are pronounced beyond the surf zone, where the wave-induced ones (energy c., gradiental c., rip c., mass transport and others, cf. Fig. 2.1) are dominant. Meandering longshore currents arise under stronger waves and their oblique incidence, while circulation cells are coupled with almost normal incidence. In the Author's observations, the width of circulation cells varied about 250 m and narrow seaward underwater outflow existed on deeper beach sections.

Wind-driven currents are essential beyond the surf zone, at a distance which depends on $h \cdot \operatorname{tg} \alpha H$. They can be computed from formulae 2.15 and 2.16. The ratio of wind-driven current velocities to respective wind speeds depends on sea depth (Fig. 2.8).

Wave currents develop much faster than the wind-driven ones.

The concept of radiation stresses is very helpful in deriving formulae for ware currents. The Author has found that the results of Longuet-Higgins (1970) basing on this concept are in agreement with empirical evidence. Simpler formulae employing the principle of mass conservation (per Bruun's Eq. 2.8 and Galvin and Eagleson's Eq. 2.9) are not quite satisfactory. Gradiental components may be computed from the Shadrin formula Eq. 2.10.

From the discussion of theoretical formulae and experimental results it follows that the velocity of longshore currents varies as a power

function of the distance from shore, with an exponent close to 1/7 at shore and with possibe shears on further distances (Fig. 3.24). This conclusion might be well true not only for wind-driven and wave-induced currents, but also for deep-sea currents (e.g. intertial) entering the coastal zone.

The vertical variation of current velocities is logarithmic and can be described with power functions (Fig. 3.24).

The Author's inshore currents spectra (Fig. 2.9) show the maximum energy peak moving toward higher frequencies at lower depths. The spectra of wind-driven currents seem to be wider than those of wave-induced ones. The turbulence intensity of weak currents does not change with depth and amounts to 20 ... 30 per cent.

Diffusion and dispersion processes undergone by wastes on their way from marine outfall to a protected zone may best be treated in terms of the semi-empirical turbulent theory. The Author shows that care must be exercised in applying empirical results for the dispersion tensor $D_{ij}(\vec{X}, t)$ to computations of the eddy diffusivities $K_{ij}(\vec{X}\, t)$ and in employ in the „4/3" law. The partial appicability of this law to coastal conditions might be due to narrow inertial subrange and the effect of adjacent energy input bands (Fig. 3.8), to the presence of the shore, which transforms the structure of turbulent eddies and changes diffusion law dramatically after a critical ratio of the distance from shore to eddy size is reached (Fig. 3.7.), and also — due to velocity field, which can undergo internal transformations to bring about modified dispersion laws (Fig. 3.10). Because of the many factors involved, dispersion can be described most simply through eddy diffusivities. The latter have been found to increase almost linearly with distance from shore up to hundreds meters offshore, while the "4/3" law can be applied on further distances (Fig. 3.24).

Hydraulic model tests on wave-induced diffusion indicate homogeneous turbulence conditions. The diffusion coefficients K_x and K_y depend on the characteristic wave parameter $\alpha = \frac{h^2}{\nu T}\left(\sinh \frac{2\pi H}{L}\right)^{-1/4}$, both in the turbulent and in the laminar regime. However, the temporal growth of dispersion under prototype conditions is often faster. Additional analysis of diffusion due to oscilations of water elements in wave motion together with random fluctuations allowed the Author to derive formula 3.49 for eddy diffusivity in the field of random waves and currents. The effect of wave — current interactions explains the acceleration of diffusion and also sheds light on the occurence of the "4/3" law.

Simple estimates were found for vertical diffusion in a density-homogeneous medium and its structure in stratified media was studied together with stratification effect on horizontal diffusion. On the basis of the turbulent energy equation the Author derives the variation of the vertical diffusion coefficient with depth (exponential in the upper layer, stability-dependent in the lower layers), which agrees with experimental data. It is also shown that stratification need not bring about any rise in the horizontal diffusion coefficient. The vertical dispersion component D_{zz} varies with distance as a pover with an exponent which depends on stratification.

Theoretical solutions have been found for the semi-empirical equation of turbulent diffusion (Par. 3.2.). The functional forms of eddy diffusivities and velocities shown in Fig. 3.24 were employed to find the concentration field 3.40, by which the Author confirms theoretically the coastal entrapment phenomenon observed in the field. All solutions presented depend on many factors and thus no generalization can be given. The simpler are shown below for a continuous line source with exponent intervals due to various stratification:

$u = \text{const}$	$K_y = \text{const}$	$\vartheta \sim x^{-1/2}\, x^{0 \div -0.8} = x^{-0.5 \div -1.3}$
$u = \text{const}$	$K_y = K_1 Y$	$\vartheta \sim x^{-1}\, x^{0 \div -0.8} = x^{-1.0 \div -1.8}$
$u = u_1 Y$	$K_y = \text{const}$	$\vartheta \sim x^{-0.7}\, x^{0 \div -0.8} = x^{-0.7 \div -1.5}$
$u = u_1 Y^{1/7}$	$K_y = K_1 Y^{6/7}$	$\vartheta \sim x^{-0.9}\, x^{0 \div -0.8} = x^{-0.9 \div -1.7}$

Heated-water discharges are governed by environmental heat transfer. All important heat transfer components (incident and reflected solar radiation, incident and reflected atmospheric radiation, back radiation, and evaporation and conduction losses) can be collectively shown as

$$\Phi_n = \Phi_r - \{4 \cdot 10^{-8} (T_w + 460)^4 + 17.2 W_z [(e_w - e_z) + 0.255 (T_w - T_z)]\},$$

where all the incident and reflected radiation terms are grouped in the net radiation term Φ_r, which is a function of meteorological variables, while, the remaining terms depend in part upon the water surface temperature.

The submerged outfall version of waste- and heated- water discharge (cf. Fig. 1.2) requires good initial dilution from sea bottom to surface. This dilution is controlled by the characteristics of jet itself (type and direction of discharge, momentum vs buoyancy, etc), thermal and density conditions of a recipient, motion of a recipient, and the initial and boundary conditions. The governing equations can be found from the conservation laws for mass, momentum flux, and density deficiency flux and from geometrical relations. The equations may not be solved in a closed analytical form, but numerical solutions can be found for various combinations of the controlling factor (Figs. 5.2, 5.3, 5.6, 5.7); some sum-

mary is provided by Shirazi and Davis (1971). Along with the stratification parameters, the Froude number controls dilution patterns. In a homogeneous medium, dilution at any level increases as the jet densimetric Froude number increases. In a linearly stratified environment, the maximum height of rise of the jet is decreased for increased Froude numbers, etc.

The Author has added to the knowledge of initial dilution under conditions with waves and currents. The jet centerline concentration falls more drastically in co-flowing and counterflowing ambient media than in a cross-flow. The concentration decrease rate depends on the ratio of jet and current velocities. The Author has elaborated a diagram for wave conditions, which together with Cederwall's diagram for currents can be used in assessment of dilution regimes. Jet dilution in a wave field was found to be dependent on the ratio $\frac{h^2}{gT^2H}$.

While the initial dilution relates to both waste and heated water discharged far off shore, the surface discharge at the shore line is recommended only for heated water. One is most justified when assuming the following regions of heated discharges: core, entrainment, stabilization, heat loss, and far field. The basic set of governing equations for every region consists of three Navier-Stokes equations together with the equations of mass conservation, heat conservation, and thermal expansion. Various assumptions taken up for this set must be substantiated empirically. Among them, entrainment poses most problems. The Author summarized the findings of others and compared their entrainment coefficients with his own values for conditions of stagnant and flowing environments. Values of $\alpha = 0.05$ to 0.8 depend on velocity ratios, flow geometry, and stratification (decreasing with higher Richardson numbers). Cross flow is generally found to deflect the jet and not to affect the dilution very much. Small bottom slopes are observed to inhibit vertical entrainment and dilution. After having analyzed all assumptions, governing equations, scope of ambient conditions, etc. the Author concludes that the fullest description of surface discharges is warranted by the computer program of Stolzenbach and Harleman (1971); the Author has added to this program some improvements, especially as to the far field turbulence.

Various experimental techniques must always bolster waste discharge-oriented theoretical analysis and design computations. The Author has used many different tools in studying the phenomena discussed herein; their summary may be found in Zeidler et al. (1969) and the Author's other works, as well as in Waldichuk (1967), Cederwall and Hansen

(1968), Ozmidov (1968), Feuerstein and Selleck (1963) and others. Drogues and floats are quite useful in coastal studies of advection and diffusion, although big amounts are necessary for higher reliability (a figure of 40 to 50 may be given as a reasonable practical amount for identifiable diffusion tracers). While using fluorescent dyes in shallow-water areas it is recommended to pump the traced water instead of to tow an underwater probe (Zeidler, 1969). Aerial photography (including infrared) also offers promise in diffusion studies.

Physical (hydraulic) modelling is often used to aid the studies discussed. In view of many factors involved and the impossibility of conforming to all inherent modelling scales it is practicable to employ at least two different models, of which the undistorted one is to reproduce the initial dilution phenomena, while the other (distorted) has to represent the far-field conditions. The distortion depends on the relative weight of friction effects, heat loss, etc. and must be estimated individually for any given case. Eqs. 8.3 and 8—11 provide criteria for surface cooling, while Eq. 8.7 allows for ambient turbulence.

Besides the hydromechanical factors, other effects must also be included into the design of waste outfalls. Biochemical and biological phenomena become substantial after longer residence times of wastes.

In a series of marine tests with rhodamine and bacteria as tracers the Author found that the decay coefficient for Coliform bacteria varies with the residence time. The half-life time $T_p = \frac{\ln 2}{\alpha}$ is 0.5 hour for about two-hour residence times and about 1.5 hour for longer times (the tests were conducted up to 6 hours). This effect is not observed in sterile marine water.

The quasi-deterministic models discussed herein are useful unless the stochastic character of the external dilution-controlling fields is taken into account. Under real conditions there exists not only microscale diffusion within the framework of statistically stationary and homogeneous hydromechanical fields but also meso-and macro-scale turbulence, which brings about more pronounced changes in those fields and adds to the microscale diffusion. Since through integral transforms it is possible to obtain some partial results only, e.g.

$$S^{\vartheta}(\omega) = S^{0}_{\vartheta}(\omega) \exp(-\chi x)\left[\cos\frac{\omega}{u}x + \bar{u}\frac{\chi}{\omega}\sin\frac{\omega}{u}x\right]$$

for the Fourier transforms of two-point concentration correlations, or

$$S_{\vartheta}(\omega) = f_1(x, y, z) \cdot \exp\left[-f_2(x, y)\sum_k \Phi_k\right]\left\{-f_3^2\frac{1}{\omega^2} + (f_3^3 f_y + f_3^6/6)\frac{6}{\omega^4} \ldots\right\}$$

as a transform of Eq. 3.40 derived for eddy diffusivities and velocities shown in Fig. 3.24, and because of unavailability of other analytical tools (multi-dimensional probability funtions are not found easily, while solutions for characteristic functionals do not exist, etc.), the mere alternative of including the randomness into the design scheme consists in the step-by-step procedure derived by the Author. The individual steps are as follows:

1. Quasi-deterministic calculation for a given time interval with statistically stationary and homogeneous conditions. Jet No. 1 flows out of a pollutant discharge structure;

2. The treatment of jet No. 1 as if it separated from the discharge outlet. Simultaneously another jet begins to flow out of the discharge structure.The external field changes its characteristics including flow direction at the transition instant 1—2, but remains unchaged during the whole time interval No. 2.

3. During subsequent time intervals new jets are produced and older patches follow their own patterns;

4. The whole procedure is repeated until the number of time steps becomes representative in the statistics of shore pollution (in practice, about 20). The final concentration for patch with initial concentration $\vartheta_o(\vec{x})$ reads

$$\vartheta(\vec{X}, t) = \int\int \ldots \int p(\vec{X}, t | \vec{X}_{n-1}, t_{n-1})\, p(\vec{X}_{n-1}, t_{n-1} | \vec{X}_{n-2}, t_{n-2}) \ldots$$
$$\ldots p(\vec{X}_1, t_1 | \vec{x}, t)\, \vartheta_o(\vec{x})\, d\vec{x}\, d\vec{X}_1 \ldots d\vec{X}_{n-1}$$

Acknowledgements

The Author should like to express his sincere gratitude to the staff of the Ralph M. Parsons Laboratory for Hydromechanics and Water Resources of the Massachussetts Institute of Technology, and particularly to Professors Arthur T. Ippen and Donald R.H. Harleman for the valuable discussions held during the Author's stay in Cambridge (Massachusetts) under the scholarship arranged by the American Government under the Senior Fulbright-Hays Program. He also highly appreciates the scientific atmosphere doveloped at the Maritime Hydraulics Division, Institute of Hydro-Engineering, Polish Academy of Sciences (Gdańsk) while headed by Professors J. Onoszko and Cz. Druet. These two factors enabled the Author to complete this work successfully.

LIST OF NOTATIONS

$A = \frac{h_o}{b_o}$ — discharge channel aspect ratio

a — ambient index; wave amplitude; coefficient
a_t — wave trough below mean wave level
B — slot jet outlet width
$B_{ij} = < V_i'(t)\, V_j'(t+\tau) >$ — Lagrangian velocity correlation
b — jet half-width; breaking index
b_o — discharge channel half-width
C — cloudiness; specific heat
c — phase velocity; centerline index
D — circular jet outlet diameter
$D_{ij} = < Y_i'(\tau)\, Y_j'(t+\tau) >$ — turbulent dispersion tensor
$\mathcal{D}$ — operator of variational derivation
$E = \frac{1}{\varrho}\frac{\partial \varrho}{\partial z}$ — stability factor; energy
F, F_L, F_o, F_r — Froude number
f — bottom friction
$\mathcal{F}$ — operator of the Fourier transform
g — acceleration due to gravity
H — water depth
$\mathcal{H}$ — heat input
h — wave height
h_o — discharge channel depth
i — index i = 1, 2, 3; imaginary versor
j — index i = 1, 2, 3; imaginary versor
K, K_{ij} — turbulent diffusion coefficient (eddy diffusivity)
$k = \frac{2\pi}{L}$ — wave number
L — wavelength
l — characteristic length; turbulence scale
l_1, l_2 — local width of surf zone
$m = \mathrm{tg}\alpha$ — bottom slope; maximum index
n — normal line axis
o — deep-water index; initial state index
P — probability; diffusion velocity

p — peak index; pressure; probability density
Q — flow rate
q — unit flow rate
$R_{\alpha\beta}$ — correlation
$R_{ij}(t) = \frac{B_{ij}(t)}{B_{ij}(O)}$ — standardized Lagrangian velocity correlation
R_e — Reynolds number
R_i — Richardson number
r — hydraulic modelling ratio index (e.g. U_r — velocity scale); radial co-ordinate; radius
S, S_{ij}, S — spectral density; radiation stress
s — longitudinal co-ordinate; energy porton
T — time; temperature; wave period
T_p — half-life time
t — time
$\vec{U}, \vec{V}$ — velocity vector (Lagrangian)
$\vec{u}, \vec{v}$ — velocity vector (Eulerian)
u, v, w — velocity components (Eulerian)
u^* — friction velocity
$\vec{W}$ — wind velocity vector
X_i, X_j, X, Y, Z — Cartesian co-ordinates (Lagrangian)
x_i, x_j, x, y, z — Cartesian co-ordinates (Eulerian)
$Y = X - x$ — dispersion distance
α — solar altitude; entrainment coefficient; decay coefficient; bottom slope
Γ — velocity gradient ("shear"); gamma function
ε — energy dissipation rate
Θ — angle (of wave incidence; of jet inclination, etc.)
Θ_{nm} — statistical moment
ϑ — concentration
φ — heat flux
ν — kinematic coefficient of viscosity
ξ_i, ξ_j — local co-ordinates
ϱ — density
ϱ_o — initial density
ϱ_w — water density
σ — standard deviation; orbital frequency
τ — time; shear stress
Φ — characteristic functional
χ — molecular diffusion coefffcient
ω — frequency

RYSZARD ZEIDLER
Polska Akademia Nauk
Instytut Budownictwa Wodnego — Gdańsk

HYDROMECHANICZNE ZAGADNIENIA ZRZUTU ŚCIEKÓW I PODGRZANYCH WÓD DO BRZEGOWEJ STREFY MORZA ORAZ PROBLEMY POKREWNE

Streszczenie

Zagadnienia badane w ramach niniejszej pracy stają się w Polsce coraz bardziej aktualne ze względu na powszechną obawę przed skażeniem naturalnego środowiska w wyniku zrzutu ścieków przemysłowych i komunalnych, łącznie z substancjami radioaktywnymi i podgrzanymi wodami elektrowni nadmorskich. Aczkolwiek przedmiotem pracy są przede wszystkim hydromechaniczne zjawiska obiegu ścieków w morzu, to dla uzyskania pełniejszego obrazu i umożliwienia projektowania właściwych zrzutni ścieków uwzględniono także czynniki biochemiczne, termiczne i inne.

Substancje zanieczyszczające zrzucane do morza rozprzestrzeniają się w dwóch zasadniczych etapach: rozcieńczania wstępnego w tzw. polu bliskim w pobliżu wylotu kolektora oraz rozpraszania w większej skali w tzw. polu dalekim. W wypadku ścieków konwencjonalnych stosuje się na ogół wylotowy dyfuzor podwodny umieszczony z dala od brzegu, podczas gdy podgrzane wody zrzucane są przede wszystkim przy brzegu morza.

Uwaga badaczy skupiona na dużym rozcieńczaniu wstępnym w wylotowym strumieniu substancji ściekowych pozwoliła na niezłe rozpoznanie tego problemu i opracowanie rozwiązań nawet dla złożonych sytuacji w ośrodkach niejednorodnych gęstościowo (najczęściej w postaci algorytmów komputerowych). Autor uzupełnił istniejące rozwiązania wynikami badań laboratoryjnych nad wpływem falowania i prądów na rozcieńczanie wstępne. Okazało się, że zarówno w wypadku płynącego, jak i falującego ośrodka, stężenia w strumieniu wylotowym zmieniają się w sposób potęgowy z wykładnikami potęg zależnymi od prędkości ośrodka i parametrów fal (rys. 5.9 i wzór 5.23). Te same czynniki wpływają również na charakter ruchu i kształt obszaru ruchu substancji ściekowych wypływających w ośrodkach płynących i falujących (rys. 5.8, 5.10).

Badanie bliskiego pola podgrzanych wód wymaga znajomości czynników termicznych, m.in. promieniowania słonecznego, parowania itd. (które przedyskutowano w rozdziale 4). Z porównania tych i innych czynników — w ramach stosunkowo spójnych modeli teoretycznych, przeprowadzonego w rozdziale 6 z uwzględnieniem rezultatów badań empirycznych — wynika, że algorytm przedstawiony przez Stolzenbacha i Harlemana (1971) opisuje najszerszą klasę zjawisk. Ponadto, stosowanie tego modelu daje wyniki zgodne jakościowo i ilościowo z pomiarami doświadczalnymi wykonanymi przez różne grupy badaczy (rozdział 6). W pierwszym przybliżeniu można posługiwać się jednak prostszymi wzorami empirycznymi zaprezentowanymi przez autora (wzory 6.7—6.10).

Teoretyczne modele wstępnego rozcieńczania omówione w rozdziale 5 (przede

wszystkim dla ścieków konwencjonalnych) oraz w rozdziale 6 (przede wszystkim dla podgrzanych wód) muszą być uzupełnione analizą prądów, falowania i turbulencji oraz ich wpływu na rozcieńczenie w dalekim polu. Badania autora (i inne) w tym zakresie zostały przedstawione w rozdziale 2 (procesy przenoszenia w strefie brzegowej) i rozdziale 3 (dotyczącym burzliwej dyfuzji).

Terenowe i laboratoryjne pomiary autora potwierdziły odmienność adwekcji w bezpośrednim sąsiedztwie brzegu (gdzie dominują prądy falowe i często występują komórki cyrkulacyjne) w ich obszarze pozabrzegowym. Energetyczne prądy falowe są dobrze opisywane ilościowo wzorami Longuet — Higginsa, niezłe zaś przybliżenie prędkości prądów gradientalnych zapewnia wzór Szadrina. Prądy falowe rozwijają się znacznie szybciej od prądów wiatrowych.

Poza wzorami (2.15) i (2.16) dla prądów wiatrowych, we wstępnych pracach projektowych można posługiwać się prostym stosunkiem prędkości wody do prędkości wiatru u/W, który zależy od głębokości (rys. 2.10). Z dyskusji wzorów i wyników pomiarów w naturze wynika, że prędkość prądów przybrzeżnych zmienia się potęgowo z odległością od brzegu, z wykładnikiem potęgi bliskim 1/7 przy brzegu oraz z odmiennym wykładnikiem dalej od brzegu (rys. 3.24). Można sądzić, że wniosek ten dotyczy nie tylko prądów wiatrowych i falowych, przedyskutowanych w pracy, ale i krążenia przybrzeżnego kształtowanego przez czynniki pozabrzegowe (np. prądy bezwładnościowe).

Zmienność prędkości prądów wzdłużbrzegowych z głębokością jest logarytmiczna, ale można ją opisać wzorami potęgowymi (rys. 3.24). Pomierzona intensywność turbulencji słabych prądów nie zmieniała się z głębokością, osiągając wartość 20—30%.

Zasadnicze rezultaty analizy dyfuzji przedstawiono również na rysunku 3.24. Pokazano, że współczynniki dyfuzji zmieniają się prawie liniowo z odległością od brzegu, co potwierdzają empiryczne badania autora. Dla pól prędkości i współczynników dyfuzji w postaci zadanej na rys. 3.24 posługując się sposobem Fouriera rozwiązano równania półempirycznej teorii dyfuzji dla różnych rodzajów źródeł substancji ściekowych. Jednym z ciekawszych wyników okazało się teoretyczne potwierdzenie „przechwytywania" zanieczyszczeń przez brzeg w wyniku istnienia gradientów prędkości i zmiennego pola współczynników dyfuzji (por. rys. 3.9). Istotny wpływ na rozpraszanie w dalekim polu ma falowanie. Laboratoryjne badania z falami regularnymi wskazują na zależność współczynników dyfuzji falowej od h^2/T i względnej głębokości (rys. 3.14). Odrębna analiza dyfuzji związanej z oscylacjami elementów wody i losowymi pulsacjami pozwoliła na wprowadzenie współczynnika widmowej dyfuzji falowej (3.49) zależnego od widma drgań swobodnej powierzchni. Przyjęcie tego współczynnika w ramach oddziaływania prądów i fal wyjaśnia obserwowane w naturze „przyśpieszenie" dyfuzji pod wpływem falowania i stawia w innym świetle często nadużywane prawo lokalnej izotropii (np. rys. 3.5). Jedną z przyczyn niepełnej stosowalności prawa 4/3 dla strefy brzegowej może być wąskość podprzedziału bezwładnościowego i wpływ sąsiednich pasm dopływu energii (rys. 3.8), inną — obecność brzegu, który przekształca pole burzliwych wirów i drastycznie zmienia prawa dyfuzji po przekroczeniu krytycznego stosunku odległości od brzegu do promienia wirów (rys. 3.7), lub wreszcie — pole prędkości, które może ulegać wewnętrznym przemianom odpowiednio modyfikując prawa rozpraszania (rys. 3.10).

Analiza danych dla pionowej dyfuzji pozwala postulować trójwarstwowy model (rys. 3.15, wzory 3.63) z wykładniczym zanikiem K_z przy powierzchni. W powiązaniu z innymi danymi dla poziomej dyfuzji analiza ta daje spójny obraz zjawisk dyfuzyjnych w przybrzeżnej strefie morza i jednocześnie umożliwia projektowanie

zrzutni ścieków w ramach modeli quasi deterministycznych (z polami mikroskalowych pulsacji nakładanych na regularne strumienie zrzucanych substancji).

Rozszerzenie zakresu badanych zjawisk turbulencji i uwzględnienie również średnioskalowych zmian, powodujących przemieszczenie i odkształcenie całych regularnych strumieni, umożliwiają metody przedstawione w rozdziale 10. Zastosowane przekształcenie Fouriera pozwala obliczać pola stężeń substancji zrzucanych w warunkach zmiennych prądów. Podobne stężenia otrzymuje się w wyniku przyjęcia innego schematu rozprzestrzeniania się ścieków, a mianowicie skokowej zmiany warunków prędowych w określonych odstępach czasowych (rys. 10.2). Uwzględnienie średnioskalowych zmian prądów prowadzi do uznania istotnego wkładu dalekiego pola do ogólnego rozcieńczenia substancji ściekowych (por. rys. 10.3).

Inne czynniki przyczyniające się do dodatkowego zaniku ścieków (zwłaszcza komunalnych) omówiono w rozdz. 9. W wyniku badań w naturze stwierdzono, że czas półzaniku ścieków pod wpływem biochemicznego i biologicznego oddziaływania morza jest krótszy na niedużych odległościach od wylotu (tj. dla krótkich czasów przebywania w morzu). Czas ten wynosi około $T_p = 0{,}5$ godziny do odległości ok. 350 m (tj. ok. 2 godzin obiegu w morzu) i dochodzi do $T_p = 1{,}5$ godz. dla większych odległości (tj. dłuższych czasów obiegu i mniejszych stężeń).

Metodykę badań empirycznych związanych z omawianym problemem poruszono w rozdziałach 7 (pomiary terenowe) i 8 (modelowanie hydrauliczne). W powiązaniu ze sposobami postępowania analitycznego i wynikami podanymi w pozostałych rozdziałach znajomość tej metodyki umożliwia przystąpienie do badań doświadczalnych, które powinny uzupełniać prace projektowe dla morskich zrzutni substancji zanieczyszczających.

REFERENCES

LITERATURA

Abraham G. (1963), *Jet diffusion in stagnant ambient fluid*, Delft Hydr. Lab. Publ., **29**.

Abraham G. (1965), *Horizontal jets in stagnant fluid of other density*, ASCE-HY, 4.

Abraham G. (1970), *The flow of round buoyant jets issuing vertically into ambient flow flowing in a horizontal direction*, Int. W.P.C. Res. 5th Conf.

Abraham G. and Eysink W. (1962), *Jets issuing into fluid with a density gradient*, J. Hydr. Res. 2.

Abramovich G.N. (1963), *The theory of turbulent jets*, MIT Press (or in Russian: *Teoriya turbulentnych strug*, 1958).

Ackers P. (1969), *Modelling of heated-water discharges*, Ch. 6 in Parker and Krenkel.

Adams E. (1972), *Submerged multiport diffuser in water with a current*, M.I.T. Report 142.

Aitsam A. (1968), *A stochastic model of marine waste disposal*, 4th Int. Conf. on Wat. Poll. Res.

Aitsam A. (1971), *Transformation of probability characteristics of pollutants in marine environment*, AIHR Congress.

Aitsam A. et al. (1970), *A method of qualification of sea water with due regard to the extent of sewage dilution (in Russian,* Gigiena *i* Sanitariya, 8, Aug).

Aitsam A. et al (1973), *Probabilistic characteristics of pollutants diffusion in marine environment,* AIHR Conf., 13th.

Anwar H.O. (1969), *Behavior of buoyant jet in calm fluid,* ASCE-HY, 7.

Anwar H.O. (1972), *Appearance of unstable buoyant jet,* ASCE-HY, 7.

Anwar H.O. (1972), *Discussion to Koh (1971),* ASCE-HY, 1.

Assaf G. et al. (1971), *Some mechanisms of oceanic mixing revealed in aerial photographs,* J. Geoph. Res., No. 27, Sep.

Atkins G.R. (1971), *Marine effluents research and marine disposal of effluents in the False Bay Area,* Wat. Poll. Control, 70 (2).

Aubert M. et al. (1969), *The diffusion of bacterial pollution in the sea,* 4th Int. Conf. on Wat. Poll. Res.

Barr D.I.H. (1967), *Discussion to Jen et al. (1966),* ASCE-PO, March.

Barret et al. (1968), *Radiotracer dispersion studies in the vicinity of a sea outfall,* 4th Int. Conf. on Wat. Poll. Res.

Barry R.E. and Hoffman D.P. (1972), *Computer model for thermal plume,* ASCE-PO, 1.

Battjes J.A. (1972), *Radiation stresses in short crested waves,* J. Mar. Res. 1.

Baumgartner D.J. (1969), *Disposal of liquid and particulate wastes to the ocean,* FWPCA, Paper.

Beckman W.J. (1970), *Engineering considerations in the design of an ocean outfall,* J. Wat. Poll. Contr. Fed. Oct.

Beer L.P. (1969), *Environmental effects of condenser water discharge in southwest Lake Michigan,* Great L. Res., 12th Conf.

Beer L.P. (1971), *Natural and unnatural water temperatures in Zion-Waukegan, Lake Michigan,* Great L. Res., 14th Conf.

Bonde G. et al. (1967), *Report on the investigations of the Swedo-Danish Committee on Pollution of the Sound 1959—1964,* Copenhagen.

Bowen A.J. (1969), *Rip currents,* 1. J. Geoph. Res., No. 23, Oct.

Bowen A.J. (1969), *The generation of longshore currents on a plane beach,* J. Mar. Res., No. 206.

Bowen A.J. and Inman D.L. (1969), *Rip currents,* 2. J. Geoph. Res., No. 23.

Bowen A.J. and Inman D.L. (1971), *Edge waves and crescentic bars,* J. Geoph. Res. Dec.

Brady D.K. et al. (1969), *Surface heat exchange at power plant cooling lakes,* Edison Elec. Institute. Publ. 69—901. Nov.

Bronfman A.M. et al. (1974), *Dynamics of the self-purification and pollution processes in the system "pelagial-sea bed" (in Russian),* Conf. „Pollution of saline seas" — Gdynia, Morski Instytut Rybacki.

Bretschneider Ch. (1967), *On the generation of wind-driven currents over the continental shelf,* 3d Ann. Meeting, A.S.C.E, San Diego.

Brook R.R. (1970), *Power law solutions for vertical plumes,* ASCE-HY, 9.

Brooks N.H. (1959), *Diffusion of sewage effluent in an ocean current Waste,* Disp. Mar. Envir. 1st Int. Conf.

Brooks, N.H. and Koh R.C.Y. (1969), *Selective withdrawal from density-stratified reservoirs,* ASCE-HY, 7.

Bruun P. (1963), *Longshore currents and longshore troughs,* J. Geoph. Res., No. 68.

Bye J.A.T. (1967), *The wave-drift current,* J. Mar. Res. 25.

Carstens T. (1970), *Turbulent diffusion and entrainment in two-layer flow*, ASCE-WW, 1.

Carter T.G. et al. (1973), *Mass-transport by waves and offshore sand bedforms*, ASCE-WW, 2.

Carter H.H. and Okubo A. (1972), *Longitudinal dispersion in non-uniform flow*, Wat. Res. Research 3 (June).

Cederwall K. (1968), *Hydraulics of marine waste water disposal*, Chalmers Inst. Techn.

Cederwall K. and Hansen J. (1968), *Tracer studies on dilution and residence time distribution in receiving waters*, 4th Int. Conf. on Wat. Poll. Res.

Cederwall K. (1971), *Discussion to Tamai et al. (1969)*, ASCE-PO, 1.

Cederwall K. (1971), *Buoyant slot jets into stagnant or flowing environments*, KH-R-25 Apr.

Ceglarski R. et al. (1972), *Die Anwendung eines Fluorometers bei in-situ-Messungen der Meeresdiffusion*, Beitr. zur Meereskunde 30/31.

Chu V.H., Goldberg M.B. (1974), *Buoyant forced-plumes in cross-flow*, ASCE--HY, 9.

Crickmore M.J. (1972), *Tracer tests of eddy diffusion in field and model*, ASCE-HY, 10.

Chao J.L. and Compurano C.M. (1972), *Simplified method of ocean outfall diffuser analysis*, J. Wat. Poll. Contr. Fed., May.

Chao J.L. and Hennessy P.V. (1972), *Local scour under ocean outfall pipelines*, J. Wat. Poll. Contr. Fed., July.

Collyer M.M. (1970), *The stability of stratified shear flows*, J. Fl. Mech., 42, 2.

Csanady G.T. (1964), *Turbulence and diffusion in the Great Lakes*, Great L. Res., 7th Conf.

Csanady G.T. (1966), *Dispersal of foreign matter by the currents and eddies of the Great Lakes*, Great L. Res., 9th Conf.

Csanady G.T. (1970), *Dispersal of effluents in the Great Lakes*, Wat. Res., 4.

Csanady G.T. (1970), *Waste heat disposal in the Great Lakes*, Great L. Res., 13th Conf.

Csanady G.T. (1970), *Dispersal of effluent in the Great Lakes*, Wat. Res., 1.

Csanady G.T. (1971), *On the equilibrium shape of the thermocline in a shore zone*, J. Phys. Ocean, 4.

Csanady G.T. (1972), *Frictional currents in the mixed layer at the sea surface*, J. Phys. Ocean, 10.

Csanady G.T. (1970), *Coastal entrapment in Lake Huron*, Int. W.P.C. Res., 5th Conf.

Csanady G.T. and Mekinda M. (1970), *Rapid fluctuations of current direction in Lake Huron*, Great L. Res., 13th Conf.

Csandy G.T. et al. (1971), *Thermal plume study at Douglas Pt, Lake Huron*, Great L. Res., 14th Conf.

Dake J.M.K. and Harleman D.R.F. (1969), *Thermal stratification in lakes; analytical and laboratory studies*, Wat. Res, 2.

Davis D.R. et al. (1972), *Bayesian decision theory applied to design in hydrology*, Wat. Res., 1, Feb.

Desnianskii V.N., Novikov E.A. (1974), *Evolutsiya spektrov turbulentnosti k rezhimu podobiya*, Fiz. Atm. Ok. 2.

Diachishin R.R. (1963), *Dye dispersion studies*, ASCE-SA, 1.

Diachishin R.R. (1963), *Waste disposal in tidal waters*, ASCE-SA, 4.

Disco M.D. et al. (1970), *Mathematical model of mixing in New Haven Harbor*, Coast. Eng. Conf., 12th.

Ditmars J.D. (1969), *Computer Program. Round Buoyant Jets into Stratified Ambient Environments*, KH-R Memo 69—1, March.

Dobroklonskii S.V., Pyzhevich M.L. (1974), *Primer rascheta kosvennymi metodami vertikalnoy skorosti techeniya i vertikalnogo koeffitsiyenta turbulentnoi viazkosti v okeane*, Issl. izmench. gidrof. poley v okeane, Nauka, Moskwa.

Dornhelm R. et al. (1970), *Velocity and temperature in a buoyant surface jet*, ASCE-PO, 1.

Druet Cz., Kowalik Z. (1970), *Dynamika morza (Sea dynamics)*, Wydawnictwo Morskie, Gdańsk.

Druet Cz., Massel St., Zeidler R. (1972), *Statystyczne charakterystyki falowania wiatrowego w przybrzeżnej strefie Zatoki Gdańskiej i otwartego Bałtyku*, Rozpr. Hydrot., z. 30.

Eagleson P.S. (1969), *Theoretical study of longshore currents on a plane beach*, M.I.T. Rept. 82.

El Mahgary Y.S. (1971), *Thermal diffusion of the warm water of power plant into a sea basin*, Journ. Env. Scie., Nov.

Elliot G.H. (1971), *A mathematical study of the thermal bar*, Great L. Res., 14th Conf.

Ellis D.W. et al. (1972), *Marine monitoring of the Victoria sewer system*, Coast. Eng. Conf. 13th.

Ellison T.H. and Turner J.S. (1959), *Turbulent entrainment in stratified flows*, J. Fl. Mech. Vol. 6, part 3, Oct.

Engelund F. and Pedersen F.B. (1970), *Surface jet at small Richardson numbers.*

Eremenko J.J. et al. (1973), *Determination of passive matter concentration in anisotropic flows*, IAHR Conf., 13th.

Fan L-N. (1967), *Turbulent buoyant jets into stratified or flowing ambient fluids*, KH-R-15.

Fan L-N. and Brooks N.H. (1969), *Numerical solutions of turbulent buoyant jet problems*, KH-R-18.

Fink L.E. (1973), *Modelling of the influence of background turbulence upon jet mixing*, AIHR Conf. 13th.

Feuerstein and Selleck R.E. (1963), *Fluorescent tracers for dispersion measurements*, ASCE-SA, 4.

Fisher H.B. (1969), *The effects of bends on dispersion in streams*, Wat. Res. Research 2.

Fisher H.G. (1971), *The dilution of an undersea sewage cloud by salt fingers*, Wat. Res. Research 10.

Fisher L.J. (1966), *Preliminary results and comparison of dye tracer studies condusted in harbours, estuaries, and coastal waters*, Intnl. Conf. Coast. Eng. 10th.

Fox D.G. (1969), *Forced plume in a stratified fluid*, J. Geoph. Res., 33 Nov.

Foxworthy J.E. et al. (1966), *Dispersion of a surface waste field in the sea*, Wat. Poll. Contr. Fed. p. 1171.

Frankel R.C. and Cumming F.R. (1965), *Turbulent mixing phenomena of ocean outfalls*, ASCE-SA, 2.

French J.A. (1972), *Internal hydraulics of multiport diffusers*, Wat. Poll. Contr. Fed. May.

Galvin C.J. (1967), *Longshore current velocity: A review of theory and data*, Rev. Geophysics, Vol. 5, No. 3.

Galvin C.J. and Eagleson P.S. (1965), *Experimental study of longshore currents on a plane beach*, R.I.T. Rept.-82.

Gameson A.L.H. and Saxon J.R. (1968), *Field studies on the effect of daylight on mortality of Coliform bacteria*, 4th Int. Conf. on Wat. Poll. Con.

Garvine R.W. (1971), *A simple model of coastal upwelling dynamics*, J. Phys. Ocean 3.

Gedney R.T. and Lick W. (1972), *Wind-driven currents in Lake Erie*, J. Geoph. Res. 15, May.

Glenn B. and Bourke R. (1972), *Coastal currents of Pacific Northwest*, ASCE-WW, 4.

Gihtman J.J. and Skorokhod A.V. (1968), *Stochastic Differential Equations* (in Russian: *Stokhasticheskiye differentsialnyie uravneniya*), Nauk. Dumka, Kiev.

Goroshko V.I. (1974), *Turbulentnaya diffuziya primesi v pribrezhnoi zone moria*, Issl. izmech. gidrof. polei v okeane, Nauka, Moskwa.

Gunnerson C.G. et al. (1970), *Marine disposal of solid wastes*, ASCE-SA, 96.

Gustafsson B. and Larsen J. (1970), *Jet diffusion on stagnant stratified waters*, Wat. Res. Research 5.

Gunther F.J. and Bugliarello G. (1973), *Computer-instant packages and data banks in environmental data collection*, AIHR Conf. 13th.

Gunwaldsen R.W. et al. (1971), *Current and temperature surveys in Lake Ontario for James A. Fitzpatrick nuclear power plant*, Great L. Res., 13th Conf.

Häggstrom S. (1972), *Surface buoyant jets in distorted models*, Coast. Eng. Conf. 13th.

Hall W. et al. (1970), *Boundary effects on jet flow patterns related to water quality and pollution problems, Illinois Univ.*, Wat. Res. Center, Res. Rept 28.

Hamblin P.F. (1971), *An investigation of horizontal diffusion in Lake Ontario*, Great L. Res., 14th Conf.

Hansen J.A. (1970), *Predetermining trapping of sewage in stratified receiving waters*, Nucl. Techn. in Env. Poll. Salzburg, Oct.

Harleman D.R.F. (1969), *Mechanics of condense-water discharge from thermal power plant*, Ch. 5 in Parker and Krenkel.

Harleman D.R.F. and Stolzenbach K.D. (1967), *A model study of thermal straticication produced by condenser water discharge*, M.I.I. Rept. 107, October.

Harleman D.R.F. et al. (1972), *Summer Session on heated water discharges*, MIT.

Harremoës P. (1967), *Tracer studies on jet diffusion and stratified dispersion*, Int. WPC Res. 3rd Conf.

Harremoës P. (1968), *Diffuser design for discharge to a stratified water*, 4th Int. Conf. on Wat. Poll. Con.

Harremoës P. (1970), *Field determination of bacterial disappearance in seawater*, Wat. Research 11.

Harremoës P. (1966), *Prediction of pollution from planned waste-water outfalls*, Wat. Poll. Contr. Fed. p. 1323.

Harris T.F.W. et al. (1964), *Mixing in the surf zone*, Int. WPC Res. 1st Conf.

Haverson D. (1970), *Mathematical model techniques for coastal waters*, Int. W.C. Res. 5th Conf.

Hayashi T. (1971), *Turbulent buoyant jets of effluent discharged vertically upwards from an orifice in a cross current in the ocean*, Int. AIHR Congress.

Hayashi T. and Shuto N. (1967), *Diffusion of warm water jets discharged horizontally at the water surface,* Int. AIHR Congress.

Hays J.R. et al. (1966), *Application of frequency-response techniques to analysis of turbulent diffusion phenomena,* Wat. Poll. Contr. Fed., p. 1669.

Higuchi H. and Iwagaki Y. (1968), *Hydraulic model experiment on the diffusion due to the coastal current,* Coast. Eng. Conf., 11th.

Hindley P.D. et al. (1971), *Thermal discharge: A model-prototype comparison,* ASCE-PO, 4.

Hindley P.D. and Miner R.D. (1972), *Evaluating water surface heat exchange coefficients,* ASCE-HY, 8.

Hirst E. (1971), *Buoyant jets discharged to quiescent stratified ambients,* J. Geoph. Res., Oct. 20.

Hirst E. (1972), *Discussion to Koh* (1971), ASCE-HY, 1.

Holley E.R., Harleman D.R.F., Fisher H.B. (1970), *Dispersion in homogeneous estuary flow,* Procedings A.S.C.E. vol. 96, No. HY8.

Holly F.M., Grace J.L. (1972), *Model study of dense jet in flowing fluid,* ASCE-HY, 11.

Hopkins T.S. (1974), *On time dependent wind induced motions.* Proceed. of Conf. on Sea Diffusion, Intnl Council Expl. Sea vol. 167, Dec., pp. 21—36.

Huang N.E. (1970), *Mass transport induced by wave motion,* J. Mar. Res., 28, 1.

Huang J.C.K. (1972), *The thermal bar, Geoph.* Fluid Dyn. vol. 3, No. 1.

Huber W.C. et al. (1972), *Temperature prediction in stratified reservoirs,* ASCE-HY, 4.

Huyer A. and Patullo J.G. (1972), *A comparison between wind and current observations over the continental shelf off Oregon, summer 1969,* J. Geoph. Res., June 20.

Inman D.L. et al. (1971), *Mixing in the surf zone,* J. Geoph. Res., 15 May.

Ichiye T. and Plutchak N.B. (1966), *Photodensitometric measurement of dye concentration in the ocean,* Limn. Ocean, vol. XI, No. 3.

IGW (1968), *Self-purification kinetics for the Bay of Puck as a recipient of wastes (in Polish — Typescript),* IGW — Gdańsk.

Inman D.L. et al. (1971), *Mixing in the surf zone,* J. Geoph. Res., 15 May.

Ivanov Yu. A., Morozov E.G., Samodurov A.S. (1974), *Vnutrennyje gravitatsionnyie volny v okeane,* Issl. izmench. gidrof. polei v okeane, Nauka, Moskva.

Iwai M. et al. (1968), *On the survey and prediction of pollution at the Omuta industrial harbour,* 4th Int. Conf. on Wat. Poll. Res.

Janowitz R.V. (1971), *The coastal boundary layers of a lake,* Great L. Res., 14th Conf.

James W.P. et al. (1971), *An aerial photographic study of wastefield from ocean outfalls,* Offshore Techn. Conf., Third Ann.

Jen Y. et al. (1966), *Surface discharge of horizontal warm-water jet,* ASCE-PO, Apr.

Johnson R.E. (1970), *Regression model of wave forces on ocean outfalls,* ASCE-WW, 2.

Jones R.H. and Stewart R.E. (1968), *Diffusion of sewage efficient from an ocean outfall,* Coll. Int. d'Ocean Medic., 4th.

Jones J.S.F. and Kenney B.C. (1971), *Turbulence in lake Huron,* Wat. Res. Research 9.

Josa F. (1967), *Bases for outfall design on the Mediterranean coast.,* Int. WPC Res. 3rd Conf.

Jurish R. (1973), *Instantaneous velocity measurements in hydraulic models by laser-Doppler anemometry*, AIHR Conf., 13th.

Kalatskii V.I. (1974), *Nekotoryie analiticheskie resheniya uravneniya balansa turbulentnoi energii*, Fiz. Atm. Okeana, 8.

Karabashev G.S. (1966), *A new device for diffusion studies in the sea (in Russian)*, Izv. AN SSSR, Fiz. atm. okeana 5.

Kennedy R.E. (1949), *Computation of daily insolation energy*, Bull. Amer. Met. Soc., vol. 30, No. 6.

Kenney B.C. (1967), *Dye plume meandering*. Great L. Res. 10th Conf.

Kitaigorodskii S.A. (1975), *Teoriya podobiya v geofizicheskoj gidromehanike*, Rozpr. Hydr., 36.

Ko S.C. (1972), *Measurements of turbulence in water at high velocity*, ASCE-HY, 12.

Koh R. C.Y. (1971), *Two-dimensional surface warm jets*, ASCE-HY, 6, (a).

Koh R. C.Y. (1971), *On buoyant jets*, AIHR Congress (b).

Koh R.C.Y. and Fan L.N. (1970), *Mathematical models for the prediction of temperature distribution resulting from the discharge of heated water into large bodies of water*, Wat. Poll. Con. Res. series. Rept., 16130 DWQ 10.

Komar P. (1971), *Nearshore cell circullation and the formation of giant cusps*, J. Geoph., 20.

Larsen J. and Sörensen T. (1968), *Buoyancy spread of waste water in coastal regions*, Coast Eng. Conf., 11th.

Lee T. and Mc Guire J.B. (1972), *An analysis of marine wastes in Southeast Florida's coast*, Int. WPC Res., 6th Conf.

Liseth P. (1970), *Mixing of mering buoyant jets* [...] *in stagnant* [...] *water* [...] *of uniform density*. Rep. HEL-23-1, Berkeley, Nov.

Long R.R. (1970), *A theory of turbulence in stratified flows*, J. Fl. Mech., 42, 2.

Longuet-Higgins M.S. (1953), *Mass transport in water waves*, Phil. Trans. Roy. Soc., London 903.

Longuet-Higgins M.S. and Stewart R.W.S. (1964), *Radiation stresses in water waves; a physical discussion with applications Deep-Sea Res.*

Longuet-Higgins M.S. (1970), *Longshore currents generated by obliquely incident sea waves*, J. Geoph. Res., Nov. 20.

Lonsane B. et al. (1968), *Effect of storage temperature and time on the coliforms in water samples*, 4th Int. Conf. on Wat. Poll. Con.

Ludwig H.F. and Onodera D. (1963), *Scientific parameters of marine waste discharge*, Int. J. Air Wat. Poll., 7, 159.

Ludwig H.F. and Storrs P.N. (1970), *Effects of waste disposal into marine waters. A survey* [...] *ten years*, Wat. Research, 4, 709.

Lukin L.D. et al. (1971), *Limitations and effects of waste disposal on an ocean shelf*, Wat. Poll. Con. Res. Series., 16070 EFG 12.

Lumley J.C., Khajeh-Nouri B. (1974), *Modeling momentum and heat transfer in stratified flow*, Fiz. Atm. Okeana, 6.

Mash F.D. (1964), *Mixing and dispersion of wastes by wind and wave action*, Int. WPC Res., 1st Conf.

Mih W.C. and Hoopes J.A. (1972), *Mean and turbulent velocities for plane jet*, ASCE-HY, 7.

Mirabel A.M. (1974), *Chislennaya model evolutsii spektrov energii i polia koncentratsii passivnoi primesi v dwumernom turbulentnom potoke*, Fiz. Atm. Okeana, 2.

Mitchell R. and Morris C. (1969), *The fate of intestinal bacteria in the sea,* Int. Wat. Poll. Contr. Conf., 4th.

Monin A.S., Yaglom A.M. (1965, 1967), *Statisticheskaya gidromehanika,* v. 1, v. 2. Nauka. Moskva.

Monin A.S., Kamenkowich V.M., Kort V.G. (1974), *Izmenchivost mirovogo okeana,* Gidrometeoizdat, Moskva.

Moore M.J. and Long R.R. (1970), *A laboratory investigation of turbulence in stratified shearing flow,* The Johns Hopkins Univ., Techn. Rept., 2, (ser. K).

Morton B.R. (1971), *The choice of conservation equations for plume models,* Jour. Geoph. Res., October 20.

Motz L.H. and Benedict B.A. (1972), *Surface jet model for heated discharges,* ASCE-HY, 1.

Murota A. and Muraoka K. (1967), *Turbulent diffusion of the vertically upward jet,* Int. Congress AIHR.

Murthy C.R. (1969), *Large-scale diffusion studies at Niagara River Mouth, Lake Ontario,* Great L. Res., 12th Conf.

Murthy C.R. (1970), *An experimental study of horizontal diffusion in Lake Ontario,* Great L. Res., 13th Conf.

Murthy C.R. (1972), *Complex diffusion processes in coastal waters of a lake,* Journ. Phys. Ocean., Jan.

Murthy C.L. (1972), *Complex diffusion processes in coastal currents of a lake,* J. Phys. Ocean, 1.

Murthy C.R. and Csanady G.T. (1971), *Experimental studies of relative diffusion in Lake Huron,* J. Phys. Ocean, 1.

Murthy C.R. and Csanady G.T. (1971), *Outfall simulation experiment in Lake Ontario,* Wat. Research 10.

Nece R.E. et al. (1966), *Single-port suction manifolds,* ASCE-HY, 1.

Okubo A. and Farlow J.S. (1967), *Analysis of some Great Lakes droque studies,* Great L. Res., 10th Conf.

Okubo A. (1970), *Horizontal dispersion of floatable particles in the vicinity of velocity singularities such as convergences,* Deep Sea Res.

Okubo A. (1971), *Oceanic diffusion diagrams,* Deep Sea Research, p. 789.

Olsen T.A. and Burgess F.J. (1967), *Pollution and Marine Ecology,* Interscience.

Orlob G.T. et al. (1969), *Mathematical models for the prediction of thermal energy changes in inpoundments,* Wat. Poll. Con. Res. Series. FWQA Rept. 16130 ext. 12.

Ozmidov R.V. (1968), *Gorizontalnaya turbulentnost i turbulentnyi obmen v okeane,* Nauka, Moskva.

Ozmidov R.V. (1973), *Issledovanie okeanicheskoi turbulentnosti,* Nauka, Moskva.

Ozmidov R.V. (1974), *Issledovanie izmenchivosti gidrofizicheskich polei w okeane,* Nauka, Moskva.

Palmer M.D. and Izatt J.B. (1970), *Determination of some chemical and physical relationships from recording meters in lakes,* Wat. Research 12.

Palmer M.D. (1969), *Simulated thermal effluent into Lake Ontario,* Great L. Res., 12th Conf.

Palmer M.D. (1972), *Some chemical and physical relationships on Lake Ontario,* Wat. Research 6.

Palmer M.D. and Izatt J.B. (1970), *Dispersion prediction from current meters,* ASCE-HY 8.

Palmer M.D. and Izatt J.B. (1970), *Lakeshore two-dimensional dispersion,* Great L. Res. 13th Conf.

Parkhurst J.D. et al. (1967), *Ocean outfall design for economy of construction,* Wat. Poll. Contr. Fed. Journ., June.

Partheniades et al. (1973), *Near-field* [...] *submerged heated jets,* AIHR Conf. 13th.

Parker F.L. and Krenkel P.A. (eds) (1969), *Engineering aspects of thermal pollution,* Vanderbitt Univ. Press.

Pearson E.A. (1957), *Submarine waste disposal installation,* Coast Eng. Conf. 6th.

Pearson E.A. et al. (1971), *A comprehensive study of San Francisco Bay,* Cal. State Wat. Resources Control Board. Subl. 42.

Pearson E.A. et al. (1966), *Some physical parameters and their significomce in marine waste disposal,* Not. Conf. Poll. Mar. Ecol., Galveston.

Pease T.E. (1972), *Analytical solutions for coastal currents,* Conf. Offshore technology, May.

Pedersen F.B. (1972), *Discussion to Koh (1971),* ASCE-HY, 2.

Petranskas Ch. (1971), *Discussion to Johnson (1970),* ASCE-WW, 2.

Phillips O.M. (1965), *The dynamics of the upper ocean,* Camb. Un. Press.

Pike E.B. et al. (1969), *Mortality of Coliform bacteria in seawater samples in the dark,* Coll. Int. d'Ocean. Medic., 4th.

Pomeroy R. (1959), *The empirical approach for determining the required length of an ocean outfall,* Waste Disp. Mar. Envir., 1st Int. Conf.

Pozdynin V.D. (1974), *Statisticheskie otsenki parametrov melkomaschtabnoi okeanicheskoi turbulentnosti,* Issl. izmench. gidrof. polei v okeane, 0000.

Pratte B. and Baines D. (1967), *Profiles of the round turbulent jet in a cross-flow,* ASCE-HY, Nov.

Pramer K. (1969), *Discussion to Aubert et al.*

Price R.K. et al. (1970), *Recirculation in shallow bays and rivers,* Coast. Eng. Conf. 12th.

Progress Report (1961), *Marine disposal of wastes,* ASCE-SA, 1.

Prych E.A. (1972), *A warm water effluent analyzed as a buoyant surface jet,* Sverige Met. Hydr. Inst. ser. Hydr., No. 21.

Putman J.A. et al. (1969), *The prediction of longshore currents,* Trans. Am. Geoph., Union 30.

Rajaratnam N. and Subramanya K. (1968), *Plane turbulent reattached wall jets,* ASCE-HY, 1.

Rajaratnam N., Pani B.S. (1974), *Three-dinensional turbulent wall jets,* ASCE-HY, 1.

Rawn A.M. et al. (1960), *Diffusers for disposal of sewage in sea-water,* ASCE-SA, vol. 86, No. 2.

Rogatzkie R.A. et al. (1969), *Summer thermal structure and circulation of Chequamegon Bay,* Lake Superior. Great L. Res., 12th Conf.

Renfro W. et al. (1971), *Oceanography of the nearshore coastal waters of the Pacific Northwest relating to possible pollution,* Oreg. State Univ., July.

Romberg G.P. et al. (1971), *Thermal plume measurements,* Great L. Res., 14th Conf.

Russel R.C.H. and Ossorio J.D.C. (1957), *An experimental investigation of drift profiles in a closed channel,* Coast Eng. Conf., 6th.

Sarikaya H.Z. (1973), *Numerical calculation of the removal ratio of suspended matter in setting basins,* AIHR Conf. 13th.

Savci R. (1973), *Longitudinal dispersion of soluble matter in submerged jets,* AIHR Conf. 13th.

Savage H.P. and Hanes N.B. (1971), *Toxicity of seawater to Coliform bacteria,* J. Wat. Poll. Contr. Fed. May.

Sharp J.J. (1969), *Spread of buoyant jets at the free surface,* ASCE-HY, 5.

Sharp J.J. (1971), *Unsteady spread of buoyant surface discharge,* ASCE-HY, 9.

Shadrin J.F. (1972), *Currents in the coastal zone of a non-tidal sea* (in Russian: *Techeniya berogovoi zony besprilivnogo moria),* Nauka, Moscov.

Shemdin O.H. (1972), *Wind-generated current and phase speed of wind waves,* J. Ph. Ocean Oct.

Shepard F. P. and Inman D.L. (1951), *Nearshore circulations,* Ch. 5.

Shirazi M.A. and Davis L.A. (1973), *Workbook on thermal prediction,* vol. 1: Submerged discharges, Wat. Poll. Contr. Res., Series 16130 ZPC, April.

Shirazi M.A., Mc Quivey R.S., Keefer Th. N. (1974), *Heated water jet in coflowing turbulent stream,* ASCE-HY, 7.

Schnert E.H. (1970), *Turbulent diffusion in the intermediate waters of the North Pacific Ocean,* J. Geoph. Res., 3 Jan.

Silvester R. and Patarapanich M. (1972), *Use of mixing tubes on marine outfalls,* Coast Eng. Conf., 13th.

Simons T.J. (1971), *Numerical models of Lake Ontario,* Great L. Res. 14th Conf.

Sleath J.F.A. (1972), *A second approximation to mass transport by water waves,* J. Mar. Res., 30, 3.

Slotta L.S. et al. (1969), *Stratified reservoir currents,* Oregon State Univ., Eng. Exp. Station, Bull. No. 44, Oct.

Sonnichsen J.C. (1971), *Jr. Lateral spreading of heated discharge,* ASCE-PO, 3.

Sonu Ch. J. (1972), *Field observation of nearshore circulation and meandering currents,* J. Geoph. Res., June 20.

Soskin I.M. (1962), *Empirichiskiye zavisimosti dla rascheta vetrovykh techeniy* (in Russian: *Empirical relationships for wind currents computations),* Trudy. GOIN 70.

Stefan H. (1970), *Modelling spread of heated water over a lake,* ASCE-PO, 3.

Stefan H. et al. (1971), *Surface discharge of heated water,* Wat. Poll. Con. Res. Series FWQA.

Stefan H. and Vaidyaraman. (1972), *Jet-type model for the three-dimensional thermal plume in a cross-current or under wind,* Wat. Res. Research 4.

Stefan H. (1972), *Dilution of buoyant two-dimensional surface discharges,* ASCE--HY, 1.

Stolzenbach K.D. and Harleman D.R.F. (1971), *Analytical and experimental study of surface discharges,* MIT Rept. 135.

Stanislav J. and Mohtadi M.F. (1971), *Mathematical solution of dispersion of pollutants in a lake with ice cover,* Wat. Research 7.

Srinivasan S.K. and Vasudevan R. (1971), *Introduction to Random Differential Equations and Their Applications,* Amer. Elsevier Inc. N. York.

Tam Ch.K. (1973), *Dynamics of rip currents,* J. Geoph. Res., Apr.

Tamai N. et al. (1969), *Horizontal discharge of warm water jets,* ASCE-PO, Oct.

Tarnowska M., Zeidler R. (1976), *Prądy przybrzeżne w naturze i laboratorium hydraulicznym,* Rozpr. Hydrot., (in preparation)

Terhune L.D.B. (1968), *Free-floating current followers,* Fish. Res. Board, Canada, Techn. Rept. 85.

Thomas R.H. (1964), *Marine dilution and inactivation of sewage*, Wat. Poll. Res. Conf., 1st.

Thornton W.R. (1970), *Variation of longshore current across the surf zone*, Coast Eng. Conf.

Tolmazin D.M. (1972), *Ob osobennosti turbulentnoi diffuzii v pribreznoi zone moria*, Fiz. Atm. Okeana 3.

Turner J.S., (1966), *Jets and plumes*, J. Fl. Mech. 26, 779.

Turner J.S. (1969), *Bouyant plumes and thermals*, Annual Review of Fl. Mech., vol. 1.

US-FWPCA (1969), *Proc. Lake Superior*, May, Sept.

US-FWPCA (1970), *Proc. Biscayne Bay*, Feb.

US-FWPCA (1970), *Proc. Lake Michigan*, Sept.-Oct.

Vigander S. et al. (1970), *Internal hydraulics of thermal discharge diffusers*, ASCE-HY, 2.

Wada A. (1968), *Studies on recirculation of cooling water in a bay*, Coast. Eng. Conf. 11th.

Waldichuk M. (1967), *Currents from aerial photography in coastal pollution studies*, Int. WPC Res., 3rd Conf.

Ward K.C. and Fischer J.T. (1973), *Transverse dispersion of pollutants in estuaries*, AIHR Conf., 13th.

Wastes management concepts for the coastal zone, Nat. Ac. Scie. (USA) 1971.

Webster F. (1972), *Estimates of the coherence of ocean currents over vertical distances*, Deep-Sea Res. 35.

Weil J., Fischer H.B. (1974), *Effect of stream turbulence on heated water plumes*, ASCE-HY, 7.

Weiss M. (1970), *Water surface temperature measurement using airborne infrared technique*, Great L. Res. 13th Conf.

Welsch J.G. (1967), *A new method of measuring coastal surface currents with markers and dyes dropped from an aircraft*, J. Mar. Res., p. 190.

Weyl P.K. (1971), *Temperature distribution of the heated effluent from the Northport Power Station (Long Island Lighting Co.)*, NY State Univ. Mar. Scie Dept., Techn. Rept. No. 10, Aug.

Wilde P. et al. (1971), *Automatic multi-sensor electrochemical monitor for sea water measurements*, Offshore Techn. Conf. 3rd Ann.

Wood J.R. and Wilkinson D.L. (1967), *Discussion to Jen et al. (1966)*, ASCE--PO, 2.

Wunderlich W.O. and Fan L.N. (1971), *Criteria for fully-mixed temperature regime in streams*, AIHR Congress.

Yih G.T. and Brutsaert W. (1970), *Perturbation solution of an equation of atmospheric turbulent diffusion*, J. Geoph. Res., 27 Sep.

Zeller R.W. et al. (1971), *Heated surface jets in steady cross-current*, ASCE-HY, 9.

Zeidler R. (1967), *Zagadnienie ruchu burzliwego podczas przepływu (Flow turbulence problems)*, Nauk. Bibl. Hydrot., 1.

Zeidler R. (1968), *Turbulencja morska ze szczególnym uwzględnieniem falowania (Marine turbulence with special reference to waves and swell)*, Rozpr. Hydrot., 22.

Zeidler R. (1970), *Prediction of relationships between dispersion and advection for low sea turbulence levels in the nearshore zone*, 7th Conf. Balt. Ocean. (a).

Zeidler R. (1970), *Problematyka zanieczyszczania Bałtyku w świetle VII Konferencji Oceanografów Bałtyckich (Problems of the Baltic Sea pollution in the light of the 7th Conf. Balt. Ocean.)*, Techn. Gospod. Morska 12 (b).

Zeidler R. (1971), *Zagadnienie odmienności laminarnego i burzliwego ruchu falowego (Laminar and turbulent wave motion)*, Rozpr. Hydrot., 28 (a).

Zeidler R. (1971), *Charakterystyka rozpraszania substancji przenoszonej znad dna ku powierzchni akwenu przy laminarnym falowaniu ośrodka (Dispersion characteristics for the motion of substance from above sea bottom toward surface under laminar wave conditions)*, Rozpr. Hydrot., 28 (b).

Zeidler R. (1971), *Turbulencja przydenna w falującym ośrodku (Bottom turbulence in a medium under wave conditions)*, Arch. Hydrot., 3 (c).

Zeidler R. (1972), *Ocena zaniku zanieczyszczenia morza w rejonie Zatoki Puckiej pod wpływem czynników biochemicznych i biologicznych (Marine pollution decay due to biochemical and biological factors in the Bay of Puck)*, Rozpr. Hydrot., 30 (a).

Zeidler R. (1972), *Versuch zur Bestimmung der Struktur der turbulenten Bewegung des Meeres in der ufernahen Zone (Determination of the structure of turbulent sea motion in the nearshore zone)*, Beitr. zur Meereskunde 30/31 (b).

Zeidler R. (1973), *Waste disposal in the marine environment (Zrzut ścieków do ośrodka morskiego)*, Rozpr. Hydrot., 32.

Zeidler R. et al. (1969), *Rozprzestrzenianie się w morzu ścieków Gdyni i kinetyka samooczyszczania Zatoki Puckiej (Marine dispersal of Gdynia wastes and self-purification kinetics in the Bay of Puck)*, Techn. Gospod. Morska 5.

Zeidler R. and Żelazny E. (1970), *Hydrographic characteristics of sea turbulence in nearshore zone at a waste disposal site.* 7th Conf. Balt. Ocean. (b).

Zeidler R. et al. (1970), *Dyfuzja zanieczyszczeń w morzu — metody badań i interpretacji dla potrzeb bezpiecznego odprowadzania ścieków (Marine diffusion of wastes, methods and techniques)*, Mater. IGW (a).

Zeidler R. et al. (1972), *Die Anwendung eines Fluometers bei in-situ-Messungen der Meeres diffusion (Use of fluorimeters in marine diffusion measurements)*, Beitr. zur Meeresk. 30/31.

Zeidler R. (1976), *Küstenstromungen unter Berücksichtigung der Ostseeverhältnissen, Beitr.* Meereskunde, 39.

Zeidler R. (1976), *Coastal dispersion of pollutants*, ASCE-WW, 2.

Glossary of Abbreviations

ASCE-PO — Proc. Amer. Soc. Civ. Eng., Power Div.,

ASCE-WW — Proc. Amer. Soc. Civ. Eng., Waterways, Harbors, and Coastal Engng.

ASCE-HY — Proc. Amer. Soc. Civ. Eng., Hydraulics Div.

Coast. Eng. Conf. — International Conference on Coastal Engineering, Proccedings.,

FWPCA — Federal Water Pollution Control Association.,

Great L. Res. — th Conf. — Proceedings of the -th Conference on Great Lakes Research.,

Int. W P C Res. Conf. — Advances in Water Pollution Research, International Conference.,

KH-R — Calif. Institute of Technology, W.H. Keck Hydr. Labor.,

M.I.T. — Ralph M. Parsons Laboratory of the Massachusetts Institute of Technology

US-FWPCA — US Dept. of the Interior, Federal Wat. Poll. Contr. Adm; Proceedings; Conference (s) on the matter of pollution of the navigable waters of ...